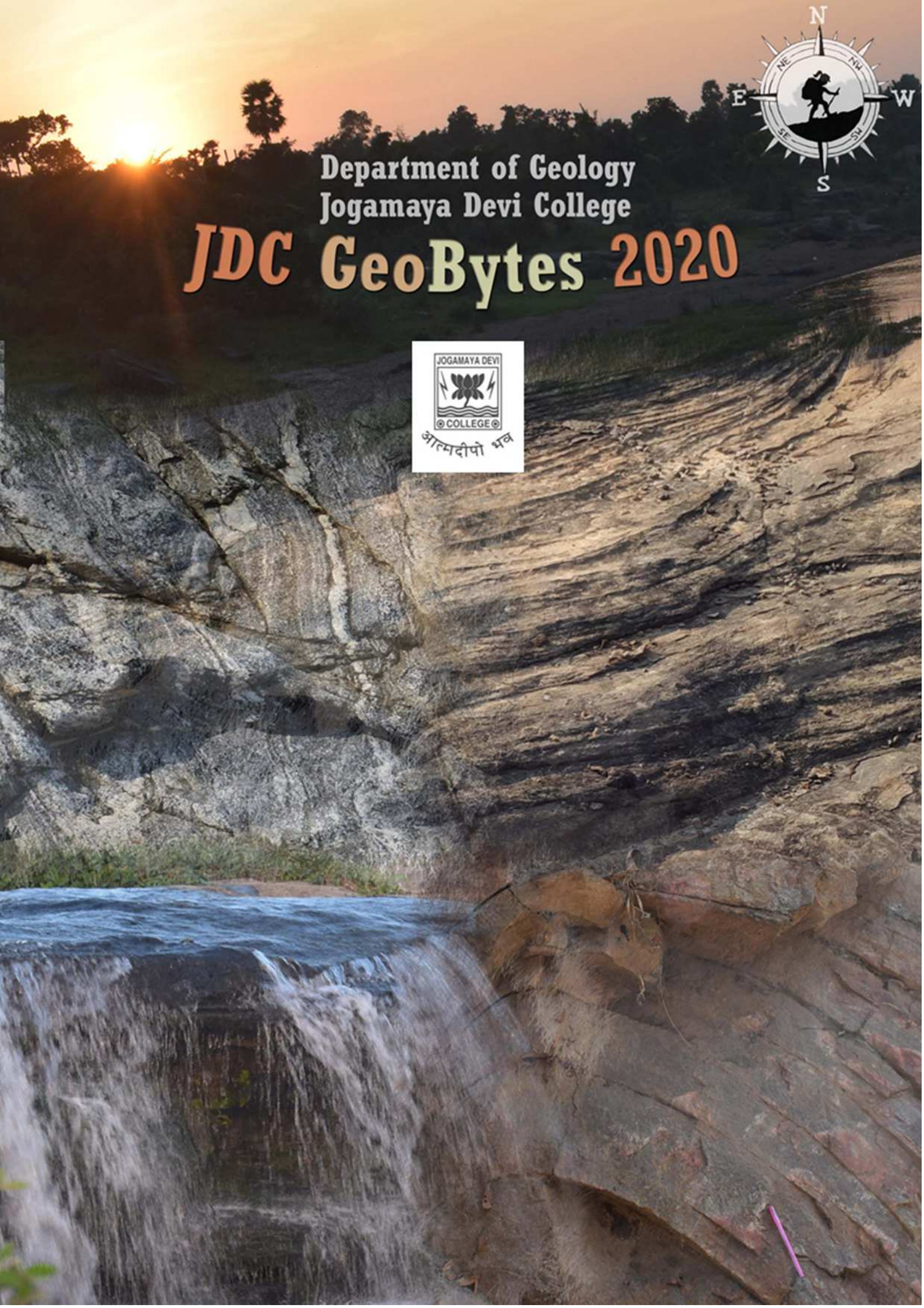




Department of Geology
Jogamaya Devi College

JDC GeoBytes 2020





JDC GeoBytes 2020

Department of Geology
Jogamaya Devi College
Kolkata
2020

Kolkata Jogamaya Devi College
92, Shyama Prasad Mukherjee Road, Kolkata 700026 and
5A, Rajeswar Dasgupta Road, Kolkata 700026

First Publication: 26th July 2020

Publication Data:

JDC GeoBytes 2020/Department of Geology, Jogamaya Devi College
(Jogamaya Devi College Departmental Magazine, Volume 1)

Joint Editors:

- Chandrabali Mukhopadhyay
- Upasna Karmakar

Editorial Board:

- Abhijit Chakraborty
- Bhaskar Ghosh
- Kaushik Kiran Ghosh
- Keya Bandyopadhyay
- Asima Kar
- Nabanita Barik
- Tiasha Mitra
- Navya Dharmdev

*Dedicated in the memory of
our revered faculty
Smt. Mahua Ganguly.*

... Being geologists, enjoying the diverse geology of our planet appears to be one of our major delights; 'a way of life' that we strive to pursue even at the face of severe challenges. In an attempt to facilitate this fascination even in recent times, as we find our way forward in this new era of the 'COVID Pandemic', we bring to you the JDC GEOBYTES 2020. This E-magazine is a product of many relentless hours of discussion, exploration, research, interaction, mending-mentoring, editing and debate; all of which was aimed at the single cause of publishing a standard magazine within our limited resources.

A range of topics has been included in this magazine issue that covers the significant domains of Earth Sciences- Petrology, Mineralogy, Geochemistry, Structural Geology, Palaeontology, Physical Geology and so on. The articles have all been contributed by our students who were mentored by the faculty members of our department. We consider this endeavour a step towards transforming this magazine into a standardized journal in the future. We sincerely hope to be able to gather more precise input and engage in intense sessions of brainstorming for our future editions.

I am certain that this magazine will attract a broad audience and foster an active interest in our fraternal concern: the Earth, the way it is. I feel great pleasure for being a part of this constructive endeavour and wish all the success to the contributors, particularly the budding geologists of our department. The College Authority is thankfully acknowledged for providing logistic help.

*Abhijit Chakraborty
Head of the Department
Geology*

CONTENT

	Page No.
1. Orogeny of Himalayan Mountain belt <i>Ankita Moulik, Asmita Roy, Asmita Singh, and Barnita Ghosh</i>	01
2. Friendships: Stories of Sandstone <i>Moumita Sen, Ritupriya Jalani, Raniria Mitra and Pallabi Saha</i>	06
3. Bio-Oxidation of Gold <i>Sampriti Dutta, Shreya Mudi, Sejuti Mondal and Shreya Mukherjee</i>	12
4. The Hadean World <i>Sneha Barik, Sneha Debnath, Sneha Mojumder and Sneha Pal</i>	18
5. Managing Natural Hazards – A Geological Approach <i>Sneha Roy, Snigdha Mondal, Sreeja Ghosh and Srijita Banerjee</i>	23
6. Tracking the Trails <i>Swagata Adhikary, Srijita Kayal and Tiasha Mitra</i>	30
7. Earthquake and its Prediction <i>Aditi Das, Ipsita Mondal, Sarmistha Das and Nandita Misra</i>	35
8. Fidelity of Terrestrial Heat Flow Data <i>Anwasha Ghosh, Srila Bhowmik and Sneha Chakraborty</i>	43
9. Volcano: Its Different Landforms <i>Ishika Chatterjee, Kankana Paul and Sampriti Dey</i>	48
10. Dynamic Recrystallization: An Outline of the Mechanism and the Microstructural Development <i>Anushka Das, Navya Dharmdev and Srija Ray Chowdhury</i>	59
11. Fun Textures in Feldspar <i>Ankita Samaddar, Tanushri Bera, Debadrita Nag and Debarati Bhowmik</i>	66
12. Plate Tectonics and CO ₂ Balance in Atmosphere <i>Nabanita Barik, Nrittwika Barui and Dakshi Sarkar</i>	80

13. Dendrochronology and Relative Age Dating 88
Aettree Karmokar, Bipasa Roy and Susmita Mandal
14. Mohr Circle: Its Application in the Representation and Measurement of Stress 96
Anwesa Sen and Debapriyaa Chakraborty
15. Mohr Circle: Its Application in the Representation and Measurement of Strain 101
DebasritaBhattacharjee, Shrestha Pal and Sumana Roy
16. Development of Tensile and Shear Fracture 107
Ankita Mukherjee, Upasna Karmakar and Tiyasa Ghosh

Orogeny of Himalayan Mountain Belt

Ankita Moulik¹, Asmita Roy², Asmita Singh³, and Barnita Ghosh⁴

Students of 4th Semester Geology Honours Course

¹ankitamoulik248@gmail.com, ²royasmita789@gmail.com

³asmitasingh2008@gmail.com, ⁴barnita.ghosh74h@gmail.com

1. Introduction

The Himalayan mountain belt, like many other fold mountain chains of the world (listed in Table 1 & Table 2), was formed by convergent motions of the lithospheric plates.

The lithospheric plates are in motion with respect to one another. Their relative motions can be convergent (the plates move towards each other), divergent (the plates move away from each other) or side-ward (the plates slide past one another along transform faults).

In case of the convergence involving two continental plates (Figure 1), continental plates being less dense than the underlying asthenosphere, neither of them can be subducted into the asthenosphere and a tremendous amount of compression gradually builds up along their contact zone. This continued compression brings about gradual buckling of the rock units in the continent-continent collision zones (Figure 2). As a consequence, there is a slow but continual formation of a long, narrow zone of higher topography, known as a collisional orogenic belt, and this process of formation is known as *Orogeny* (Greek *oro*: mountain, *geny* genesis or creation). A list of the major collisional orogenic belts of the world is given in Table 1 and Table 2.

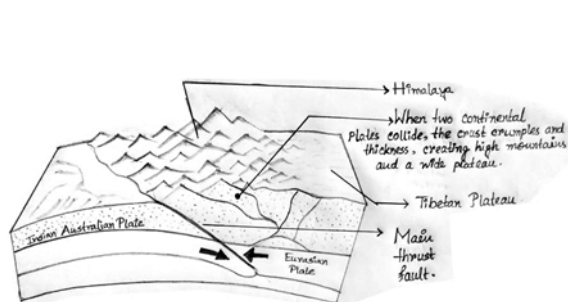


Figure 1: Continent-Continent Convergence. (Press & Seiver, 5th Edition)

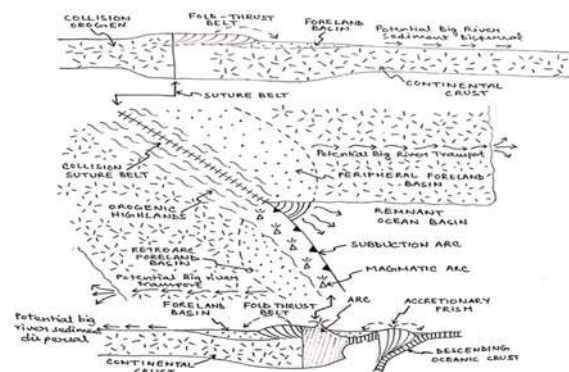


Figure 2: Evolving Collisional Boundary (Condie 1976)

2. Breakup of Gondwana Land and Northward Movement of Indian Plate

The Gondwana Land, a Southern Hemisphere super-continent comprising the present day landmasses of South America, Africa, Arabia, Madagascar, India, Antarctica, and Australia, and surrounded by the Tethys Ocean to its north, began to split apart into smaller fragments around 160 Ma (million annum, i.e. 10^6 years) before present (Scotese 1991, Storey 1995). This fragmentation was triggered by mantle plume and hot spots that caused the generation of

Large Igneous Provinces and Continental flood basalt provinces, the largest and most conspicuous among which is the Deccan Volcanic Province, the continental flood basalt province covering an area of 500,000 s.q. km in the western and central India (Vaidyanadhan & Ramakrishnan 2010). The African landmass began to drift away from India-Antarctica during the Middle to Late Jurassic. The Indian plate began rapid northwards motion in Cretaceous to drift towards the Eurasian plate. About 80 million years ago, India was located roughly 6,400 km south of the Asian continent, moving northward at a rate of about 9m a century.^[1] This northward movements topped around 40-50 Ma ago when the two plates collided, initiating the Himalayan orogeny described in the next section.

Name of Mountain Belt	Location	Elevation (m)	Length (km)	Width (km)	Highest Point	Area (km ²)
Himalaya ^[i]	Southern Asia	8,848	2,300	200-400	Mount Everest	595,000
Alps ^[iii]	Europe	4,810	1,200	250	Mont Blanc	298,128
Andes ^[iv]	South America	6,961	7,000	500	Aconcagua	3371,000
Rocky ^[v]	North America	4,401	3,000	110 - 480	Mount Elbert	991, 691
Appalachian ^[vi]	North American	2,037	2,400	160	Mount Mitchell	1909,000
Ural ^[vii]	Western Russia	1,895	2,500	150	Mount Narodnaya	2225,000
Zagros ^[viii]	Iran	4,409	1,600	240	Zardkooh	533,512

Table 1. The geographic description of major collisional orogenic belts of the world.

^[i]Yang, Qinye; Zheng, Du (2004); ^[iii]Wadia, D. N. (1931); ^[iii]“Alpine Convention” July 29, 2011; ^[iv]Andes Mountains, Encyclopaedia Britannica online; ^[v]Rocky Mountains, Encyclopedia Britannica online; ^[vi]“The Mountains That Froze the World”. AAAS. November 3, 2009. ; ^[vii]Ural Mountains, Encyclopædia Britannica online; ^[viii]Zagros Mountains, Encyclopaedia Britannica online

Mountain Belt	Age of Mountain Building	Converging Plates
Himalaya ^[i]	66Ma Still Active	The Eurasian Plate in the North and The Indian Plate in the South
Alps ^[iii]	65-2.5 Ma Still Active	The Eurasian Plate in the North and The African Plate in the South
Andes ^[iii]	Middle to Late Cretaceous Still Active	The South American Plate in the East and The Nazca Plate in the West
Rocky ^[iv]	80-55 Ma Still Active	The North American Plate in the East and The Pacific Plate in the South
Appalachian ^[v]	First Phase: middle Ordovician Second Phase: Cainozoic	The North American Plate and The North African Plate
Ural ^[vi]	Late Palaeozoic	Collision between Laurussia and Kazakhstania
Zagros ^[vii]	Late Cretaceous to Early Miocene Still Active	The Arabia in the south west and Eurasian plate in the north

Table 2. Tectonic Settings of major collisional orogenic belts of the world.

^[i]The Himalayas: Two continents collide; ^[iii]Schuster & Stüwe (2010); ^[iii]“Mountains on a plate form the Andes”; ^[iv]“Rocky Mountains | Location, Map, History, & Facts”; ^[v]Geologic Provinces of the United States: Appalachian Highlands Province”. USGS. ^[vi]Brown et al. (2008). ^[vii]Scheffel et al. (1980).

3. Different Stages of Formation of Himalayan Mountain Belt

3.1 Ridging up of Asia-India Junction–Formation of Indus-Tsangpo Suture

The Indus-Tsangpo Suture Zone (I-TS) is a tectonic suture in southern Tibet and across the north margin of the Himalayas which resulted from the collision between the Indian plate and the Eurasian plate in early Cainozoic. The rocks of the suture zone consist of an ophiolite mélanges composed of Neotethys oceanic crustal flyschs and ophiolites; the Dras Volcanics, dacites and minor radiolarian cherts, and the Indus Molasse which are an Eocene or later continental clastic sediments.^[2]

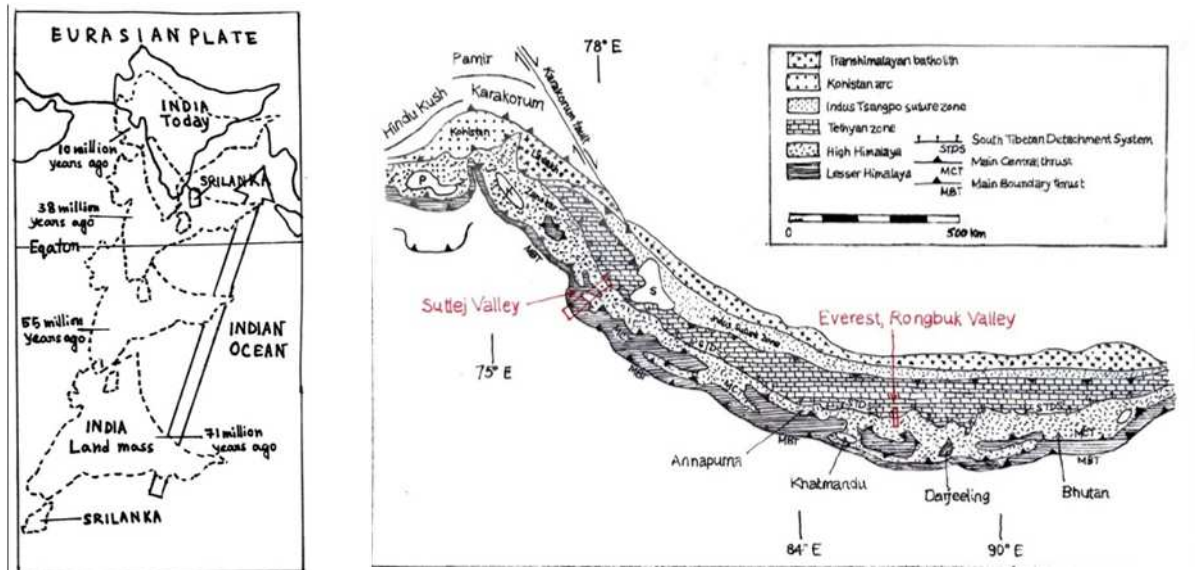


Figure 3: Northward Movement of India.^[3]

Figure 4: Geologic Sketch Map of Himalayan Orogen (sketched by the authors after Lawetal. 2004)

3.2 Formation of Main Central Thrust and Trans-Himalayan Fault

With continued compression between the Indian and Tibetan land masses across the I-TS, brittle deformation took place concurrently to buckling and produced two major thrusts of regional scale from Late Oligocene to Early Miocene (25–20 Ma): Trans-Himalayan Fault (T-HF, also known as South Tibetan Detachment Fault System) in the north of I-TS, and the Main Central Thrust: (MCT) in its south. They are approximately parallel to the I-TS, and at the eastern extremity (near Namcha Barwa) sharply bend towards SSW. MCT consists of multiple surfaces of dislocation dipping 30°–45° towards north, along which intense mylonitization and development of pervasive northerly-plunging lineation took place. The basement of metamorphic and granitic rocks was fractured and thrust along the MCT, and the Greater Himalayan Range or Himadri emerged. The granitic magma, generated by melting of the downthrown lithospheric plate, rose up and crystallized to form the frame work of the Himadri. With continued tectonic movement, the deformed sedimentary sequences were thrust tens of kilometres southward along the MCT upon the rocks of Lesser Himalaya. Displacement upto 125 km has been recorded at a few places.

Down-warping of the Indian plate along the southern edge of Lesser Himalaya occurred synchronously to the emerging upward, producing the foreland basins. It gradually formed

the Sirmur (or Sirmaur) foreland basin in Paleocene, which was a site of vigorous sedimentation till Early Miocene.

Around 18.3Ma, further down-warping to the south of Sirmur basin produced the long, narrow, east-west trending Siwalik Basin, extending from Potwar in the north-west to Arunachal Pradesh in the east. It contains a thick pile (~7000m) of largely fluvial molasse sediments derived from the Himalayan detritus.

3.3 Formation of Main Boundary Thrust

A powerful tectonic event in late Pliocene (2.5–2.0 Ma ago) deformed the Siwalik sediments to produce a series of roughly east–west trending hill ranges. It also thrust the Lesser Himalayan rocks over the Siwalik sediments along a series of faults collectively known as the Main Boundary Thrust (MBT). The MBT, roughly parallel to the MCT, is another inclined thrust system dipping steeply near the surface but becomes gradually gentler at deeper parts.

3.4 Evolution of Foreland Basins and Indo-Gangetic Alluvial Plane

The revival of tectonic movement in Pleistocene (1.6–1.1Ma ago) lifted the Himalayan mountain to tremendous height (Valdiya 1992). It broke the southern boundary of the Siwalik sediments along a series of northerly dipping steep faults—the Himalayan Frontal Fault (HFF, also called Main Frontal Thrust, MFT by Gansser 1976). The river basin to the south of HFF has been filled up by the sediments of Indus, Ganges and Brahmaputra river systems, to form the Indo-Gangetic alluvial plane.

4. Conclusion

The Himalayan mountain belt is the highest, youngest and one of the best studied continental collision orogenic belts. The geology of the Himalaya is a record of the most dramatic and visible creations of modern plate tectonic forces. The Himalaya-Tibet region supplies fresh water for more than one-fifth of the world population, and accounts for a quarter of the global sedimentary budget. Topographically, the belt has many superlatives: the highest rate of uplift (nearly 10mm/ year at Nanga Parbat), the highest relief (the 8848m high Mt. Everest), among the highest erosion rates at 2–12 mm/ year, the source of some of the greatest rivers and the highest concentration of glaciers outside of the polar regions. This last feature earned the Himalaya its name, originating from the Sanskrit for “the abode of the snow”.

Acknowledgement

We would like to express our special thanks of gratitude to our mentor Bhaskar Ghosh, Department of Geology, Jogamaya Devi College, who gave us the opportunity to write this article.

Reference

Condie, C. K, 1976. Plate Tectonics and Crustal Evolution. Fourth edition, Butterworth & Heinemann

Grotzinger, J., Thomas H., Press, Fr., Seiver, R. Understanding Earth. Fifth edition, W. H. Freeman and Company, New York

Vaidyanadhan, R., Ramakrishnan, M., 2010. Geology of India, Volume 2. Geological Society of India, Bangalore

Valdiya, K. S., 1998. Dynamic Himalaya. Hyderabad: Universities Press.

Weblinks

- [1] <https://pubs.usgs.gov/gip/dynamic/himalaya.html>
- [2] https://en.m.wikipedia.org/wiki/Indus-Yarlung_suture_zone
- [3] <https://www.geolsoc.org.uk/Plate-Tectonics/Chap3-Plate-Margins/Convergent/Continental-Collision#:~:text=The>

Friendships: Stories of Sandstones

Moumita Sen¹, Ritupriya Jalani², Raniria Mitra³ and Pallabi Saha⁴

Students of 4th Semester Geology Honours Course

¹moumita.2000k@gmail.com, ²jalaniritupriya1999@gmail.com

³riarani2000@gmail.com, ⁴pallabisaha830@gmail.com

1. Introduction

Sand is a very tiny particle 0.0625mm – 2mm in diameter (Pettijohn 1975), but a very important thing in our life. A large amount of sand helps you to build your house and make you happy while playing on the beach. Do you ever imagine the world of sand? How they were born? Do you know how they mature? How do they actually become small? Do you know about their friendship among themselves?

Today we are going to tell you the story of friendships. Friendships between sands. Just like humans change their looks, behaviour and their friendships with time & places, sand also have certain attributes in their lifetime. In geological terms we call those as depositional environments. Sands behave differently according to their depositional environments changing their shape and size.

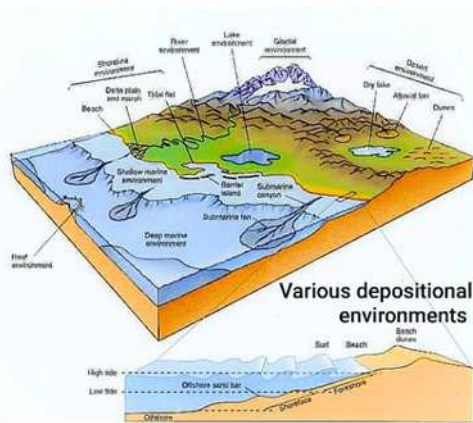


Figure 1: Depositional environments associated with sandstone.^[1]

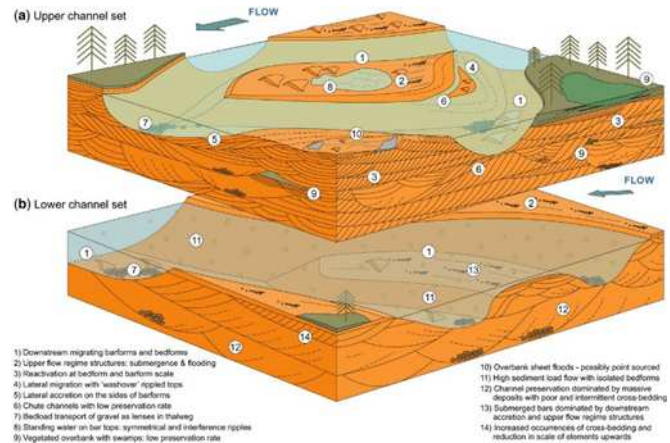


Figure 2: Fluvial sandstone with trough cross beds.^[2]

The depositional environments are very important, as they determine what type of sand grains will be accumulated there. The sandstone beds range from terrestrial to deep marine, including: Fluvial (alluvial fans, river sediments); Deltaic (levees, distributary deposits, mouth bars and other sediments formed where river meets a lake or sea); Aeolian (wind-blown dune sands formed in coastal and desert environments); Shoreline (beaches, barrier bars, tidal deltas and similar deposits formed in coastal areas); Glacial (sandy materials in tillites and other glacier deposits); and Deep-sea sediments, including contourite sands formed by ocean-bottom currents, turbidites and submarine fan deposits, formed by gravity-driven mass movements. (Figure 1) (Scholle & Spearing 1982). However, depositional

conditions vary from one location to another and within individual rock units. These changes result in variations in porosity, permeability and hence fluid distribution.

2. Fluvial sandstones: Tough but good bonding

Fluvial or alluvial sandstones are not well sorted sand deposits containing carbonaceous debris and clay trapped in the spaces within the framework grains (Tucker 2001, Collison & Thompson 1989), like friends with crazy haircuts, friends with good and bad grades. Just like that sand grains also vary in sizes and shapes.

They are formed in river channel deposits and are commonly developed on eroded surfaces. Sand beds in meandering and braided stream deposits are as thick as the depth of the river. They often show a fining upward particle size sequence especially with meandering streams; where sands grade into shales. Trough and planar cross beds occur in the main part of sandstone beds (Figure 2) dipping essentially downstream. In plan view, fluvial sandstones have abrupt terminations of sand bars.



Figure 3: Cross bedded deltaic sandstone.^[3]



Figure 4: Shoreline sandstone.^[4]

3. Deltaic sandstones: Fights and argues but has each other's back

Principal reservoirs are formed in delta-front sands. These deltaic sandstones (Figure 3) form as deltas build out over the deeper-water deposits. Vertical stacking in deltaic sandstones is common, giving rise to multiple zones. This is mainly due to individual delta lobes typically building out over and beside earlier lobes as subsidence proceeds and basin fills (Boggs 2005). Deltaic sandstones typically have a coarsening upward sequence, with individual sand bodies often elongate, lobate, or parallel to the paleo-shoreline but discontinuous along strike (Tucker 2001, Collison & Thompson 1989) which shows that they are really good friends as they support one another, putting their own ego aside and helping each other as a team.

4. Shoreline sandstones: Healthy competition

Shoreline sandstones are convex upwards, lenticular sand deposits with associated marine and lagoon shales serving as source rock (Tucker 2001, Collison & Thompson 1989); these sands are best developed along gently sloping shoreline areas, subjected to transgression and/or regression with fluctuations in sea level, (Boggs 2005), but most significantly are

those formed by beaches and offshore (Figure 4); including coastal barriers and tidal channels. Shoreline sandstones deposited on beaches are narrow, linear, elongate and oriented parallel to the shoreline while barrier shoreline sandstones are finer grained than the beach deposits, and are more discontinuous laterally. However, both beach and barrier shoreline sands are typically clean, well sorted; with little muddy matrix and good porosity and permeability.

This is how a healthy competition should be. Each sand grain wants to be better than the other which keeps this competition going. This benefits them as a group. It's what makes one strive to be better resulting in a more productive group.



Figure 5: Turbidites formed in deep sea environment.^[5]



Figure 6: Tertiary Sandstone near Corrine on the island of Arran.^[6]

5. Deep sea sandstones: Impulsive

Deep marine sandstones are formed by processes operating in deep oceanic environment such as gravity flows and turbidity currents, driven by down-slope movement of sediment under gravity, and ocean-bottom currents driven by movement of ocean water in three-dimensional circulation pattern, at depths of > 200m and on the continental slope and adjoining abyssal plain, and are often associated with pelagic limestone, which represents carbonate ooze formed by accumulations of planktonic organisms, and are commonly part of a submarine fan deposit (Scholle & Spearing 1982).

There are some friends in our life whom we admire for their bravery and also their quality of stealing the spotlight. Similarly, in the world of sand these deep marine sandstones prove to be the adventurous ones.

6. Glacial sandstones: Acquaintance

Glacial sandstones are poorly sorted bouldery sand deposits consisting of sands, lenses left by meltwater streams with reservoir potential and other glacial deposits left by retreating glaciers as moraine deposits (Scholle & Spearing 1982). They are not friends at all, they prefer to be in their own way and these sand particles hardly know one another. Glacial sandstones may also be deposited in marine areas (Figure 6), giving rise to muddy sediments with dispersed

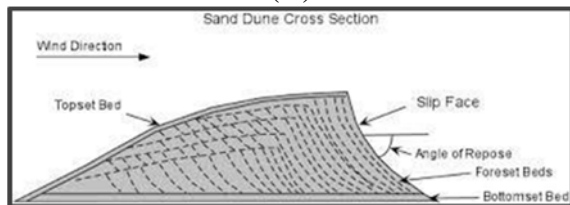
boulders. These may however be locally reworked by wave action in shallow areas resulting into potential reservoir sand bed for example Ordovician oil- bearing glacial sands found in Algeria and Permo-carboniferous hydrocarbon glacial sands in southern Oman.



(A)



(B)



(C)

Figure 7a: Longitudinal dunes (Wind direction from lower part to upper part).^[7]

Figure 7b: Transverse dunes (Wind direction from lower left to upper right).^[8]

Figure 7c: Sand dune cross section.^[9]

7. Aeolian sandstones: Companion

Aeolian sandstones are wind-blown sand dunes of coastal and desert environments. Dunes are ridges of sand (Figure 7c) with crests either parallel to wind direction (longitudinal dunes) (Figure 7a) and perpendicular to the prevailing wind (transverse dunes) (Figure 7b) although they may also be crescent-shaped (Tucker 2001, Collinson & Thompson, 1989). Dunes advance down-wind direction by erosion of sand from up-wind side and depositing sand on the down-wind (lee side). These sand grains are friends for a very short duration of time. These friends come and go. Sometimes they will be there for you. Sometimes they won't. Some will love, some will not. This tide will never be still, but no matter they always remain as a part of life.

The up-wind face has a gentle inclination while the down-wind face has a steeper slope where sand added and building cross beds which when buried within the dune forms large scale high-angle cross beds (Figure 8); whose dips are in the same direction as wind direction. Aeolian sandstones are extremely well sorted because of their wind-blown nature and hence have good porosity and permeability. However, with desert deposits, they are less likely than other types of sand to be associated with organic accumulations that would act as hydrocarbon source rocks and provide a petroleum charge. Aeolian sandstones are commonly associated with evaporites which are salt deposits. They can thus have a complex diagenetic history, which may in some cases block the pores of the sand with chemically precipitating cementing materials.

8. The unfinished story: To infinity and beyond

The friendship between sands depends on the process by which sands transform into hard rock is a fascinating geological journey that we actually cannot witness directly – it takes place at depth over eons. However, like tourists we have identified the different stages of this journey of friendship, in the first instance by examining rock outcrops at the surface and second by drilling into the crust. Geologists commonly refer to this transformation as diagenesis.

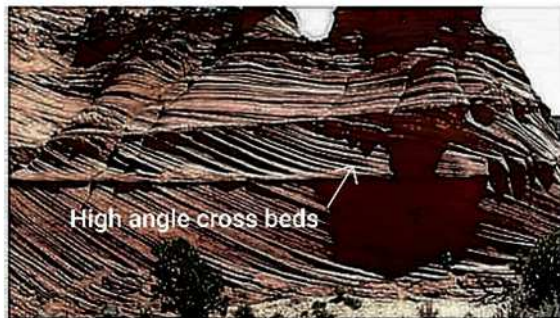


Figure 8: Large scale high-angle cross beds.^[10]

In our life, we can see that communication skill, personality and sense of humour help us to make good friends. Similarly, there are three important ingredients that contribute to the transformation of sand into rock: Pressure, temperature and chemical reaction.

The journey of the sandstone starts at or near the earth's surface where the sand-layer is deposited. Over millennia, the layer of sand is buried by other layers of sediment. The weight of overlying sediment layers compact the sand grains. Hence, the sands move close together and a strong bond of friendship develops between them. An important process that takes place during compaction is that fluid squeezes out from between the sand grains, which plays an important role in chemical reaction. As it does so, minerals are precipitated (Crystallized). We know that temperature increases as we probe deeper in the earth's crust. So, as the sand layer is buried increasing temperature makes the chemical reactions faster, so that their friendship becomes stronger. Typical chemical reactions that contribute to the formation of 'rock' include the precipitation of quartz and calcite crystals and clay minerals. The minerals 'Cement' the sand grains together to make their friendship unbreakable. In this way sandstone is formed.

But, the bitter truth is, this friendship does not stay permanently. The sandstone may be uplifted to the surface, carried by wind, water or ice and broken down by weathering and erosion into small fragments. Thus, the friend, who remained together over a million years, are now separated from each other. Again, they are carried out in different ways, deposited in different depositional environments and make friendship with other sands having different characteristics.

In this way, the friendship between sand grains is recycled over years. Some grains have more than 10 such cycles, each of which lasts on the order of 200 million years.

Acknowledgement:

We would like to express special thanks and gratitude to our mentor Asima Kar, Department of Geology, Jogamaya Devi College, who guided and encouraged us throughout the article.

References:

- Boggs, S. Jr., 2005, Principles of Sedimentology and Stratigraphy, 4th Edn., Prentice Hall, New Jersey.
- Collison, J. D., Thompson, D. B., 1989. Sedimentary Structures, Allen & Unwin, London.
- Pettijohn, F. J., 1975, Sedimentary Rocks, 3rd Edn., Harper and Row, New York.
- Scholle, P.A., Spearing, D. (ed.) 1982. Sandstone Depositional Environments (AAPG Memoir 31) 1st edition, American Association of Petroleum Geologists.
- Tucker, M. E., 2001, Sedimentary Petrology – an introduction to the origin of sedimentary rocks, Blackwell, Oxford.

Weblinks

- [1] <http://academic.brooklyn.cuny.edu/geology/grocha/monument/images/deposit.gif>
- [2] <https://sp.lyellcollection.org/content/specpubgsl/488/1/181/F11.large.jpg>
- [3] <https://fifegeology.files.wordpress.com/2012/08/cross-bedded-deltaic-sandstone-5.jpg>
- [4] https://as1.ftcdn.net/jpg/02/12/48/90/500_F_212489062_Xwmw0OON5QqK7OToOEpxotjBDFIQV3It.jpg
- [5] <https://upload.wikimedia.org/wikipedia/commons/thumb/c/cf/Turbidite-California.jpeg/1200px-Turbidite-California.jpeg>
- [6] <https://c8.alamy.com/comp/DXERMH/tertiary-sandstone-and-glacial-erratics-near-corrie-on-the-island-DXERMH.jpg>
- [7] <https://www.mediastorehouse.com/p/632/desert-parallel-longitudinal-sand-dunes-sandy-10130257.jpg>
- [8] <https://cdn.hswstatic.com/gif/sand-dune-4.jpg>
- [9] https://www.researchgate.net/profile/Chris_Goldfinger/publication/269097755/figure/fig1/AS:667692608544782@1536201731934/Typical-subaerial-dune-cross-section-http-wwwtulaneedu-sanelson-images-dunegif.ppm
- [10] <https://smallpond.ca/jim/sand/overview/cross-strata.jpg>

Bio-Oxidation of Gold

Sampriti Dutta¹, Shreya Mudi², Sejuti Mondal³ and Shreya Mukherjee⁴

Students of 4th Semester Geology Honours Course

¹sampriti.29600@gmail.com, ²mudishreya667@gmail.com

³sejuti.mondal17@gmail.com, ⁴Shreya.muku@gmail.com

1. Introduction

Gold is a mineral and a native element. Its chemical symbol is Au (Aurum). Gold is mainly recovered by bioleaching process. In mining industry, beneficiation is a process that improves the economic value of the ore by removing the gangue minerals which produces a higher-grade product and a waste stream from the proto ore. In the case of small scale gold mining in different countries, for the pre-concentration, gravity separation is used and amalgamation is used for final concentration ^[1] (Figure 1).



Figure 1: Mineral Gold.^[2]

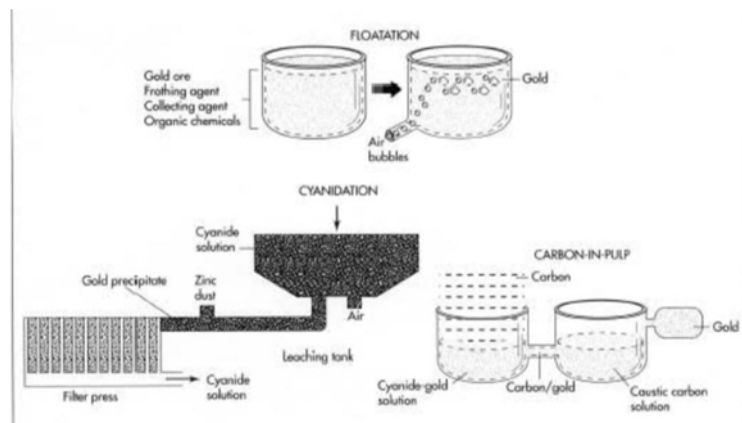


Figure 2: Geochemical prospecting.^[3]

2. Different methods of prospecting

Now a days so many processes are used to extract gold. Some of them are:

Geochemical prospecting: In this method high concentrations of metals surround the deposit, and the dispersion of metals laterally or vertically along fractures or faults creates a halo surrounding the deposit. Halos are very useful in prospecting because they may be hundreds of times larger than the deposit they surround and helps to locate deposition ^[4] (Figure 2).

Biological prospecting: Plants, humus, and bacteria have been successfully used as aids in mineral prospecting, and under certain conditions they may assist the prospector in locating buried mineral deposits. Laboratory and pilot plant scale studies of bio-oxidation of sulphidic gold ores have been conducted with pure cultures of pyrite-oxidizing bacteria, mixtures of laboratory cultures, and consortia of microorganisms cultured from environments where pyrite is undergoing oxidization (Ahmadi et al. 2011) Conventional and electrochemical bioleaching of chalcopyrite concentrates by moderately thermophilic bacteria at high pulp density. Hydrometallurgy 106:84–92)

(Figure 3).



Figure 3: Gold in contact with pyrite and chalcopyrite.^[5]

Hydrological prospecting: As groundwater flows through the deposits, minute amounts of gold are leached from the rock. These can sometimes be detected in ground water samples collected from wells located down gradient from the deposit.

3. Biological agent of gold:

Bio-oxidation refers to the microbiological oxidation of the metal ores containing metal compounds, the metal values remaining in solid residues in concentrated forms. Normally metal sulphides get oxidized by certain bacteria namely *Thiobacillus ferrooxidans* resulting in the formation of metal sulphate and sulphate acids. Hemp is an herbaceous oil plant with hydrophobic properties originating from strong oil secretion which serving as a significant collector for hydrophobic matter including gold. Thiolate bonding that occurs on sulphur rich amino acids in Methionine and Cystine in Hemp results in the adsorption of nanogold via plant uptake.^[6]

4. Bio-oxidation

The oxidation of different metal sulphides with different crystal structures proceeds through mineralization of various metals from gold containing ores by different ion oxidising bacteria and fungi on the basis of three biochemical reactions – acydolysis, complexolysis, redoxolysis. Dump leaching also require prevention of uncontrolled loss of metals in underground aquifers. Therefore, tank leaching processes for the bacterial treatment of gold containing refractory ore concentrates have been developed for expeditions collection of gold through three different pretreatment methods-mainly roasting, pressure leaching and biological leaching. Gold is usually disseminated in Pyrite and Arsenopyrite containing ores. One of the pretreatment techniques for recovery of Gold locked in the sulphide mineral fraction by cyanidation or Thiourea extraction is the microbiological oxidation of arsenopyrite and pyrite concentrates. The presence of organic carbon in the ore hampers the process and recovery of low gold is achieved if the ore contains more than 0.1%

carbonaceous material. The deactivation of carbonaceous fraction can be achieved with chemical methods of blinding with kerosene or chlorination. Microorganisms oxidise metal sulphide ores by direct mechanism when microbial attached to the surface of the mineral as oxidation electrons and directly transferred from the microbial cells. The mineral as oxidation electrons and directly transferred from the microbial cells without help of ferric or ferrous ions or the indirect mechanism when electrons are transmitted to the oxidising agent of the sulphide ores first from iron to sulphur then to oxygen. (Lindstrom, Gunneriusson, Tuovinen)

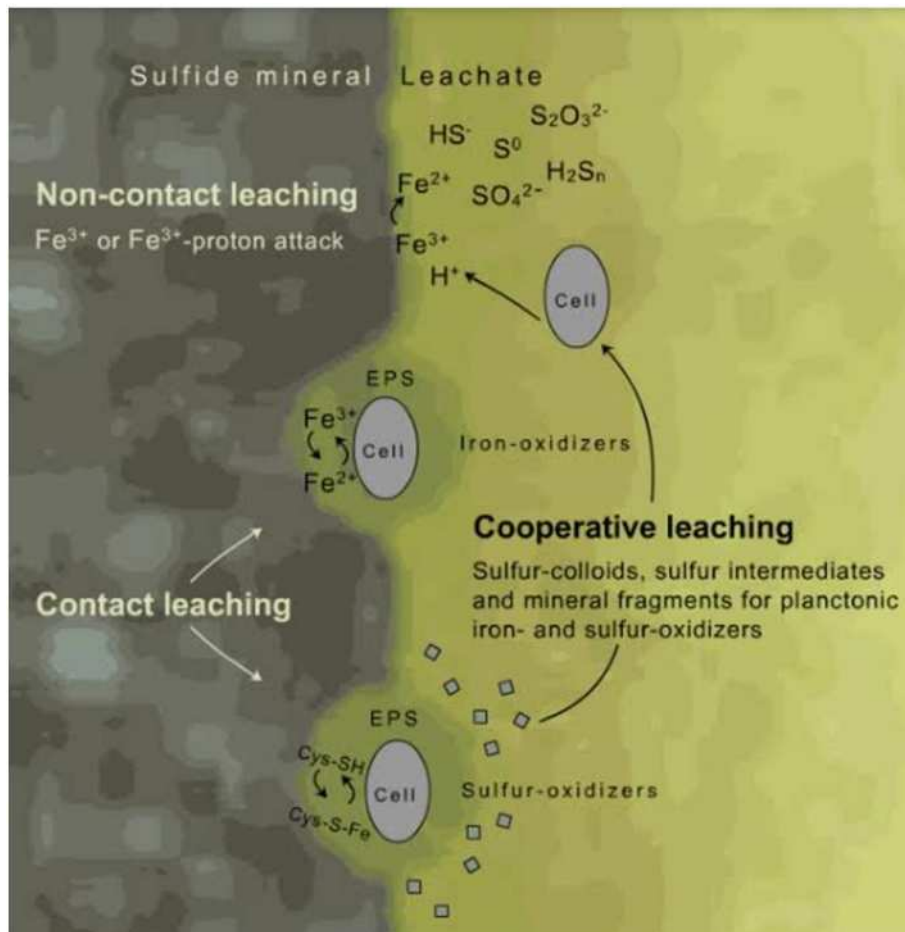
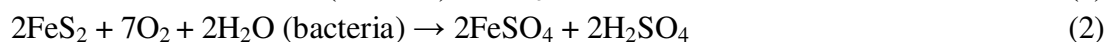


Figure 4: sulphide mineral bacterial leaching.^[7]

5. Leaching Microorganism

Depending on the type of the ore or concentrate to be leached, the nature of the bacteria to be used in the process also differs. For liberation of locked-up gold particles from sulphide minerals such as pyrite, arsenopyrite, pyrrhotite and chalcopyrite, bacterial treatment with *Thiobacillus ferrooxidans*, *Thiobacillus thiooxidans* and *Leptospirillum ferrooxidans* will be very beneficial. (Ehrlich 2002) (Figure 4).

The reaction is performed at bacterial cell membrane. In the process, free electrons are generated and used for the reduction of oxygen to water which produces energy in the bacterial cell.



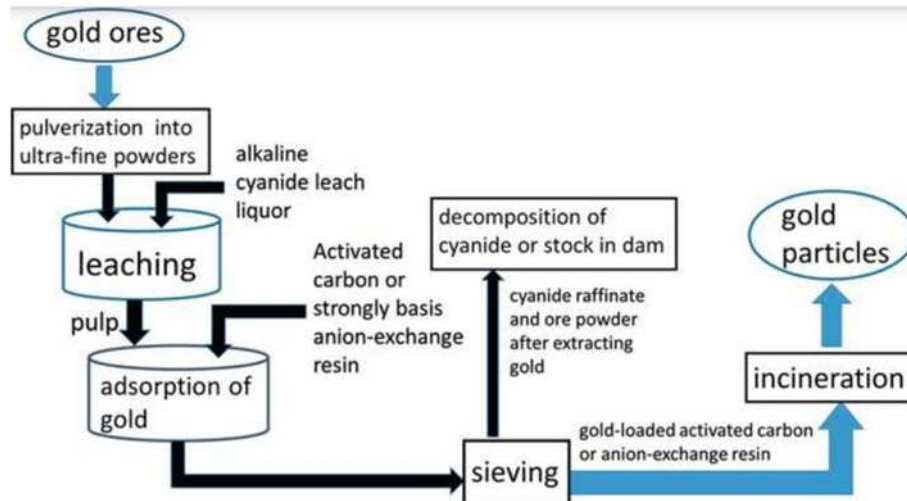
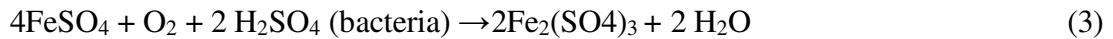


Figure 5: Leaching processes.^[8]

6. Bioleaching Mechanism

Bioleaching is a biochemical mining technique in which specific biological organism is used for the removal of a specific metal from impure ore. Organisms that conduct this bioleaching technique get their metabolic energy by the oxidation of sulphides and ferrous ions. Inorganic substrates such as sulphides, elemental Sulphur are enzymatically converted into ATP by oxidation phosphorylation for supplying chemical energy. Direct bacterial leaching has sometimes been separated from the ferric iron mediated leaching. Direct oxidation is envisaged to involve a bacterial attack on the mineral surface, yielding water soluble products, with electrons being scavenged by the bacteria for the electrons transport system. The electron transport system in iron and Sulphur oxidizing Thiobacilli is bidirectional. Downhill transport couples the flow of electrons and protons with the reduction of oxygen to produce water and established a proton-motive force to produce ATP. The uphill flow of electrons and is ultimately coupled to produce reducing equivalents $[(\text{NAD(P)H} + \text{H}^+)]$ to support the reductive fixation of carbon dioxide. Ferric iron-mediated indirect leaching is based on the presence of (Fe^{3+}) as the primary oxidant. Ferric iron is an electron acceptor, coupled with the chemical oxidation of reduced compounds of Sulphur. Bacterial reoxidation of Fe^{2+} is a key reaction in both the direct and indirect types of leaching reaction (Critical reviews in Biotechnology 12(1/2):133-155 (1992)) (Figure 5).

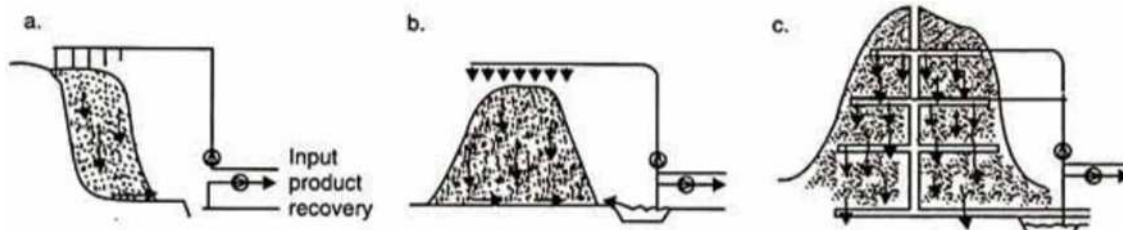


Figure 6: Process of bioleaching (a) slope leaching (b) heap leaching (c) in-situ leaching.^[9]

7. Common commercial bioleaching processes

Slope Leaching: In this technique, fine ore is kept in a large slope-shaped dump and a water solution made of inoculum is continuously sprayed over the ore. Then, the remaining liquid is gathered at the base and processed for supplemental metal recovery.

Heap Leaching: In this technique, the ore is arranged in large heaps and an aqueous mixture of microorganisms is spread over the leach pile. After that the solution is collected and processed to help recover even more metal.

In-situ Leaching: In this technique, the ore remains in its natural state while the leaching process happens. Water that contains thiobacillus is pushed through drilled passageways within the ore. The leach fluid is then stored until it is time for metal recovery^[10] (Figure 6).

8. Advantage of bioleaching

- (i) Bioleaching is simple process cheaper to operate and maintain.
- (ii) Bioleaching can extract metals from ore that are too poor for other technologies which means less waste.
- (iii) Environment friendly process.

Acknowledgement

We would like to express our special thanks of gratitude to our mentor Kaushik Kiran Ghosh, Department of Geology, Jogamaya Devi College, who gave us the opportunity to write this article.

References

- Ahmadi A, Schaffie M, Petersen J, Schippers A, Ranjbar M (2011) Conventional and bacteria at high pulp density. *Hydrometallurgy* 106:84–92
- Lindstrom E. B., Gunneriusson E., Tuovinen, O. H. 2008 *Bacterial Oxidation of Refractory Sulfide Ores for Gold Recovery*,
- Ehrlich, H.L. 2002 *Geomicrobiology*. Marcel Dekker, New York, 4th Ed.

Weblinks

- [1] <http://www.nzdl.org/gsdldmod?e=d-00000-00---off-0hdl--00-0----0-10-0---0---0direct-10---4-----0-11--11-en-50---20-about---00-0-1-00-0--4----0-0-11-10-0utfZz-8-00&c1=CL2.19.7&d=HASHc096d161f676b196cfad56.19.6>=1>
- [2] ALT: <https://s.yimg.com/aah/yhst-135466925550166/index-10.gif>
- [3] <http://www.madehow.com/Volume-1/Gold.html>
- [4] <https://www.911metallurgist.com/gold-prospecting-methods/>
- [5] <https://www.americangeosciences.org/sites/default/files/CI-112-Chalcopyrite-USGS-170919-1200x800.jpg>
- [6] journal homepage: www.elsevier.com/locate/mineng
- [7] <https://s3-us-west-2.amazonaws.com/courses-images/wp-content/uploads/sites/1950/2017/06/02023352/t-and-cooperative-leaching.png>
- [8] <https://api.intechopen.com/media/chapter/66110/media/F14.png>
- [9] https://www.biotechnologynotes.com/wp-content/uploads/2018/07/clip_image006-2.jpg
- [10] <https://www.angloamerican.com/futuresmart/our-industry/mining-explained/mining-terms-explained-a-to-z/bioleaching-definition-and-process>

The Hadean World

Sneha Barik¹, Sneha Debnath², Sneha Mojumder³ and Sneha Pal⁴

Students of 4th Semester Geology Honours Course

¹snehabarik91@gmail.com, ²sneha01112@gmail.com

³snehamojumder@gmail.com, ⁴snehapal435@gmail.com

1. Introduction

The Hadean is a geologic eon of the Earth predating the Archean. It began with the formation of the Earth about 4.6 billion years ago and ended, as defined by the International Commission on Stratigraphy (ICS), 4 billion years ago. Though evidences from the Hadean eon are very less, its contribution is vast for creating the present Earth. The “*Hadean*” was named after Hades, the ancient Greek god of the underworld- the world of the dead. In fact, it got its name due to the hellish conditions that prevailed on the Earth, after it had just formed and was still very hot owing to enormous heat released through its planetesimal accretion. Our Solar system was formed from a rotating cloud of stellar dust and gases known as solar nebula and the formation of the Earth is related to the formation of the Solar system.^[1] (Press & Siever 2007).

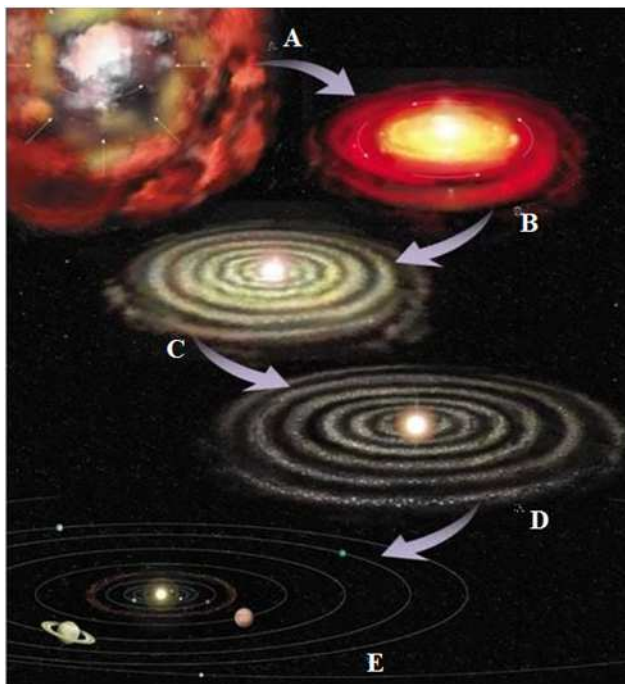


Figure 1: Schematic representation of condensation of solar nebula showing A. Supernova and formation of primordial dust cloud; B. Condensation of primordial dust, C. Proto Sun and planets begin to form. D. Accretion of planetesimals and differentiation of planets and moon. E. Existing solar system takes shape.^[2]

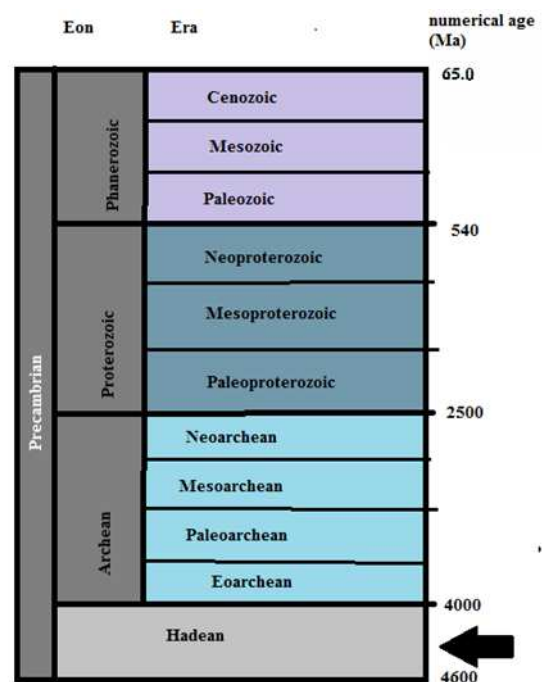


Figure 2: Geological time scale showing the span of the Hadean eon (black arrow pointing it). Reference- International Commission on Stratigraphy (ICS).^[3]

2. Position in the Geological Time scale

The Hadean is the first of the four eons of the Earth's history. During this period the Earth was formed (Figure 2). The boundary of Hadean was never properly defined.

3. History of the early Earth rock formation

Due to the acute scarcity of Hadean rocks, the composition of Earth's primitive crust during the Hadean eon is unknown, thus limiting our ability to understand how the earliest rocks evolved. Whether the Hadean Earth was dominated by mafic composition crust similar to today's oceanic crust, or included significant amounts of continental crust, remains an unsolved question that carries major implications for the earliest atmosphere, origin of life and the evolution of the crust-mantle system. Rocks that formed had melted back into the molten Earth, so no evidence of permanent rocks remained to study. Geochemical data provides direct evidence that Zircons of 4.1 billion years were found on the Earth. They are the oldest material of terrestrial origin. They are very durable and resistant to degradation.

(Reimink et al. 2016).

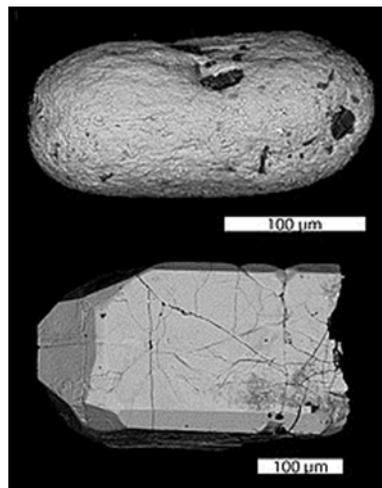


Figure 3: Backscatter electron micrograph of detrital zircons from the Hadean metasediments of the Jack hills, Narryer Gneiss Terrane, Western Australia.^[4]

4. Formation of the atmosphere, continent, and ocean

4.1. Early Earth atmosphere

The Hadean atmosphere was very different from present day atmosphere. At that time volcanic eruptions spewed gases like nitrogen, carbon dioxide, hydrogen sulphide and water vapour but no free oxygen. The atmosphere was likely reducing in nature due to methane, ammonia, water vapour and carbon dioxide. Later the event was followed by cometary infall and further degassing of planet's interior, which created the primordial atmosphere. Later the Earth's atmosphere quickly evolved to produce an environment suitable for the creation and support of life (Goodwin 1996).

4.2. Formation of the protocontinent in the Earth:

The Hadean crust started evolving around 4.45 Ga. The crust was largely basaltic in nature, but internal differentiation was unavoidable. It led to the formation of evolved rock types of Granitoid composition which was preserved in Hadean zircons. Few zircons grains were recorded that persisted beyond 3.7 Ga. In Hadean eon, the mantle convection was faster than present day, which had dynamically recycled the thin proto crust back into the mantle, thus destroying it (Kranendonk et al. 2007.).

4.3. Formation of the Ocean

Presently $\frac{3}{4}$ of the planet is covered with oceans, calling it a blue planet. The oceans had been there for 4 billion years but they were not as gigantic as they are now. The reasons for their formation were continuous volcanic eruption during Hadean, released enormous water vapour. As the Earth began to cool down slowly, it formed clouds, causing it to rain for thousands of years. The continuous downpour filled the low-lying areas, possibly creating the first oceans. But the water was still not enough; the rest came from the outer space. In early years, the Earth was hit by thousands of comets, composed of rocks and ice. By the end of bombardment, ice from the comets delivered loads of water to the Earth creating oceans.^[4]

5. Life on the early Earth

Life during Hadean is unimaginable. During that time meteorite impacts, volcanism, etc. increased the temperature of the Earth making it impossible for life to exist or survive at that time. Earth's first few hundred million years was a sterile, lifeless, hot planet that was constantly being bombarded by meteorites. But primitive oceans, crust and atmosphere that formed during Hadean set the cradle of life that first emerged in post Hadean.^[1]

6. Tectonics in the Hadean eon

Plate tectonics required a specific global scale rheology, but from Hadean to Eoarchean the Earth lacked this rheology and depended on the mechanical properties and dynamic force. It was different from recent times. At that time Hadean surface was incredibly unstable and mantle convection caused movements of the molten rocks on the surface and the negative buoyancy of the lithospheric mass, which was 20-25 km in thickness, would be sufficient to drive the plate. The movement of the plates were very fast, almost 20 times faster than now; this is one of the reasons that lead to cooling of the mantle to its present state^[5] (Kranendonk et al. 2007).

7. Difference between Hadean and post Hadean

The Hadean is the time period during which the Earth was formed from the solar nebula. The molten materials solidified into rocks as the Earth slowly cooled, thus forming primitive crust. But most of the evidences of primitive crust were destroyed by intense meteoritic bombardment and deep subduction as mantle convection was more vigorous than the Post

Hadean. But later in Post Hadean, as the interior of the Earth cooled, mantle convection became less vigorous and differentiation and growth of continental lithosphere became more important. By the end of Archean, several super-cratons or ancestral supercontinents such as Kenorland were formed. Primitive oceans and atmosphere were first formed during Hadean, as evident from the detrital zircon dating 4.1 billion years old. Primitive crust-ocean-atmosphere system in Hadean eon set the cradle for prebiotic life on Earth which first emerged in post Hadean (beginning of the Archean eon). The atmosphere at that time was of reducing nature due to rich in methane, ammonia, carbon dioxide. Later in Post Hadean (during Meso to Neoproterozoic), concentration of free oxygen were generated from O₂-producing photosynthesis by marine phytoplankton which gradually changed the atmosphere from reducing to oxidizing one.^[6]

8. Conclusion

The Hadean world is a hidden mystery of the world. The presence of few terrestrial rocks and mineral grains from Hadean limits our ability to understand the Earth's history chemically and isotopically. Meteoritic impacts increased the heat and temperature on the Earth's surface, thus making it impossible for any life to exist on it. Moreover, the study of lunar formation shows that the Earth/moon system was continuously bombarded by frequent asteroid collisions throughout the Hadean. Since the Hadean gives us very little information about itself, thus concluding it as 'the hidden mystery of the world'. (Kranendonk et al. 2007)

Acknowledgement

We would like to express our sincere gratitude to our mentor Keya Bandyopadhyay, Department of Geology, Jogamaya Devi College, for providing guidance and support for writing this article.

References

- Bennett, V. C., Kranendonk, M. J. V., Smithies, R. H., 2007. Earth's Oldest Rocks First edition, Elsevier
- Chacko, T., Creaser, R. A., Davies, J. H. F. L., Heaman, L. M., Pearson, D. G., Reimink, J. R., Stern, R. A., Sarkar, C., Schaltegger, U., 2016. No evidence for Hadean continental crust within Earth's oldest evolved rock unit.
- Goodwin, A. M., 1996. Principles of Precambrian Geology, Academic press, Page no. 274-275.
- Grotzinger, J., Jordan, T. H., Press, F., Siever, R., 2007. Understanding Earth (Fifth Edition). W. H. Freeman and company. New York.

Weblinks

- [1] https://en.wikipedia.org/wiki/History_of_Earth/
- [2] <https://www.pmfias.com/wp-content/uploads/2019/09/formation-of-the-solar-system->

nuclear-disc-model.jpeg

[3] <https://stratigraphy.org/icschart/ChronostratChart2020-03.pdf>

[4] <https://en.wikipedia.org/wiki/Hadean>

[5] www.geologypage.com

[6] <https://www.sciencedirect.com>

Managing Natural Hazards – A Geological Approach

Sneha Roy¹, Snigdha Mondal², Sreeja Ghosh³ and Srijita Banerjee⁴

Students of 4th Semester Geology Honours Course

¹roysneha361@gmail.com, ²snigdha14thnov@gmail.com
³sreejaghosh31@gmail.com, ⁴srijitabanerjee0202@gmail.com

1. Introduction

A natural hazard represents a risk if it potentially threatens human population and its activities. Many of these natural risks, which cover a wide spectrum of phenomenon, are induced by solar energy, with or without gravity playing any role. The negative effect of the natural hazards which actually happens and harms the human life can be termed as natural disaster.

Natural hazard can be broadly classified in two broad categories namely 1) Geological hazard and 2) Biological hazard. In this discussion we will throw light only on the geological hazard and its mitigation.

The geological hazards include several types of adverse geological conditions rooted in deeper Earth. The main energy source for these phenomena is essentially Earth's internal heat while disseminating to the surface.

2. Natural hazard and Disaster

Natural hazard is a naturally occurring event will have negative effect on human life and property. It may be defined as “extreme events that originate in the biosphere, hydrosphere, lithosphere or atmosphere” or “a potential threat to human and their welfare” (Madigan 2018).

Disaster is a hazardous effect caused due to natural hazard that occurs for a limited time in a defined area. During the past few decades, natural calamities such as earthquakes, floods, and hurricanes have killed several millions of people on this planet earth (Keller et al. 2012). Some natural disasters were discussed in detail:

Landslide

Landslide is defined as the movement of a mass of rock, debris or earth down the slope, when the shear stress exceeds the shear strength of the material, we can say landslide may occur because the strength of the material is weakened. This reduces the power of the 'glue' that cements rock or soil grains together. Located on a slope, the rock is then no longer strong

enough to resist the forces of gravity acting upon it. Landslides have the potential to cause significant damages to infrastructure such as roads, dams, buildings and in cases the loss of human life. Of special importance are the frequent small landslides which affect transportation networks and have high cost of remediation.

Earthquake

As the Earth's crust deforms, the rocks which span the opposing sides of a fault are subjected to shear stress. Slowly they deform, until their internal rigidity is exceeded. Then they separate with a rupture along the fault; the sudden movement releases accumulated energy, and the rocks snap back almost to their original shape. The previously solid mass is divided between the two slowly moving plates, the energy released through the surroundings in a seismic wave. This is known as the elastic-rebound theory, an explanation for how energy is released during an earthquake.

Volcanic eruption

Volcanoes occur mainly near the plate boundaries along both divergent or convergent. Volcanoes erupt when the molten rock called the magma rises to the surface as being lighter than the surface rock. There are nearly 1900 active volcanoes present on earth surface. Almost 90% are situated near the Pacific ring of fire belt. Some volcanoes also occur in the interior of the plate near "Hotspots" like Hawaii Island. Most of the active volcanoes are hidden from our view as they occur on the ocean floor along spreading ridges e. g. Mount Fuji in Japan, Stromboli in Italy.^[1]

Tsunami

Tsunami arises due to sudden displacement of gigantic water masses due to seabed earthquake, under water, volcanic eruption and landslide or meteorite impact. About 85% of all tsunami resulted from so called seaquake.

Mostly beaches and coastline are affected by tsunami. About 1500 tsunamis are documented through worldwide but only 15% has led to catastrophic destruction. Only 10% has caused some destructive effect so far e. g. 17th July, 2006 in Java, Indonesia and 26th December, 2004 Sumatra.^[2]

3. Classification of hazards

Hazards are mainly classified as two types: 1) Natural and 2) Anthropogenic

Natural hazard:

Natural hazard can be further classified as: 1) Geologic Hazards 2) Atmospheric Hazards and 3) Other Natural Hazards.

Geologic Hazard – This is the main topic of discussion and it includes:

- Earthquakes

- Volcanic eruptions
- Tsunami
- Landslides
- Flood
- Subsidence
- Impacts with space objects.

Atmospheric Hazard - It includes:

- Tropical cyclones
- Tornadoes
- Drought
- Severe thunderstorm
- Lightening

Other Natural Hazards - These are hazards that occur naturally but do not fall under the above categories. They are:

- Insect infestations
- Disease epidemics
- Wildfire

Anthropogenic hazard - These are the hazards that caused due to human interaction with the environment. They include:

- Exposure to hazardous substance
- Side effects of acid rain on human life
- Destruction of ozone layer and global warming.^[3]

4. Effect of hazards

Hazardous process of all types can have primary, secondary and tertiary effects.

- *Primary Effect* - This is the result of the cause itself. For example, damage during flood and collapse of building during earthquake.
- *Secondary Effect* - effect occurs due to the primary effect. For example, disruption of power supply and water supply due to flood or earthquake.
- *Tertiary Effect* - long term effect caused due to primary effect. For example, loss of habitat due to flood and earthquake.

5. Problems of Natural Hazard

1. Geological hazard including earthquakes, volcanisms, plate tectonic activity, landslides leads to loss of life and property both locally and globally.
2. Flood, landslide, rock fall, wave action, cyclone, solar storm can affect civilisation.
3. Epidemic infestation, spread of poisonous gases, viruses, aerosols, smog which leads anarchy in the ecosystem.

4. Mass extinction event happened by meteoritic impact in Earth's surface. e. g. dinosaurs extinct due to a large meteoric impact.
5. Aerosols create a blanket of dust around the earth atmosphere which increases the greenhouse effect. Some aerosols reflect the incoming solar radiation that would further create earth cooling.

6. Mitigation Plans

The hazard management process consists of a number of activities carried out before, during and after a hazardous event in order to reduce loss of life and destruction of property. The plans are:

Pre-event measures

- a. Mitigation of natural hazard
 - Data collection and its analysis
 - Vulnerability reduction
- b. Preparation for natural disasters
 - Prediction
 - Emergency preparedness (including monitoring, alert, evacuation)
 - Education and training

Measures during and immediately after natural disasters

- a. Rescue
- b. Relief

Post-disaster measures

- a. Rehabilitation
- b. Reconstruction

The mitigation mechanisms are:

1. Natural hazard assessments: Natural hazard assessments provide information of the probable location and intensity of danger and specific time period of natural phenomena. These studies mainly based on scientific information including geologic, geomorphic and soil maps; aerial photograph, satellite imagery etc.
2. Vulnerability assessments: Vulnerability assessment estimate the degree of loss or damage that would result from the occurrence of natural phenomenon.
3. Risk assessments: Information from the analysis of an area's hazards and its vulnerability to them is integrated in an analysis of risk. Once risk is assessed, planner has the basis for incorporating mitigation measures.

4. Vulnerability reduction: Risk from natural hazards can be substantially reduce by the introduction of mitigation measures, both structural and non-structural.^[4]

7. Disaster Preparedness

Disaster preparedness refers to measure taken to prepare for and reduce the effect of disaster. Preparedness programme for disaster assigns two broad events such as long term and short term. Short term preparedness demands instant course of action to combat the immediate multidimensional sufferings of extremity. Whereas long term preparedness programme includes situational and permanent action planning to resettle the victimised people and relocate the habitats of wild animals from disaster prone zones. Disaster preparedness programs can only be made successful by public awareness programs, education to the society and use of advanced technology such as remote sensing.

Hazard zonation map provides important information which helps to understand the risks of natural hazards and helps to prepare mitigation programme. (Bell 1999).

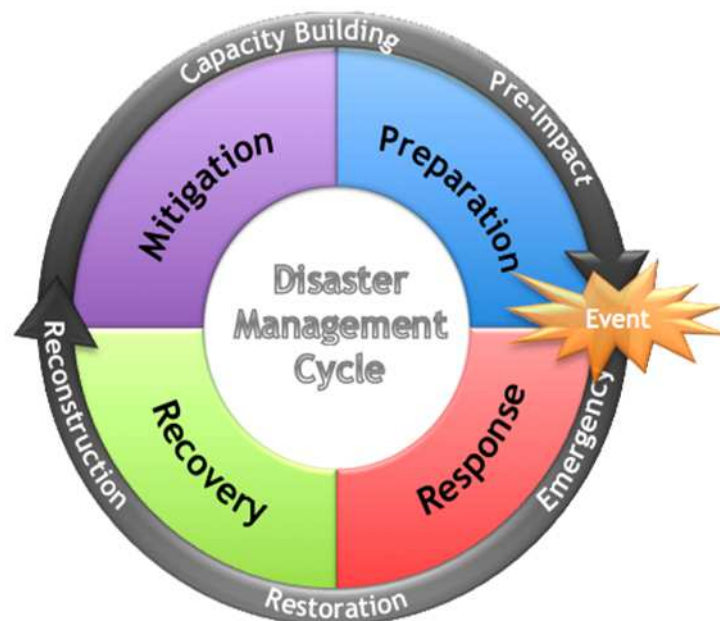


Figure 1: Disaster management cycle showing the relation between its different approaches.^[7]

8. Prediction Methods

Risk and vulnerability can sometimes be reduced if there is an adequate means of predicting a hazardous event. We cannot prevent natural hazard but we can predict that with the help of the prior knowledge to handle disasters and advanced technologies. Prediction of natural disasters, using technologies, requires extensive research and funding. By comparing past records with present data scientists can suggest the probability and intensity of the events that would occur in the coming future. Trends are used to predict earthquakes, tsunamis, and volcanic eruptions.

Another way in which technology is used in the prediction of natural disasters is with constant surveillance. Using off-shore cameras in hurricane-prone areas ensures that strong winds and waves can be recognised which helps to predict tsunamis. Meteorologists recognize patterns in weather data collected through remote sensing and on-the-ground observation that show cyclonic storms or tornadoes are developing.^[5, 6]

9. Recent Measures Taken

The computerised multi-hazard geographic information system stores the huge information in the easily accessible devices that can help the professionals in hazard preparedness and decision making.

Government and non-government organisations are taking actions in promoting awareness program with the help of professional expertise to educate common people regarding the natural disaster.

Mitigation training programme needs to be organised for research on mitigation strategies for all types of hazards.

Implementation of new technologies viz. advanced telecommunication capabilities to ensure broader dissemination of warnings.^[8]

10. Conclusion

Natural hazards pose risks to society and human life. There are still no full-proof methods to stop the hazardous natural phenomenon. The lack of accurate information on these losses is a barrier to more effective hazard mitigation that has to be solved by prediction.

Acknowledgement

We express our sincere gratitude to Abhijit Chakraborty, Department of Geology, Jogamaya Devi College, for giving us the opportunity to take part in this project. We are indebted to Kaushik Kiran Ghosh and Ms. Saheli Ghosh Dastidar for their guidance during the preparation of the article.

References

- Bell, F. G., 1999. Geological Hazards: their assessment, avoidance and mitigation. E & FN Spon.
- Keller, E. A., DeVecchio, D. E., Blodgett, R. H. 2012. Natural Hazards: Earth's Processes as Hazards, Disasters, and Catastrophes, 3rd Edition. Pearson Education Inc., Boston.

Madigan, Michael L., 2018. Handbook of Emergency Management Concepts A Step-by-Step Approach. CRC Press.

Weblinks

- [1] <https://www.popsci.com/environment/article/2009-03/top-10-volcanic-eruptions/>
- [2] https://en.m.wikipedia.org/wiki/2006_Pangandaran_earthquake_and_tsunami
- [3] https://www.tulane.edu/~sanelson/Natural_Disasters/introduction.htm
- [4] <https://www.oas.org/dsd/publications/unit/oea54e/ch09.htm>
- [5] <https://sites.google.com/site/naturaldisasterpreventiongin/prevention-prediction>
- [6] <https://sites.google.com/site/naturaldisasterpreventiongin/prevention-prediction/limitations>
- [7] <http://www.plymptonhalifaxexpress.com/wp-content/uploads/2015/10/Cycle-disastermgmt.png>
- [8] <https://www.oas.org/dsd/publications/Unit/oea66e/ch11.htm#chapter%2011%20%20%20geologic%20hazards>

Tracking the Trails

Swagata Adhikary¹, Srijita Kayal² and Tiasha Mitra³

Students of 4th Semester Geology Honours Course

¹swagataadhikary98@gmail.com, ²kayalsrijita2000@gmail.com, ³tiashamitra2000@gmail.com

1. Introduction

Varied benthic taxa delineate trails, as continuous traces indented on soft substrates as the trail makers' move, keeping a portion of their body in constant contact with the later. However, traces are not always taxon specific (Bromley 1996). Rather they often indicate similar behaviour (ethology) responding to similar environment or ecological compulsions. Accordingly, different ichnotaxa have been described based on the morphology of the traces or ichnofabric (Häntzschel 1975), notwithstanding their generic or taxonomic allegiance (Seilacher 2007). So it is important to objectively describe and diagnose an ichnofabric with precision. Trails are discretely different from tracks that are represented by discontinuous fabric. However, distinguishing subtypes in the trails require further detailing of the features. There are a number of curvilinear trails other than straight linear trails. Curvatures (or sinuosity or tortuousness) in trails are often used as a reliable criterion for the diagnosis of different ichnotaxa (Häntzschel 1975). However, description of such sinuosity is utterly qualitative that requires varied qualifying terms like, 'sinuous', 'sinuous with loops', 'sinuous to randomly meandering', 'winding' etc. (see Bromley 1996, Knaust & Bromley 2012) to describe a trail fabric. These qualitative descriptions further fail to detect and distinguish minor, yet significant generic or ethological types that are encoded in their specific trail sinuosity. Describing sinuosity (or tortuousness) by a more specific, quantitative expression might help resolving this ambiguity. Quantitative expressions for these putative evidences are seldom worked out (Deuke & Burrough, 1988 and references therein). In the present work, we have examined the quantitative difference of trail types in gastropods based on the tortuosity of their trails. We also compared these gastropod trails with the worm trails to scrutinize the validity and sensitivity of the chosen parameter (i.e., tortuousness) at different taxonomic hierarchy. In the present work, we have selected few sinuous trails of two known trace makers (viz. gastropods and worms) that are most dominant trail makers in coastal environment. We have attempted identification and diagnosis of these two apparently similar, curvilinear trail types quantitatively instead describing them in conventional and less descriptive terms, qualitatively (see Fan et al. 2018). We further delved into the quantitative aspects of varied trail subtypes (viz. reminiscent of feeding, mating, locomotion etc.) within the same broad groups (viz. gastropod and worm trails).

2. Materials & Methods

Trail photographs were taken (Source: Chakraborty, pers. Comm.) for extant gastropods and worms from coastal fringes of Bay of Bengal, India (Figure 1). Trails were then manually

traced (using light trace) from the photographs and processed in ImageJ public domain free software maintaining the same scale to get the fractal dimension (FD) values (through box count method) indicated by the individual trails. FD values were extracted for each trail, at three different scales of magnifications of trail segments (of same length) to check the scale independence of the trail patterns (Figure 2). FD values were batched for trails made by gastropods and worms (Holotheurids) at three scales of magnifications. A simulation was attempted (Figure 3) to understand the effect of sinuosity on FD values.

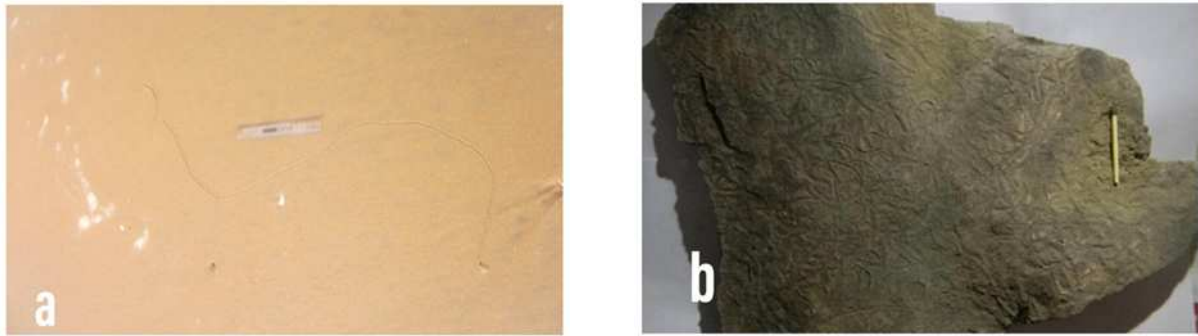


Figure 1: Figure a: Worm trail, b: Gastropods trail (Photo source: Chakraborty 2020, Personal communication)

Picture ID	C2	C3	C4	C6	C8	C12	C16	C32	C64	D
Fig21-Gastro-NoMag-8cm	596	348	238	145	103	64	46	21	9	1.197
Fig21-TwiceMag-8cm	852	444	290	160	104	67	48	24	9	1.277
Fig21-ThriceMag-8cm	1214	599	378	206	129	74	48	18	8	1.453
Fig23-Gastro-NoMag-8cm	642	370	248	154	105	64	48	22	10	1.193
Fig23-Gastro-TwiceMag-8cm	970	502	322	177	120	69	50	22	9	1.332
Fig23-Gastro-ThriceMag-8cm	1406	697	432	225	147	84	54	22	10	1.431
Fig24-Gastro-NoMag-8cm	667	395	266	169	116	74	58	28	14	1.108
Fig24-TwiceMag-8cm	964	506	345	195	139	82	64	29	13	1.222
Fig24-Gastro-ThriceMag-8cm	1175	634	387	215	149	86	60	26	13	1.306
Fig25-Gastro-NoMag-8cm	426	256	179	111	81	51	37	16	8	1.149
Fig25-TwiceMag-8cm	699	378	252	142	97	58	41	18	8	1.283
Fig25-ThriceMag-8cm	929	472	306	162	113	61	46	21	11	1.286
Fig27-Gastro-NoMag-8cm	444	269	182	119	84	53	35	18	8	1.153
Fig27-TwiceMag-8cm	642	360	227	126	89	52	37	18	9	1.236
Fig27-ThriceMag-8cm	915	467	297	166	113	69	51	18	9	1.329
Fig01-Worm-NoMag-8cm	836	483	338	207	150	92	65	28	12	1.213
Fig01-Worm-TwiceMag-8cm	1577	828	526	299	202	123	85	42	18	1.272
Fig01-Worm-ThriceMag-8cm	2395	1204	748	404	259	152	102	43	18	1.402
Fig03-Worm-NoMag-8cm	806	450	327	195	141	83	62	28	14	1.169
Fig03-Worm-TwiceMag-8cm	1073	563	365	207	140	80	61	27	12	1.284
Fig03-Worm-ThriceMag-8cm	1473	743	464	252	165	95	65	27	13	1.368
Fig04-Worm-NoMag-8cm	697	412	283	180	119	83	56	26	13	1.149
Fig04-Worm-TwiceMag-8cm	1463	770	514	280	201	124	80	36	19	1.26
Fig04-Worm-ThriceMag-8cm	1941	989	634	335	233	134	93	44	19	1.321
Fig05-Worm-NoMag-8cm	730	435	312	195	140	92	60	31	14	1.133
Fig05-Worm-TwiceMag-8cm	1200	647	429	244	170	102	73	31	15	1.262
Fig05-Worm-ThriceMag-8cm	1422	723	464	257	175	99	71	35	17	1.272
Fig09-Worm-NoMag-8cm	952	547	377	244	170	104	78	38	17	1.146
Fig09-Worm-TwiceMag-8cm	1536	811	522	307	199	136	91	43	19	1.247
Fig09-Worm-ThriceMag-8cm	2179	1114	698	370	257	141	102	46	24	1.308

Table 1: FD values computed for gastropod and worm trails at 3 scales of magnifications

3. Observations

Fractal dimensions (FD) worked out for 5 specimens each for gastropod and worm trails at three scales of magnification are documented in Table 1. Values of chosen statistical parameters (Mean/average, range, median, dispersion, and variation) indicate small but persistent and characteristic difference in FDs (at all scales of magnifications) between gastropod and worm trails, the later showing values at lower end.

4. Discussion and Conclusions

Utility of trail marks of varied benthic animals in palaeoecological and palaeoenvironmental reconstruction cannot be overemphasized. Trail characteristics envisages varied ethological expressions - viz., feeding, dwelling, mating, locomotion, escape from predation (Erlandsson & Kostylev, 1995, Bromley 1996, Seuront 2010, Ng et al. 2013).

Parameters	Gastropod Trails	WormTrails
AVERAGE	1.263666667	1.253733333
STDEV	0.098993266	0.080283842
VARIANCE	0.009799667	0.006445495
MEDIAN	1.277	1.262
Range	0.345	0.269
Max	1.453	1.402
Min	1.108	1.133

Table 2. Statistical parameters showing small yet distinct differences between FDs of gastropod and worm trails.

Positive relationship between habitat complexity and species diversity, and the potential for fractal analysis to be related with more traditional biological and ecological approaches in entangling the complex relationship between habitat heterogeneity and species diversity (Seuront 2010).

Myriad gastropod species from a variety of coastal environments over the globe suggest a Curvatures (or sinuosity) in trails are often used as a reliable criteria for the diagnosis of different ichnotaxa (Häntzschel 1975). However, description of such sinuosity is utterly qualitative that requires varied qualifying terms like, 'sinuous', 'sinuous with loops', 'sinuous to randomly meandering', 'winding' etc. (see Knaust & Bromley 2012) to describe a trail fabric, albeit less specifically. These qualitative descriptions further fail to detect and distinguish minor, yet significant generic or ethological types as encoded in their specific trail sinuosity. We suggest, describing sinuosity (or tortuousness) by a more specific, quantitative expression may help resolving this ambiguity. A significant correlation between the tortuousness of linear trails and corresponding FD values is observed in the present work. This might help to discern ichnotaxonomic or ethological proximity from the narrow dispersion and low variance of FD values of their trails. Though certain quantitative, diagnostic criteria is suggested for the discrimination of trails (viz. of worms and gastropods), a more robust dataset is required for any conclusive statement on this.

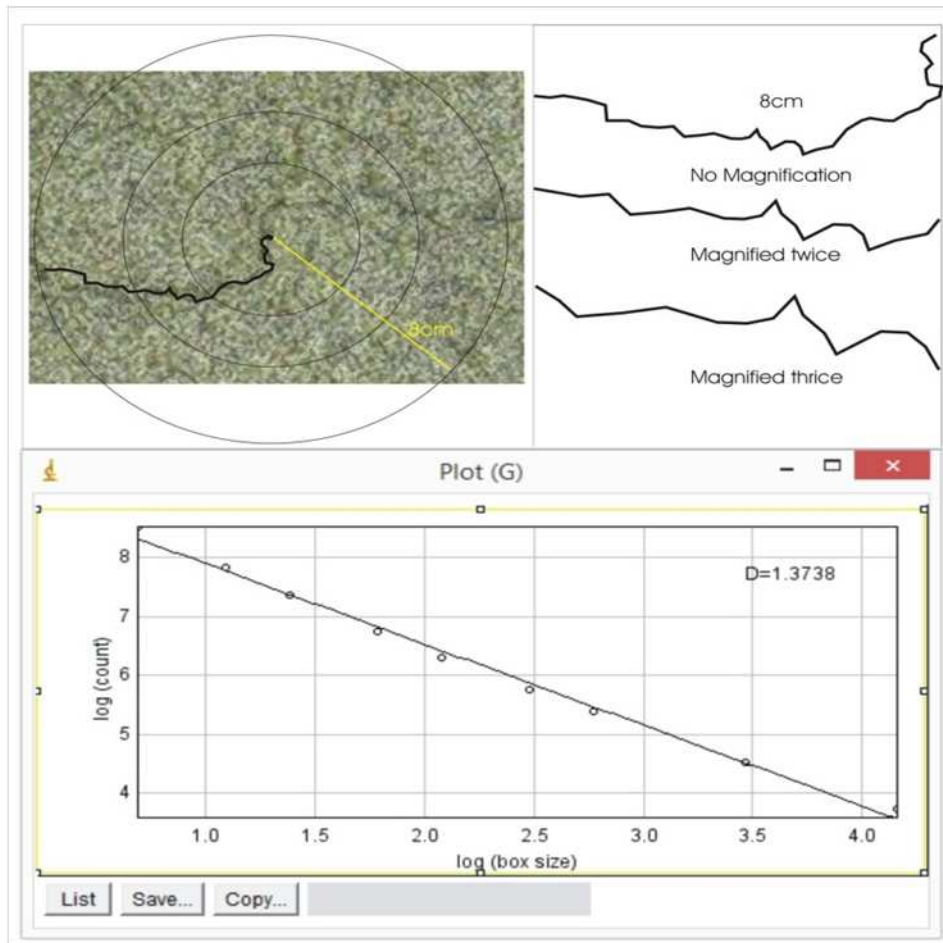


Figure 2: Scale of trail pattern
 Photo source: Chakraborty 2020, Personal communication

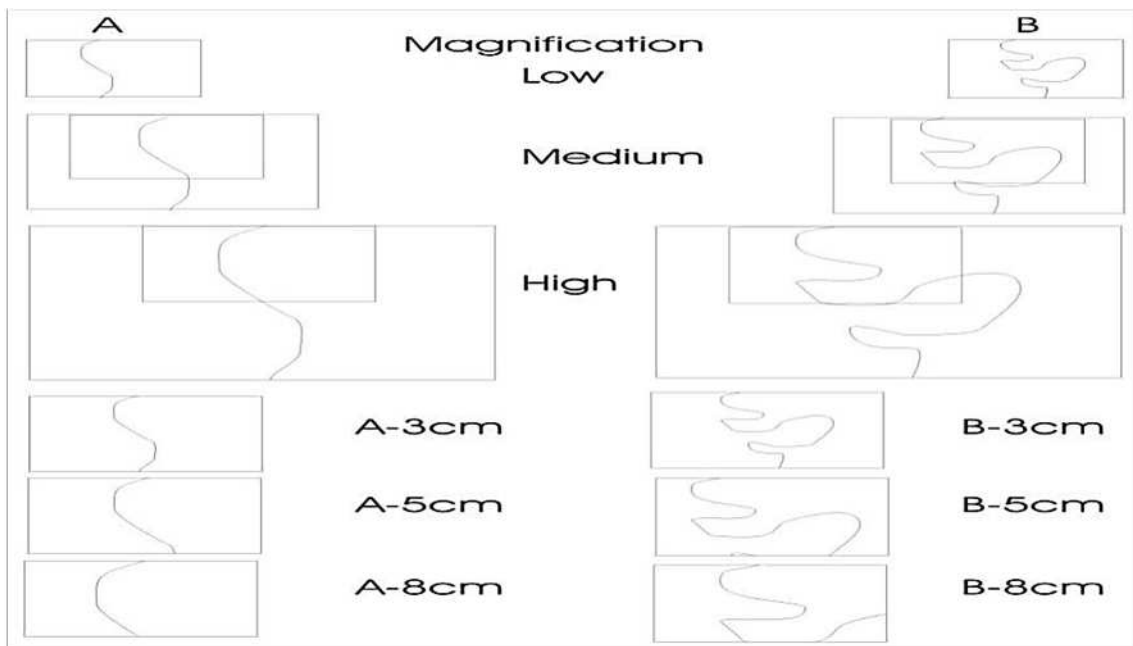


Figure 3: image of magnified trail pattern
 Photo source: Chakraborty 2020, Personal communication

Acknowledgement

We would like to express our sincere gratitude to our mentor Abhijit Chakraborty, Department of Geology, Jogamaya Devi College, for providing guidance and support for writing this article.

References

- Dicke, M., Burrough, P. A., 1988. Using fractal dimensions for characterizing tortuosity of animal trails. *Physiological Entomology*. 13, 393-398
- Erlandsson, J., Kostylev, V., 1995. Trail following, speed and fractal dimension of movement in a marine prosobranch, *Littorina littorea*, during a mating and a non-mating season. *Marine Biology*, 122, 87-94.
- Fan, R.Y., Gong, Y-M., Uchnman, A., 2018. Topological analysis of graphoglyptid trace fossils, a study of macrobenthic solitary and collective animal behaviors in the deep-sea environment. *Paleobiology*: 1-20. DOI: 10.1017/pab.2018.1
- Häntzschel, W. 1975. Trace fossils and problematica. In: Teichert, C. (ed.), *Treatise on Invertebrate Paleontology, Part. W. Miscellanea, Supplement 1*, Geological Society of America and University of Kansas Press. W269p.
- Knaust, D., Bromley, R. 2012. Trace fossils as indicator of Sedimentary Environments, Volume 64, 1st edition.
- Richard G. Bromley, 1996, Trace fossil: Biology, Taphonomy and its Application, Geological Institute, University of Denmark
- Seilacher, A., 2007. Trace Fossil Analysis. 226p. Springer Berlin Heidelberg New York Publ. ISBN-13 978-3-540-47225-4.
- Seuront, L., 2010. Fractals and Multifractals in Ecology and Aquatic Science. 344p. CRC Press, Taylor & Francis Group. ISBN 978-0-8493-2782-7.

Earthquake and Its Prediction

Aditi Das¹, Ipsita Mondal², Sarmistha Das³ and Nandita Misra⁴

Students of 2nd Semester Geology Honours Course

¹aditidas7679@gmail.com, ²ipsitamondal22295@gmail.com

³sarmipriyanka@gmail.com, ³nanditamisra2019@gmail.com

1. Introduction

An earthquake is a trembling or shaking of the ground caused by the sudden release of energy stored in the rocks beneath the earth's surface.

The strain built up over years of slow deformation by tectonic forces is released in a few minutes as seismic waves when the fault breaks due to an earthquake. The two blocks of rock on both sides of the fault slip suddenly, setting off the ground on vibration (Figure 1)



Figure 1: Building across Kathmandu, the capital of Nepal, collapsed in the devastating earthquake, 2015.^[1]

2. Anatomy of Earthquake

The Elastic Rebound Theory gives a detailed explanation for how energy is released during earthquakes. As tectonic plates on opposite sides of fault are subjected to force and shift, they accumulate energy and slowly deform until their internal energy is exceeded. At that time, a sudden movement occurs along the fault releasing the accumulated energy.

The point below the fault plane from which the tremendous accumulated energy is released, is called the focus or hypocentre of the earthquake (Figure 2)

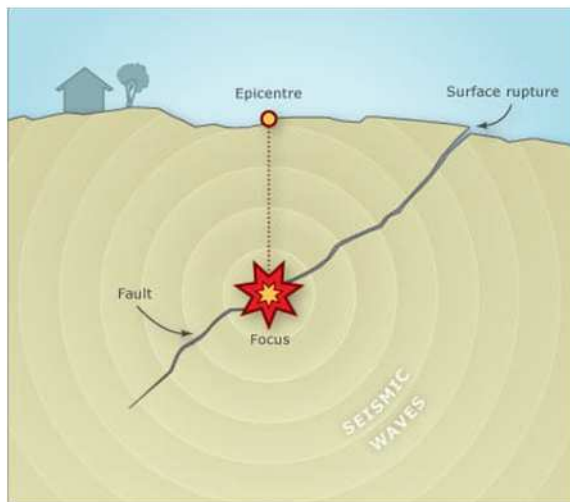


Figure 2. Focus and epicentre of earthquake.^[2]

3. Relation between Earthquake and plate boundaries

Tectonic plates are large rigid slabs of rock, which moves across earth's surface. These tectonic plates contain continents and sea-floors on its upper surface. The concept of plate tectonics is that continents and the sea-floors are in motion.

Earthquakes mostly occur in the plate boundaries- the regions of the earth's crust or upper mantle where stresses are concentrated and straining of the crust is intense. According to plate tectonics, earthquakes are caused by the interaction of plates along plate boundaries.

There are three types:

Earthquakes at divergent boundaries

At divergent plate boundaries, two tectonic plates move away from each other. This makes molten rocks to gush out from the mantle and erupt along the opening. Cooling of molten materials gives rise to a new crust and the former crust is pushed apart. This results in cracking of crust and formation of faults where earthquakes generate. Generally, earthquakes due to divergent boundaries occur at mid-oceanic ridges (MOR). Shallow focus earthquakes are generally found in these regions.

Earthquakes at convergent boundaries

At convergent plate boundaries, two tectonic plates move towards each other and collide. There are two kinds of convergent boundaries.

Subduction boundary

When a continental plate meets with an oceanic plate, oceanic plate being more dense sinks beneath the less dense and thick continental plate. This phenomenon is called subduction. About 80% of earthquakes occur when rocks are pulled down under continental plates, they begin to melt and molten lava rises to the surface.

Collision boundary

When two continental plates meet head-on, neither plate being stronger than another, they crumple and get pushed up, which causes release of energy in the form of earthquakes.

Earthquakes at transform boundaries

Along the transform boundary, two tectonic plates slide past each other and thus there is a strike-slip fault. This happens when the frictional resistance in the fault system overcomes and the plates suddenly move causing shallow focus earthquakes (Figure 3).

(Hyndman & Hyndman)

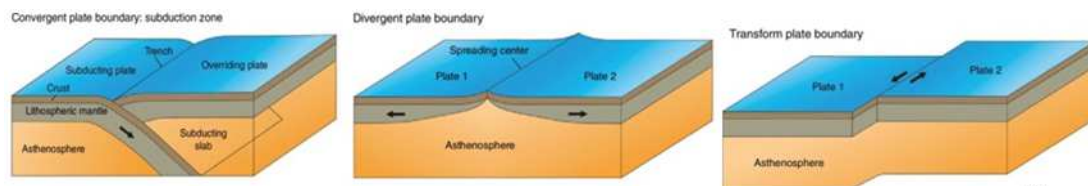


Figure 3: Convergent, Divergent and Transform plate boundaries are related to earthquake.^[3]

4. Predictions of Earthquake

Earthquake prediction gives information of future earthquakes with its time, location and magnitude in order to warn the population. Therefore, scientists look over various prediction methods to reduce seismic hazards as much as possible. (Hyndman & Hyndman 2011).

Table 1: Different prediction methods of earthquake.

Name	Principle behind it	Success rate
1. Long term prediction methods:		
1.1 Historical Earthquake Records (Paleoseismology)	(a) Study of prehistoric earthquakes, their location, timing and size (Hyndman & Hyndman 2011).	From 1910-1940, studies of two large earthquakes in Nevada, Pleasant Valley 1915 and Cedar Mountain, 1932.
1.2 Slip-rate on Active Fault	(a) Fault’s behaviour, its length and connectivity provide the magnitude, intensity, range and frequency of earthquakes.	.
1.3 Seismic Gaps	(a) Active fault areas which are prone to produce earthquakes but have not produced yet, such areas are called seismic gaps. (b) Length of seismic gap provides maximum possible length of future quake.	<i>The Loma Prieta</i> earthquake, 1989 filled a seismic gap in the San Andreas fault (Figure 3A). (Hyndman & Hyndman 2011)
1.4 Seismic Hazard Maps	(a) Seismic hazard map identifies relative hazards in different areas.	First seismic zoning map for Indian subcontinent was compiled by the Geological Survey of India in 1935, delineating Indian subcontinent into different zones to serve moderate and slight damage (Figure 4).
1.5 Theory of Surface Latent Heat Flux	(a) The SLHF data collected from the satellite to epicentre of three coastal	SLHF method depends on atmospheric changes.

(SLHF) earthquakes (Figure3B).

2. Short term prediction methods:

2.1	Seismic-wave Velocity	(a) There are two types of seismic waves: primary wave and secondary wave. They travel at different velocities, p-wave velocity (V_p) depends on density and compressibility whereas s-wave velocity (V_s) depends on density and rigidity. (b) V_p/V_s ratio dropped for a period of time and length of period increased with magnitude of impending earthquake. Magnitude increases to normal value just before the earthquake occurred.	Observations of s-wave splitting have been used to predict earthquakes in Iceland, with reported success for a single M5 event.
2.2	Ground Deformation	(a) Changes in land elevation due to the swelling of rocks because of strain building on faults which may lead to small earthquakes (Keller & DeVecchio 2012)	Observed in every earthquake. Can be a minute or hour analysis prior to an earthquake.
2.3	Foreshocks	Almost all earthquakes are preceded by minor shocks called foreshocks, which provide clues for an inevitable earthquake.	Prior to the 1975 earthquake in China.
2.4	Changes in Humidity and Groundwater Level	(a) Can be detected via humidity measurements in soil and temperature difference in fault area.	Water level rose by 3 cm a few hours prior to the earthquake in Meckering, Australia, 1968.
2.5	Hydrochemical Changes	(a) Abrupt change in chemical composition of underground water.	Observed before the Kobe earthquake, 1995.
2.6	Changes in Temperature	Considerable rise in temperature and fall in pressure observed in earthquakes preparation area before the earthquake.	Observed in Lunglin, China (1976) and Prezhevalsk, Russia (1970) with considerable rise in temperature by 283.15K-288.15K.
2.7	Oil Wells	(a) Fluctuations of oil flow from oil wells are observed prior to earthquakes. (b) Tectonic stress accumulates. (c) Pore pressure within a deep oil bearing strata reach its breaking strength causing oil to sprout out along oil wells.	Reported in Israel, Northern Caucas (Europe) and China occurring in 1969, 1971 and 1972 respectively.
2.8	Changes in animal behaviour	(a) Dogs barking, cats jumping, rats running out before earthquakes by detecting the arrival of p-wave (Kirschvnik 2000).	Oarfish appeared on the coast prior to Japan's earthquake and tsunami, 2011 (Figure 3E).

3. Recent techniques:

3.1	Electromagnetic anomalies	(a) Predicting earthquakes by magnetic sensor. (b) Magnetic field generated by the electro-kinetic (EK) effect (Figure 3D) (Cheng 2016).	Such anomalies were observed before the Wenchuan earthquake, May 12, 2008.
3.2	Radon Gas Monitoring	(a) Radon emission is monitored as a potential earthquake precursor. (b) Short-term increase in radon	Observed in the groundwater of Tashkent, Uzbekistan, 1966 for the first time.

concentration of groundwater (Figure 3C)
(Chen et al. 2011).

3.3 Van Technique

Consists of recorded telluric currents using a wide network of stations covering a particular region (Cheng 2016).

Observed during the extensive 1966 earthquake swarm in *Matsushiro*, Japan. (Derr 1973, 1986).

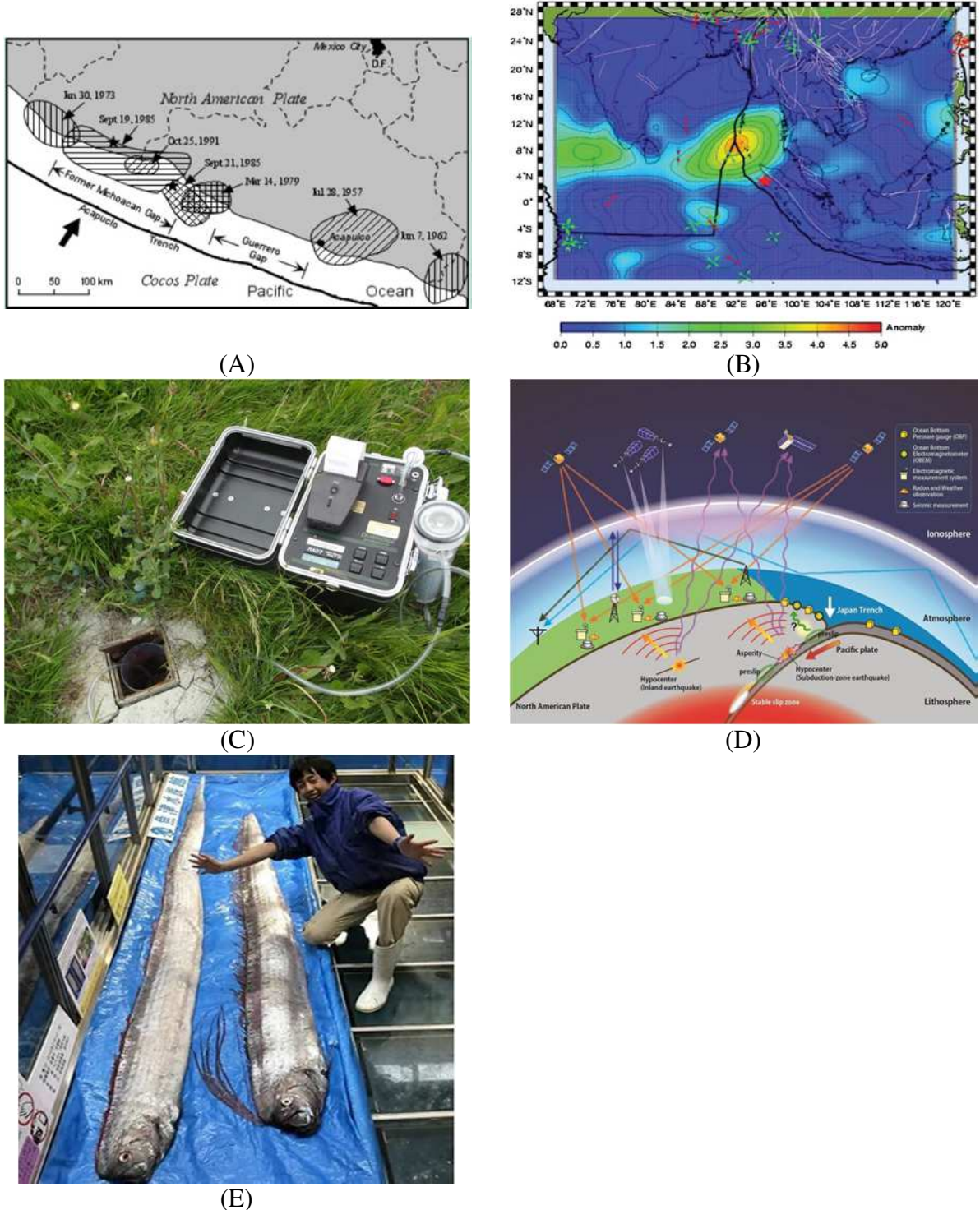


Figure 4: Different methods for predicting earthquakes

(A) The San Francisco, Loma Prieta, and Parkfield Seismic Gaps in the west coast of USA (Anderson et al. 1986)

- (B) Surface latent heat flux anomalies for Sumatra earthquake, M=9.0, 26 December 2004, Indonesia.^[4]
- (C) Radon gas monitoring process.^[5]
- (D) Conceptual diagram of an integrated satellite and terrestrial framework for multi-parameter Observation of pre-earthquake signals in Japan. The ground component includes electromagnetic observation, radon weather, ocean bottom electro-magnetic sensors, seismic measurement.^[6]
- (E) Japanese folklore got these oarfish when they move to shallower seas before under water earthquakes, possibly due to electromagnetic changes that occur with tectonic activity. (Source: ndtv.com)

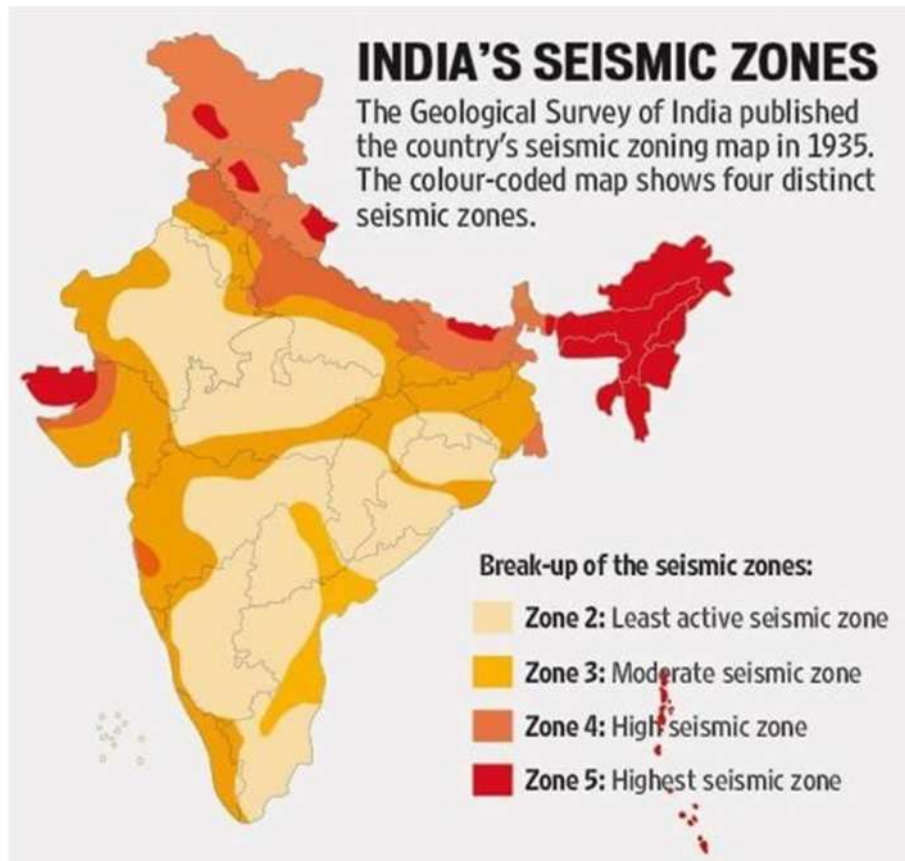


Figure 5: Seismic hazard map of India published by geological survey of India (GSI) in 1935 (Source: PTI)

5. Seismic hazard areas of India

The Bengal basin is formed by Ganga-Brahmaputra River System and is one of the world's largest delta. The dynamic nature of Bengal basin can be attributed to the interaction of mainly three plates namely Indian, Tibetan and Burma plates (Nath et al. 2014). The intensity and pattern of plate to plate interaction varied with time and affects the basin architecture and sedimentation style. The Bengal basin is slowly tilting towards the east because of neo-tectonic movement forcing greater freshwater input to Sunderbans.

Thus due to major plate tectonic phenomena severe violent earthquakes occur in this delta region and this causes rise of sea water for a considerable period.

6. Conclusion

Earthquake prediction has been a challenging research for the geologists and is the ultimate goal for seismology but forecasting earthquakes is an exigent task for the scientists. It is undeniable that the seismologists have been unsuccessful in developing methods to predict ensuing earthquakes due to lack of technology in accurately monitoring the changes in pressure and temperature beneath the crust.

Acknowledgement

We are very much thankful to Kaushik Kiran Ghosh for encouraging us to pursue with this this topic.

References

- Anderson, J. G., 1986. Implication of Attenuation for Studies of the Earthquake Source, in Das, S., Boatwright, J., Scholz, C. H. (Ed). Earthquake Source Mechanics, Volume 37, Geophysical Monograph Series, Advancing Earth and Space Science (AGU).
- Ansell R., Taber J., 1996 Caught in the crunch, Auckland: Harper Collins, 45, Te Ara- The Encyclopedia of New Zealand (Last visited on 10.06.20)
- Chen, Yun-Tai., Paolo, G., Madariaga, R., Main, I., Marzoechi, W., Papadopoulos, G., Sobolev, G., Yamaoka, K., Zschau, J., 2011. Operational Earthquake Forecasting. Annals of Geophysics, 54, 4
- Cheng, Kuei-hsiang., 2016. Earthquake Prediction. Transactions on Science and Technology, Vol.3 No.3, 507-516
- Chen, Yun-Tai., Paolo, G., Madariaga, R., Main, I., Marzoechi, W., Papadopoulos, G., Sobolev, G., Yamaoka, K., Zschau, J., 2011. Operational Earthquake Forecasting. Annals of Geophysics, 54, 4.
- Hyndman, D., Hyndman, D., 2011. Natural Hazards and Disasters, Third Edition. Yolanda Cassio
- Keller, E. A., DeVecchio, D. E., 2012. Natural Hazards, Third Edition. Pearson Education
- Kirschvnik, J. L., 2000. Earthquake Prediction by Animals: Evolution and Sensory Perception. Bulletin of the Seismological Society of America, 90, 2, 312-323
- Kulkarni, R., Kulkarni, R., 2017. Earthquake Prediction Using Data Mining. International Journal of Science and Research. Vol.6:11, 487-491
- Nath, S.K., S. K., Adhikari, M. D., Maiti, S. K., Devaraj, N., Srivastava, N., Mohapatra, L. D. 2014. Earthquake scenario in West Bengal with emphasis on seismic hazard microzonation of the city of Kolkata, India. Nat. Hazards Earth Syst. Sci., 14, 2549–2575.
- Skelton, A., Classen, L., Wasteby, N., Andren, M., 2012. The dilatancy-diffusion hypothesis and earthquake predictability. Geological Society of London. 367, 215-23

Turcotte, D. L., 1991. Earthquake Prediction. *Annu. Rev. Earth Planet. Sci.* 263-281

Weblinks

- [1] https://assets.climatecentral.org/images/made/5_21_15_Brian_NepalQuake_720_480_s_c1_c_c.jpg
- [2] <https://teara.govt.nz/files/di-4399-enz.jpg>
- [3] https://www.researchgate.net/profile/Joao_Duarte9/publication/305782020/figure/fig1/AS:508759652790272@1498309161471/Schematic-representation-of-the-three-types-of-plate-boundaries-convergent-top_W640.jpg
- [4] https://www.researchgate.net/figure/Surface-latent-heat-flux-anomalies-for-the-Sumatra-earthquake-M-90-26-December-2004_fig18_41163234
- [5] <https://www.ggs-uk.com/ground-gas-services/radon-services/>
- [6] <https://www.yourarticlelibrary.com/wp-content/uploads/2013/12/1171.jpg>

Fidelity of Terrestrial Heat Flow Data

Anwasha Ghosh¹, Srila Bhowmik² and Sneha Chakraborty³

Students of 2nd Semester Geology Honours Course

¹*anwasha2001g@gmail.com*, ²*srilabhowmik@gmail.com*, ³*chakrabortysneha14@gmail.com*

1. Preamble

Terrestrial Heat flow (HF) is the outward transfer of thermal energy from the interior of the earth. Heat sources include residual or mantle heat, radiogenic heat, shearing induced heat and plume heating. HF measured for unit cross sectional area per unit time is negligible except in certain areas of abnormally high surface HF anomalies. However, the total energy released across the terrestrial surface is order higher in magnitude compared to energy released through volcanism and earthquakes. Heat transfer is achieved by lattice conduction in solid crust and through layer confined convection involving asthenosphere and upper mantle (see Richter & McKenzie 1981). Radiation plays an order higher effective and faster mode of heat transfer at a depth window between 150-600km below surface (Wyllie 1971, Philpotts & Ague 2009). Explanation on surface HF anomalies is still a matter of debate. All heat sources taken together cannot explain HF anomalies in most of the tectonic sites and in mid-continental areas. Lateral variation in the sub-crustal thermal structure is noted from the presence of several low velocity zones (Dziewonski et al. 1975, Haenel et al. 1988). Besides, the heat transfer through solid crust is also influenced by several other factors that include the rheology and heat conductivity of the earth layers; plate thickness and nearness of a data point to the mantle heat source, conc. of radioactive elements in the crust; proximity to a cooling pluton, presence/absence of a plume as an additional heat source etc (Bott 1982). Beyond these uncertainties pivoting around the relative contribution of heat sources, thermal assays on terrestrial HF distribution is intrinsically troubled with the lack of consensus on HF data presentation. A dramatic increase in the number of available terrestrial HF data has changed our concept over terrestrial HF anomalies. This includes the ever increasing identification of abnormally high heat flow areas (popularly known as hotspots) over the years. Morgan (1972) listed 19 hot spots while Crough and Jurdy (1980) mention 42 such hotspots. Subsequently Wilson (1973) and Vogt (1981) listed 66 and 117 hotspots. Distribution of these hotspots over the surface of globe appears to be unbiased. These are reported from different tectonic sites and even from mid-plate areas. Mid-plate high HF values were causally related to plumes (a mantle heat source). No discrete characterization is, however, available for these plumes as regards their origin. High HF around diverging plate boundaries are better explained as these are directly correlated with crustal thinning. HF profiles along the subduction zones, however, depict differences for younger and older subduction zones. As a whole, the definition of HF anomaly is still in the state of flux. Here we delve into the root of major differences over the predictions on HF averages suggested for global as well as terrestrial and marine realms in last few decades (Lee & McDonald 1963, Lee & Uyeda 1965, Pollack 1993, Davies 2013) based on published data.

2. Methodology

Plots of HF data averaged at varied grid scales ($5^{\circ}\times 5^{\circ}$, $1^{\circ}\times 1^{\circ}$ and $30'\times 30'$) have been compared to reveal the area-wise data coverage and HF anomalies on a global scale. Corrections have been made for age, rock types, depth and other local factors (viz. presence of plutons, hydrothermal seepages, geysers etc.) to reduce noise in HF data that reflects regional residual heat coming from deep interior of the earth. HF values are given in SI unit (mWm^{-2}).

3. Observation

Terrestrial HF data as plotted on the global surface (as $5^{\circ}\times 5^{\circ}$ grid averaged data) reveals large areas ($\sim 37\%$) for which no HF data is available (Figure 1a). Null grid points further increases as much as 85% (Figure 1b) and 94% (Figure 1c) when HF data is averaged at $1^{\circ}\times 1^{\circ}$ and $30'\times 30'$ grid sizes respectively (Table 1).

4. Discussion and Conclusion

Discrete determination of global HF average is the precondition for identifying HF anomalies. However, with the addition of new HF data, the global HF averages are observed to reveal dramatic changes (see Table 1). Accordingly, HF anomalies are redefined over the surface of globe. So HF anomalies are basically, sort of arbitration. Our present investigation of HF values as averaged and plotted in different grid maps reveal that HF peaks (anomalies) appear in different places on globe, even using the same set of HF data (see Figures 1a-c). This triviality in data presentation may often lead to ambiguous and non-comparable thermal modelling and subsequent interpretations based on varied distribution of heat peaks and lows spread over the surface of globe. HF anomalies in global scale or in oceanic and continental areas have been variously correlated with the inhomogeneity of subcrustal low velocity zones (Pollack et al., 1993), rock types (Davies 2013), higher conc. of radioactive elements in continental crust (Wyllie 1971). Earth's surface heat flux is a fundamental out-put of the dynamic solid Earth's heat engine. Therefore, a better understanding of Earth's surface heat flux helps us to constrain the modelling of internal state of the mantle, its evolution and geochemistry (Davies, 1989, Dye 2012, Korenaga 2008, Loydet al. 2007, McDonough and Sun 1995, Schubert et al. 1980); thermal structure of the crust and mantle (Furlong et al. 1995) and hence to lithospheric rheology, which is sensitive to temperature (Houseman et al. 1981, Ranalli 1987, Bird et al. 2008).

With the new addition of plethora HF data, we are now in a better position to judge the situation. In a recent work, Davies (2013) demonstrated that $2^{\circ}\times 2^{\circ}$ grid averaged HF plots can represent $\sim 40\%$ global surface with at least one HF data for each grid (Table 1). Subsequent plots of 67, 801 HF data (Chakraborty et al. 2020; pers comm.) in $5^{\circ}\times 5^{\circ}$ grid averaged map covers 63% global areas. Interestingly, HF data averaged at $1^{\circ}\times 1^{\circ}$ grid is same (i.e., 15%) as worked out by Davies (2013). This perhaps indicates a stable scenario of HF

anomalies at least when averaged for $1^\circ \times 1^\circ$ grids with sufficient HF data. Perhaps more HF data is required to resolve HF anomalies at lower grid sizes. Fidelity of HF data is thus largely dependent on proper grid averaging that might help to detect different dimensions of events and sources responsible for HF anomalies. It may be concluded at present that terrestrial HF anomalies has strong grid dependence. Any thermal modelling on terrestrial HF must consider averaging of HF data at proper grid size. Otherwise, it may generate pseudo-anomalies that are the artifacts of gridding or else, it may fail to recognize true HF anomalies due to improper averaging with juxtaposed high low HF areas.

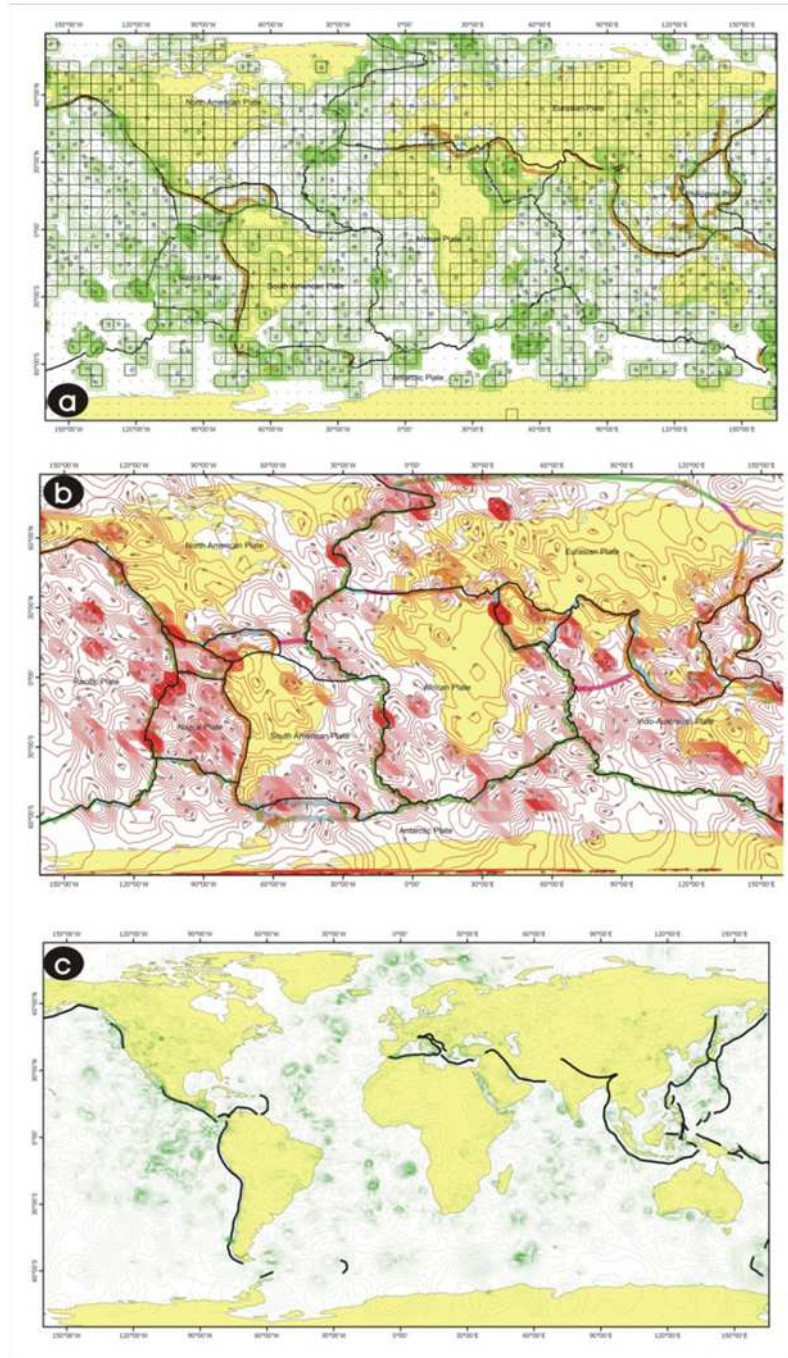


Figure 1: Global HF distribution (of 67,801 HF data) averaged at (a) $5^\circ \times 5^\circ$ grids, (b) $1^\circ \times 1^\circ$ and (c) $30' \times 30'$ grids (Source:Chakraborty et al. 2020; pers. comm.). Note the varied pattern of heat peaks when averaged at different grid sizes.

Global HF Avg	Continental HF Avg	Oceanic HF Avg	Grid Size	Area Coverage (%)	Reference	Data Points
64	67	62			Lee & McDonald 1963	757
62.7	-	-	5°x5°	-	Lee & Uyeda 1965	1150
87	65	101	5°x5°	65	Pollack 1993	22420
61	-	-	Random		IHFC 1993	58536
83	64.7	95.9	2°x2°	40	Davies 2013	38734
60	44.5	66.6	5°x5°	63	Chakraborty et al. 2020 (Pers. Comm.)	67801
58.69028	43.1	69.4	1 ° x 1 °	15		
58.97364	46.4	71.3	30 Min x 1Deg	6		
59.65211	49.8	72.8	15 Min x 15 Min	2		

Table1. Heat Flow (in mWm^{-2}) average estimated by different workers

Acknowledgement

We would like to express our thanks and gratitude to Abhijit Chakraborty, Department of Geology, Jogamaya Devi College for his constant support and guidance in completing the article.

Reference

- Bird, P., Liu Z., Rucker W. K., 2008. Stresses that drive the plates from below: Definitions, computational path, model optimization, and error analysis, *J. Geophys. Res.*, 113, B11406, doi:10. 11029/12007JB005460.
- Bott, M. H. P., 1982. *The Interior of the Earth: Its Structure, Constitution and Evolution*. 2nd edition.
- Davies, G. F. 1989. Mantle convection model with a dynamic plate: Topography, heat flow and gravity anomalies, *Geophys. J. Int.*, 98, 461–464.
- Dye, S. T. 2012. Geoneutrinos and the radioactive power of the Earth, *Rev. Geophys.*, 50, RG3007, doi:10. 1029/2012RG000400.
- Dziewonski, A. M., Hales, A. L., Lapwood, E. R.: 1975. 'Parametrically Simple Earth Models Consistent with Geophysical Data', *Phys. Earth Planet. Interiors* 10, 12-48.
- Furlong, K. P., Spakman, W., Wortel, R. 1995. Thermal structure of the continental lithosphere—Constraints from seismic tomography, *Tectonophysics*, 224, 107–117.
- Haenel, R., Rybach, L., Stegena, L., (eds) 1988. *Handbook of Terrestrial Heat –Flow Density Determination*. Kluwer Academic Publishers, Holland. 486p. DOI: 10. 1007/978-94-009-2847-3.
- Houseman, G. A., McKenzie D. P., Molnar P. 1981. Convective instability of a thickened

boundary layer and its relevance for the thermal evolution of continental convergent belts, *J. Geophys. Res.*, 86, 6115–6132.

Korenaga, J., 2008. Urey ratio and the structure and evolution of Earth's mantle, *Rev. Geophys.*, 46, RG2007, doi:10.1029/2007RG000241.

Lee, W, H, K. (ed.), 1965. *Terrestrial Heat Flow*, Geophys, Monogr. 8, Amer. Geophys. Un., Washington D. C., 276 p.

Lee, W. H. K., Uyeda S., 1965. 'Review of Heat Flow Data', in Lee, W. H. K. (ed.) *Terrestrial Heat Flow*, Geophys. Monogr. 8, Amer. Geophys. Un., Washington D. C., 27-190.

Lloyd, S. J., Becker, T. W, Conrad C. P., C. Lithgow-Bertelloni, Corsetti, F. A., 2007. Time variability in Cenozoic reconstructions of mantle heat flow: Plate tectonic cycles and implications for Earth's thermal evolution, *Proc. Natl. Acad. Sci. U. S. A.*, 104, 14, 266–14, 271.

McDonough, W., Sun, S., 1995. The composition of the Earth, *Chem. Geol.*, 120, 223–253.

McKenzie, D. P., 1967. 'Some Remarks on Heat Flow and Gravity Anomalies', 1. *Geophys. Res.* 72, 6261-6273.

Philpotts, A. R. and Ague, J. J., 2009. *Principles of Igneous and Metamorphic Petrology*. Second Edition, Cambridge University Press, 667p.

Pollack, H. N., Hurter, S. J., Johnson, J. R., 1993. Heat Flow from the Earth's Interior: Analysis of the Global Data Set. *Reviews of Geophysics*, 31 (3): 267-280.

Ranalli, G. 1987, *Rheology of the Earth*, Allen and Unwin, Boston, Mass.

Richter, F. M., McKenzie, D. P., 1981. On some consequences and possible causes of layered mantle convection. *86(7): 6133-6142*. doi.org/10.1029/JB086iB07p06133

Schubert, G., Stevenson D., and Cassen, P. 1980, Whole planet cooling and the radiogenic heat source contents of the Earth and Moon, *J. Geophys. Res.*, 85, 2531–2538.

Wyllie, P. J., 1971. *The Dynamic Earth: Text book in Geosciences*. John Wiley & Sons Inc. 416p.

Volcano: Its Different Landforms

Ishika Chatterjee¹, Kankana Paul² and Sampriti Dey³

Students of 2nd Semester Geology Honours Course

¹ishika.bkp@gmail.com, ²kankanap083@gmail.com, ³cutesampriti52@gmail.com

1. Introduction

Volcanoes are very important part of earth system. Volcano is a conical hill or mountain, built up around an opening or rupture in the Earth crust through which lava, hot gases, ashes and rock fragments are ejected. Volcanoes are of great importance as it played a key role in forming and modifying our planet. More than 80 % of Earth surface below and above the sea level is made up of volcanic rock. Volcanic eruption is going on at any time somewhere on Earth. (Figure 1)



Figure 1: Volcanic Eruptions.^[1]

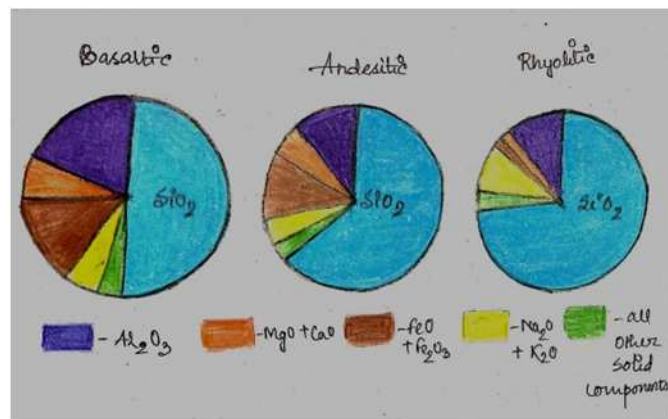


Figure 2: Pie charts on Basaltic-Andesitic-Rhyolitic magma composition.^[2]

2. Magma composition and types with their characteristics

Magma is a mixture of molten or semi-molten rock, volatiles, suspended crystals and dissolved gases.

There are three basic types of magma: basaltic, andesitic, and rhyolitic, each of which has a different mineral composition. All types of magma have a significant percentage of silicon dioxide. Basic or basaltic magma is low in silica (45%-55%) and high in iron, magnesium, and calcium but low in potassium and sodium. Intermediate or andesitic magma has intermediate silica content (55%-65%) and moderate amounts of these minerals. Acidic or rhyolitic magma is high in silica (65%-75%) and high in potassium and sodium but low in iron, magnesium and calcium.

Characteristics of different types of magma have been shown in Figure 2 and Table 1.

Change of viscosity of magmas with temperature is shown in Figure 3

Volcanic Rock type	Basalt	Andesitic	Rhyolitic
Rock Description	Black to dark grey	Medium to dark grey	Light coloured
Volume on earth surface	80%	10%	10%
Silica content	45-55%	55-65%	65-75%
Temperature	1000°C- 2000°C	800°C- 1000°C	600°C- 900°C
Viscosity	Low	Intermediate	High
Gas escape from magma	Easy	Intermediate	Difficult
Eruption style	Peaceful	Intermediate	Explosive

Table 1: Types of magma and characteristics.^[3]

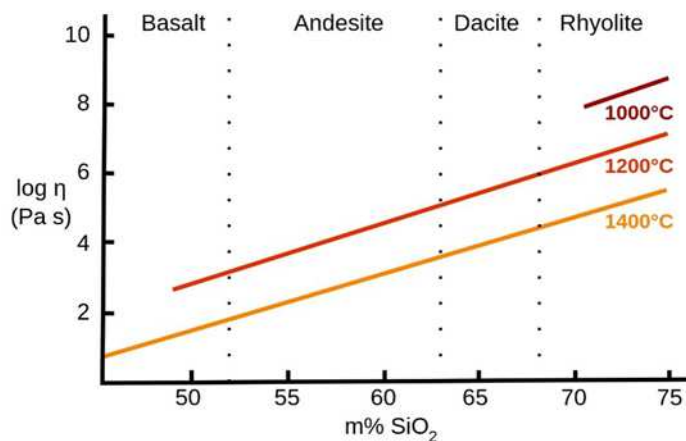


Figure 3: Graphical representation of viscosity change silica content and temperature of magma.^[4]



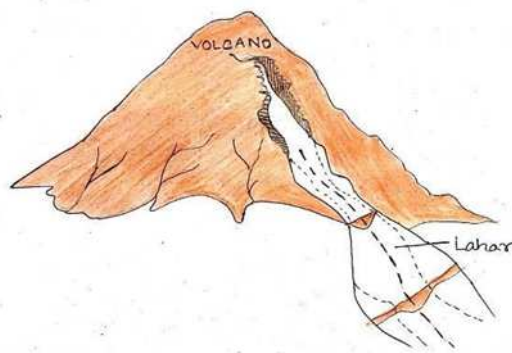
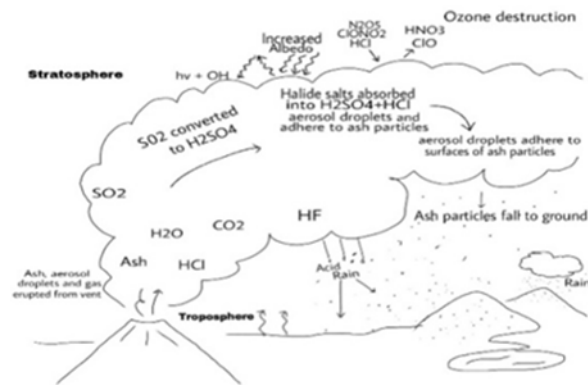
Figure 4: Tephra materials: Bombs, Blocks, Pumice

3. Eruption products

- **Lava:** Lava is the hot liquid rock that pours from an erupting volcano. When magma reaches the surface, it becomes lava.^[5]
- **Tephra:** Tephra is an unconsolidated pyroclastic material produced by volcanic eruption (Table 3).
- **Blocks:** Angular fragments that were solid when ejected (Figure 4).
- **Bombs:** Having an aerodynamic shape indicating they were liquid when ejected (Figure 4).
- **Pumice:** Bombs and lapilli consisting mostly of gas bubbles (vesicles) result in a low density highly vesicular rock fragments called Pumice (Figure 4).^[6]
- **Lava flows:** Lava flows are streams of molten rock that pour or ooze from an erupting vent.
- **Lahars:** Hot mudflows formed when water mixes with hot pyroclastic debris. (Figure 5)
- **Volcanic gases:** Gases erupting from volcanoes. (Figure 6)

Average Particle Size (mm)	Unconsolidated Material (Tephra)	Pyroclastic Rock
> 64 mm	Bombs or Blocks	Agglomerate
2 – 64 mm	Lapilli	Lapilli Tuff
< 2mm	Ash	Ash Tuff

Table 3: Tephra and Pyroclastic rocks.^[6]

Figure 5: Lahar.^[7]Figure 6: Eruption of Volcanic Gases^[8]

4. Types of lava

- *Pa-hoe-hoe Lava*: Fluid basaltic lava having ropy or corrugated appearance. The corrugations are usually less than 2cm high, with axes perpendicular to or convex to the flow direction.
- *A'a' Lava*: A rubbly flow, with a molten core, with higher viscosity (but same composition) which, therefore, tends to move more slowly and produce thicker flows (typically 3-20 m).
- *Pillow Lava*: Pillow lavas are lavas that contain characteristic pillow-shaped structures that are attributed to the extrusion of the lava under water, or subaqueous extrusion.
- *Blocky Lava*: Blocky flows are common if the silica content of lavas is higher. Blocky Lava resembles

A'a'-Lava but have much larger chunks than the latter. Blocky flows grow higher as they advance and may reach more than 100 meters in height. Refer to Figure 7

5. Volcanic Landforms

Volcanic Landforms (Figure 8) are the product of geological processes operated on them before and after their formation. These landforms are the characteristic of the type of materials these are made of these landforms can be modified by later processes. The major volcanic Landforms are discussed before with their characteristics.

Shield Volcano (Figure 9)

- Upper slope(5°), lower slope(10°) [Broad shield like]
- Lava thin, non-viscous.
- Mafic (Fe, Mg rich), low silica content lava (basalt)
- Usually quiet eruptions.
- Very little pyroclastic materials
- E. g. The Hawaiian volcanic chain
- Basaltic lava also erupts along mid-oceanic ridges, seafloor spreading, many volcanic islands along mid-Atlantic Ridge



Figure 7: Different types of Lavas.^[9]

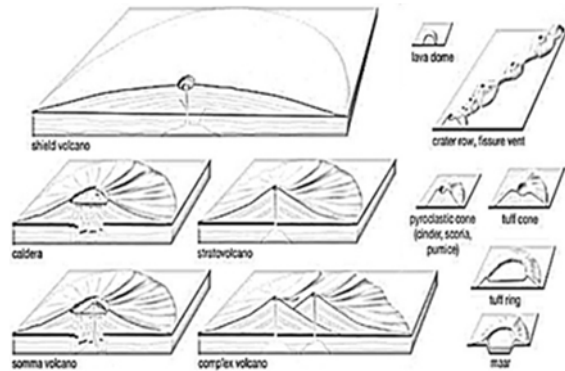


Figure 8: Three dimensional view of the Volcanic Landforms.^[10]

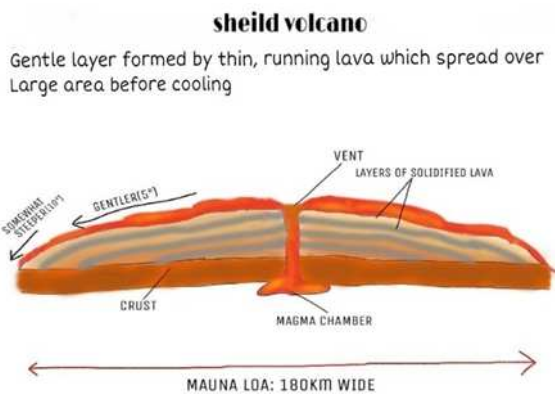


Figure 9: Shield Volcano

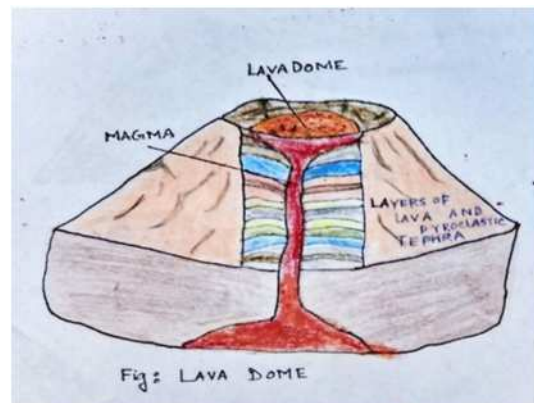


Figure 10: Lava Dome.^[11]

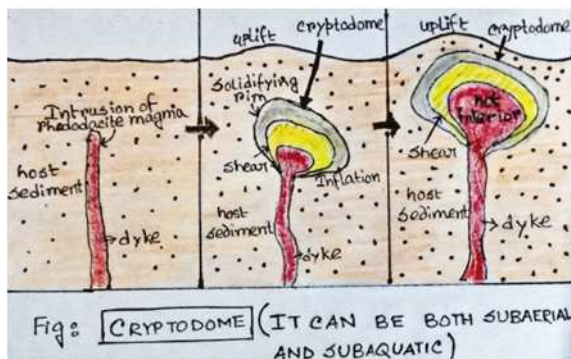


Figure 11: Cryptodome.^[12]

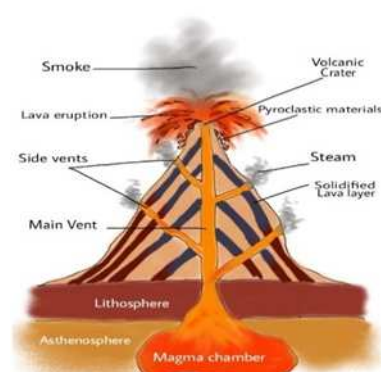


Figure 12: Stratovolcano

Lava Domes and Cryptodomes:

- Lava domes form when largely degassed viscous silicic magma such as dacite or rhyolite (less commonly andesite) erupt effusively and more slowly onto the surface and then piling up around the vent (Figure 10).
- A cryptodome literally means “hidden dome” and refers to a lava dome which is hidden within the structure of the volcano^[13] (Figure 11).

Stratovolcano (Figure 12)

- Volcano constructed of multiple layers of lava and tephra
- Low slopes on the flanks (6°-10°), about 30° near the top
- High Viscous magma

- Lavas and pyroclasts (50%) are usually andesitic to rhyolitic in composition
- Long period of repose.
- More explosive
- E. g. Mount Fuji (Japan).

Cinder Cones (Figure 13)

- Eruption of small pieces of scoria and pyroclastic
- Cone shaped hills ~ 30-400m height
- Erupts only once
- Basaltic
- Asymmetric; e.g. Sunset crater in Arizona. (Figure 14)

Craters and Calderas

- A crater is a circular depression develops at the top of the volcanic cone (formed by the solid products of eruption, accumulate around a conduit) either during eruption as materials accumulate around the summit vent or just after eruption as summit collapses into the drained conduit ^[14] (Figures 13 and 14).
- A caldera is a large depression formed when a volcano erupts and collapses. During a volcanic eruption, magma present in the magma chamber underneath the volcano is expelled, often forcefully ^[15] (Figures 15 and 16)
- Example: A famous example is Crater Lake Caldera, Oregon, USA (Figure 17).

Compound Volcano

- A compound volcano is defined as one that consists of a complex of two or more vents, or a volcano that has an associated volcanic dome, either in its crater or on its flanks. (Figure 18)
- Example: Mt. Shasta, California. ^[16]

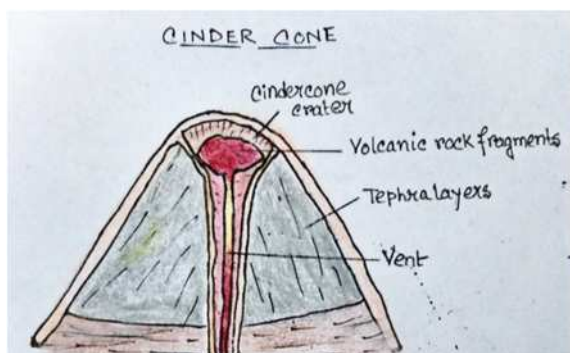


Figure 13: Cinder Cone



Figure 14: Sunset Crater in Arizona. ^[17]

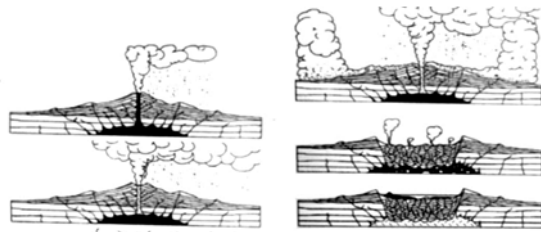


Figure 15: Formation of Caldera.^[18]

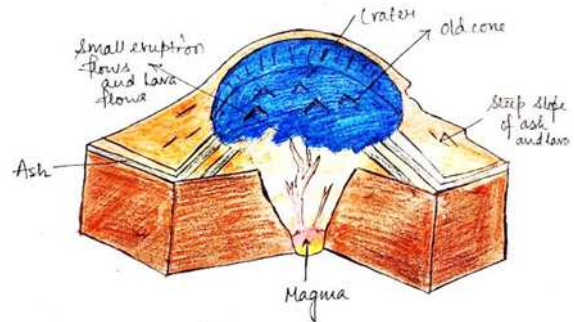


Figure 16: Caldera



Figure 17: Caldera formation.^[19]



Figure 18: Compound Volcano.^[20]

Supervolcano:

- An unusually large volcano having the potential to produce an eruption with major effects on the global climate and ecosystem ^[21] (Figure 19).
- (Source:<https://www.lexico.com/definition/supervolcano>)

Submarine Volcano:

- Submarine volcanoes are underwater fissures in the Earth's surface from which magma can erupt ^[22] (Figure 20).

Subglacial Volcano:

- A volcanic edifice constructed whole or in part by eruption beneath ice ^[23] (Figure 21).

Resurgent Domes:

- The central highlands in many calderas formed by gradual upwarping of caldera floor after caldera collapse due to renewed magma intrusion ^[24] (Figure 22).



Figure 19: Supervolcano.^[25]



Figure 21: Subglacial Volcano.^[26]

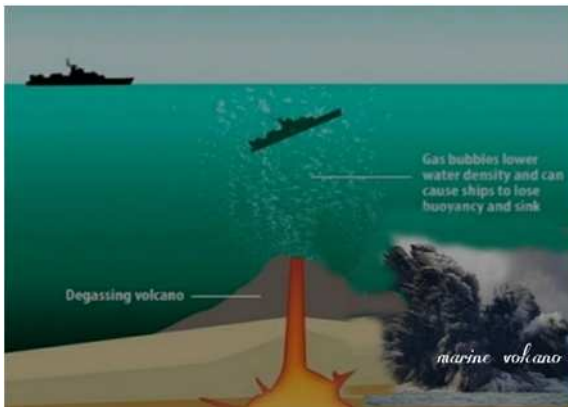


Figure 20: Submarine Volcano.^[27]

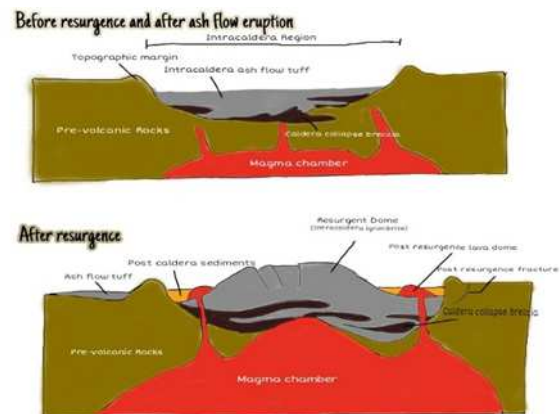


Figure 22: Resurgent Dome.^[28]

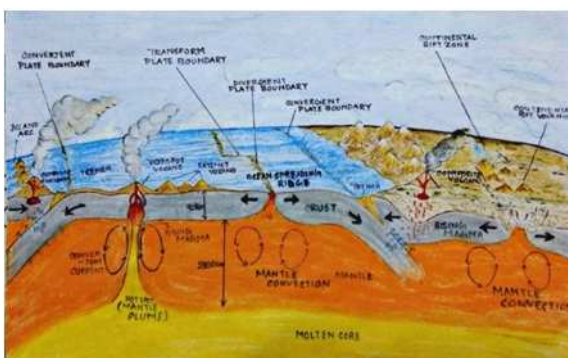


Figure 23: Volcano and Plate Tectonics.^[29]

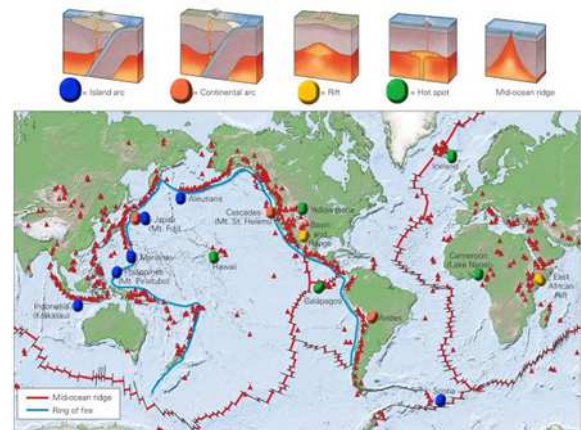


Figure 24: Global Distribution of Volcanoes.^[30]

6. Processes

Volcanic processes are related to the formation of different volcanic landform is the eruption of the molten rocks known as magma through the central vents or fissures into the surface.

They include all the processes that result from intrusion into bedrock and extrusion onto the Earth's surface. These processes have contributed to the construction of landforms and features of the Earth's surface over millions of years.^[31]

When a part of the earth's upper mantle or lower crust melts, magma forms. A volcano is essentially an opening or a vent through which this magma and the dissolved gases it contains are discharged. Although there are several factors triggering a volcanic eruption, three

predominate: the buoyancy of the magma, the pressure from the exsolved gases in the magma and the injection of a new batch of magma into an already filled magma chamber. What follows is a brief description of these processes.

As rock inside the earth melts, its mass remains the same while its volume increases--producing a melt that is less dense than the surrounding rock. This lighter magma then rises toward the surface by virtue of its buoyancy. If the density of the magma between the zone of its generation and the surface is less than that of the surrounding and overlying rocks, the magma reaches the surface and erupts. As this magma moves toward the surface, the solubility of the water in the magma decreases, and so the excess water separates from the magma in the form of bubbles. As the magma moves closer to the surface, more and more water exsolves from the magma, thereby increasing the gas/magma ratio in the conduit. When the volume of bubbles reaches about 75 percent, the magma disintegrates to pyroclasts and erupts explosively.

Another process that causes volcanic eruptions is an injection of new magma into a chamber that is already filled with magma of similar or different composition. This injection forces some of the magma in the chamber to move up in the conduit and erupt at the surface.^[32]

Shield volcanoes are formed by lava flows of low viscosity - lava that flows easily. Consequently, a volcanic mountain having a broad profile is built up over time by flow after flow of relatively fluid basaltic lava issuing from vents or fissures on the surface of the volcano.^[33]

Cinder cones are the simplest type of volcano. They are built from particles and blobs of congealed lava ejected from a single vent. As the gas-charged lava is blown violently into the air, it breaks into small fragments that solidify and fall as cinders around the vent to form a circular or oval cone.^[34]

As the name implies, *Stratovolcanoes* are formed of stratified layers of both viscous lava flows and fragmental material. Classic symmetrical stratovolcanoes such as Shishaldin in the Aleutian Islands and Mayon in the Philippines are the exception rather than the rule. Most stratovolcanoes are complex structures formed by multiple eruptions from summit and flank vents.

Compound stratovolcanoes may form when the focus of eruptions shifts, forming multiple overlapping edifices. Some stratovolcanoes may form in a few thousand years, but may remain active for tens to hundreds of thousands of years.^[35]

7. Global Distribution of Volcanoes

The relationship between volcanic activity and Earth's tectonic plates has great importance. Stratovolcanoes tend to form at subduction zones, or convergent plate margins, where an

oceanic plate slides beneath a continental plate and contributes to the rise of magma to the surface (Figure 23). At rift zones, or divergent margins, shield volcanoes tend to form as two oceanic plates pull slowly apart and magma effuses upward through the gap. Volcanoes are not generally found at strike-slip zones, where two plates slide laterally past each other. “Hot spot” volcanoes may form where plumes of lava rise from deep within the mantle to Earth's crust far from any plate margins ^[36] (Figure 24).

8. Conclusion

Volcanoes have some impact on people and environment. The study of volcanoes can reduce the hazards or adverse impact and its benefits can be utilized properly for mankind. Early volcanic eruption led to the Earth's atmosphere. It creates new land, the volcanic soil are fertile and rich in minerals. From the eruption of volcano, better understanding of the Geographical processes involved and the composition of the interior Earth is possible.

Acknowledgment

We would like to express our gratitude towards our mentor and teacher, Smt. Asima Kar, Department of Geology, Jogamaya Devi College for the support and guidance. We would like to extend our thanks to our anonymous reviewer for reviewing our article.

Weblinks

- [1] <https://cdn.britannica.com/16/77416-120-6D5A3D41/volcano-Mount-St-Helens-south-eruption-May-18-1980.jpg>
- [2] <https://image.slidesharecdn.com/magmaandvolcanoes-130903134651-/95/magma-and-volcanoesepcclm4-6-638.jpg?cb=1378216119>
- [3] <https://image.slidesharecdn.com/lecture2-globalsignificanceofvolcanicactivity-130121024148-phpapp01/95/lecture-2-global-significance-of-volcanic-activity-9-638.jpg?cb=1358736173>
- [4] https://upload.wikimedia.org/wikipedia/commons/thumb/e/e1/Viscosity_of_magma_EN.svg/1200px-Viscosity_of_magma_EN.svg.png
- [5] <https://www.vocabulary.com/dictionary/lava>
- [6] <https://www.tulane.edu/~sanelson/eens1110/volcanoes.htm>
- [7] <https://earthhow.com/wp-content/uploads/2019/07/Lahar-675x493.png>
- [8] http://www.geo.mtu.edu/volcanoes/vc_web/overview/graphics/volimpact-19.gif
- [9] https://dr282zn36sxxg.cloudfront.net/datastreams/f-d%3A97c49b8d1fbc6eee0205af2cc8d416a96937680fe1d5d0da4de24d18%2BIMAGE_THUMB_POSTCARD_TINY%2BIMAGE_THUMB_POSTCARD_TINY.1

- [10] <https://cdn.britannica.com/51/4951-004-CC7C675A/Profiles-landforms-cinder-cone-left-right-scale.jpg>
- [11] <https://i.pinimg.com/originals/da/d5/8e/dad58ed07a5f36aaea700b6655c44eae.jpg>
- [12] https://www.researchgate.net/publication/332293506/figure/fig1/AS:745754742255616@1554813194127/A-Schematic-model-of-the-growth-of-the-Ogariyama-dome-which-has-an-asymmetric_W640.jpg
- [13] <http://www.explorevolcanoes.com/Volcano%20Glossary%20cryptodome.html>
- [14] <https://www.nationalgeographic.org/encyclopedia/crater/>
- [15] <https://www.nationalgeographic.org/encyclopedia/calderas/>
- [16] <https://indianexpress.com/article/explained/explained-why-eruption-of-a-tiny-complex-volcano-is-causing-concern-6216667/lite/>
- [17] <https://www.azcentral.com/story/travel/arizona/2016/08/22/sunset-crater-volcano-national-monument/88806972/>
- [18] https://www.tulane.edu/~sanelson/Natural_Disasters/volclandforms.htm
- [19] https://www.universetoday.com/wp-content/uploads/2009/05/crater_lake_oregon.jpg
- [20] <https://www.usgs.gov/media/images/mount-shastas-west-slope-a-view-facing-east-ca>
- [21] <https://www.lexico.com/definition/supervolcano>
- [22] <https://www.crystalinks.com/volcanosubmarine.html>
- [23] https://link.springer.com/referenceworkentry/10.1007/978-1-4614-9213-9_551-1
- [24] https://volcanoes.usgs.gov/vsc/glossary/resurgent_dome.html
- [25] <http://www.geologyin.com/2018/03/early-humans-survived-massive.html>
- [26] https://www.vatnajokulsthjodgardur.is/static/files/svaedin/Vatnajokull-HorfandiJoklar/Myndir/3_9b_gjalp_mtg.jpg
- [27] <https://2rdrtx4bt29lo91s31mjhkji-wpengine.netdna-ssl.com/wp-content/uploads/2016/03/Underwater-volcanoes-02.jpg>
- [28] https://www.researchgate.net/profile/Donald_Sweetkind/publication/236934763/figure/fig1/AS:648955809525761@1531734530205/Generalized-diagram-of-ash-flow-caldera_W640.jpg
- [29] <https://opentextbc.ca/physicalgeologyearle/wp-content/uploads/sites/145/2016/06/volcanic-tectonics.png>
- [30] <http://geologylearn.blogspot.com/2016/03/relation-of-volcanism-to-plate-tectonics.html>
- [31] https://www.researchgate.net/publication/317031379_Volcanic_processes_and_landforms
- [32] <https://www.scientificamerican.com/article/what-causes-a-volcano-to-erupt-and-how->

do-scientists-predict-eruptions/

[33] https://www.sciencedaily.com/terms/shield_volcano.htm

[34] <https://pubs.usgs.gov/gip/volc/types.html>

[35] https://volcano.si.edu/learn_galleries.cfm

[36] <https://kids.britannica.com/students/assembly/view/156130>

Dynamic Recrystallization: An Outline of the Mechanisms and the Microstructural Developments

Anushka Das¹, Navya Dharmdev² and Srija Ray Chowdhury³

Students of 2nd Semester Geology Honours Course

¹anuuu3781011@gmail.com, ²navya.dha29@gmail.com, ³srijaraychowdhury@gmail.com

1. Introduction

Recrystallization, a process closely associated with metamorphism, mylonitization, and development of microstructures in a shear zone, is defined as the reorganisation of material with a change in grain size, shape and orientation within the same mineral (Passchier & Trouw 2005). In contrast to neocrystallization, it does not involve formation of new minerals. The textural changes are affected by the creation of new crystal nuclei within the old grain.

Recrystallization leads to the growth of less deformed crystals at the cost of its more deformed neighbour by the creation and/or movement of grain boundaries. It brings about the gradual replacement of old grains (known as porphyroclast) by the new grains of relatively smaller size.

There are two types of recrystallization: dynamic and static. Dynamic recrystallization occurs during intracrystalline deformation. Static recrystallization, on the other hand, takes place when the deformation stops or slows down. This article briefly describes the different types of the dynamic recrystallization processes and the microstructures produced by them.

2. The three mechanisms of dynamic recrystallization

There are three major mechanisms of dynamic recrystallization, occurring in different metamorphic conditions. They are: Bulging recrystallization (BLG), sub-grain rotation recrystallization (SGR), and grain boundary migration recrystallization (GBM). Among these three, BLG takes place at lowest temperature ranges and GBM at the highest temperature ranges.

These three mechanisms are briefly explained in the next three subsections.

2.1 Bulging Recrystallization

As described by Baily and Hirsch (1962), Drury et al. (1985), Shigematsu (1999), Stipp et al. (2002) (as referred by Passchier & Trouw 2005) this mechanism is driven by the difference of dislocation concentration in the adjacent crystal grains (Figure 1A). At low temperature, the local mobility of the grain boundary may cause it to bulge locally into a neighbouring

grain with higher dislocation density (Figure 1B). This bulge may gradually develop a new independent small grain (Figures 1C, 1D). It mostly occurs at the boundary of old grains (Figure 2).

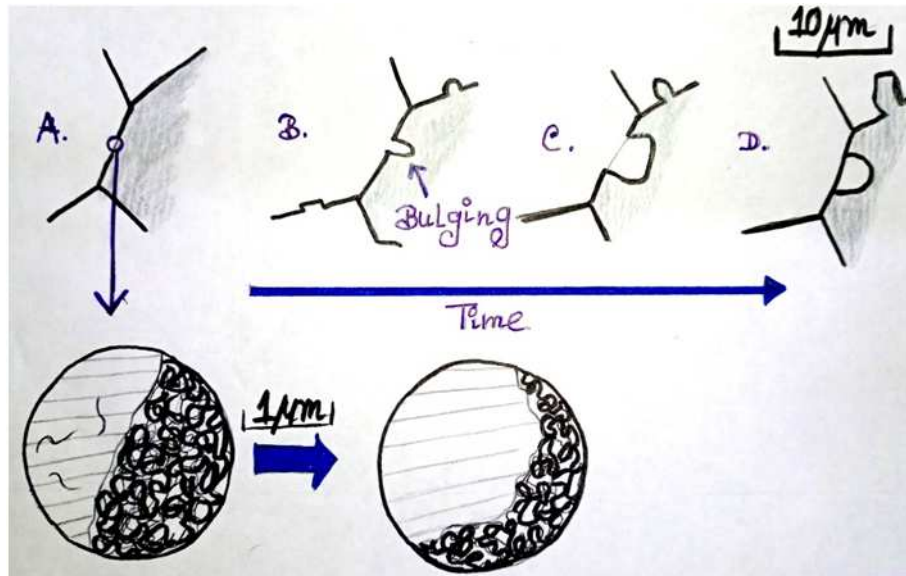


Figure 1: Bulging recrystallization (BLG). A. Two adjacent grains are there one with higher dislocation density than the other (inset; grey lines indicate crystal lattice) B. The grain boundary starts bulging towards the grain with higher dislocation density C. Bulging continues and a new separate grain is about to form D. A new independent grain is formed in expense of the old grain (Passchier & Trouw 2005)

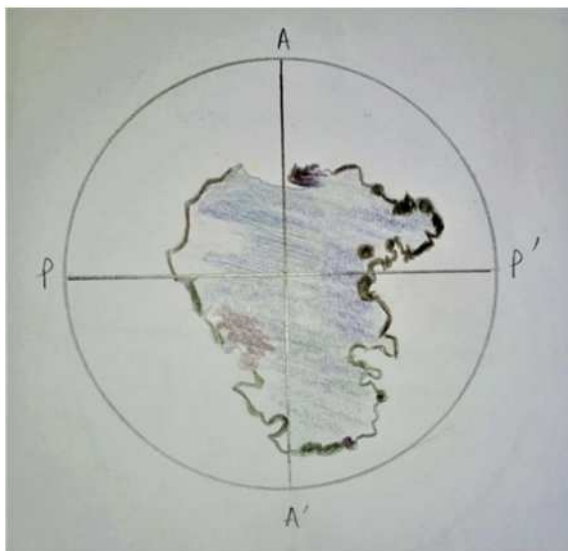


Figure 2: Quartz. The grain boundary is moving due to 'strain induced grain boundary migration' or BLG.

The bulges (black ones near the boundary) are formed due to the migration which eventually form new grains. One new grain is observed at top right (black coloured). The quartz was found in a deformed granite from the Bega Batholith (Vernon 2004).

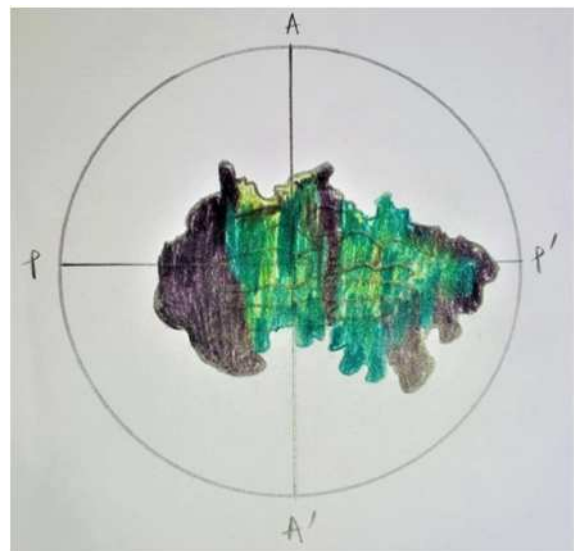


Figure 3: 'Core mantle structure' in Olivine. The elongated grains (elongated bordered with black) are surrounded by new recrystallized grains. The new grains are recrystallized grains, formed during intracrystalline deformation by BLG. The process of recrystallisation has not yet completed that is the reason why all the grains are not yet recrystallized.

Thus the old sub-grains are surrounded by new grains forming 'core-mantle-structure' indicating incomplete recrystallisation process (Vernon 2004).

This process is also known as 'low-temperature grain boundary migration', local grain boundary migration, and 'slow grain boundary migration', to distinguish it from GBM which is fast grain boundary migration at high temperature, occurring along the entire grain boundary.

At relatively lower temperature, the old grains are slightly deformed and may show fractures. Bulging produces undulose extinction, kink, deformation lamellae (Figure 4), and irregular or serrated grain boundaries at higher temperature. If the process of recrystallization is not complete, then the remains of the old grain may be surrounded by the new recrystallized grain, this feature is known as core-mantle structure (Figure 3).

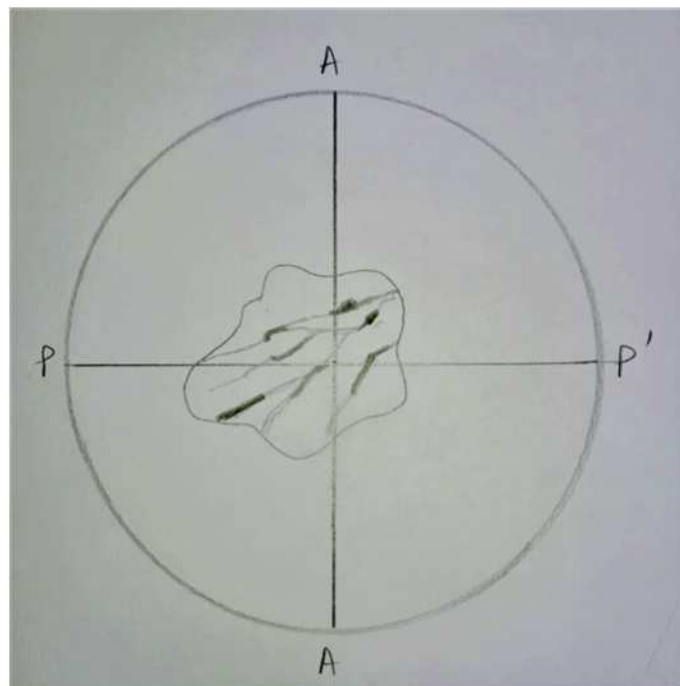


Figure 4: Quartz grain with deformation lamellae (sub vertical) containing new grains (black ones) formed by 'low temperature grain boundary migration'. Quartz vein in mica schist. Southern Alps, Italy. Width of view 1.8 mm. CPL (Passchier & Trouw 2005)

2.2 Sub-grain rotation recrystallization (SGR):

This occurs when the dislocations are added continuously to the sub-grain boundaries, and can climb from one lattice plane to another (known as climb-accommodated dislocation creep). Then the lattice angles increase in both side of the boundary, until the grain no longer occurs to be part of the old grain and thus a new grain is developed (Figure 5).

This occurs in a higher temperature condition than BLG. Old grains tend to deform in a ductile manner to develop more elongated grains, with numerous sub-grains (Figure 6).

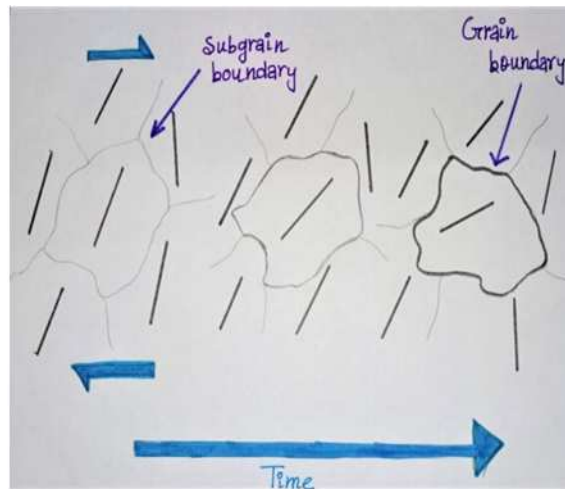


Figure 5: Sub-grain rotation recrystallisation (SGR). Dislocations are continuously added to the grain boundaries (when only SGR can occur). The lattice angle increases subsequently on either side of the grain boundary and finally forming a new grain (Passchier & Trouw 2005).

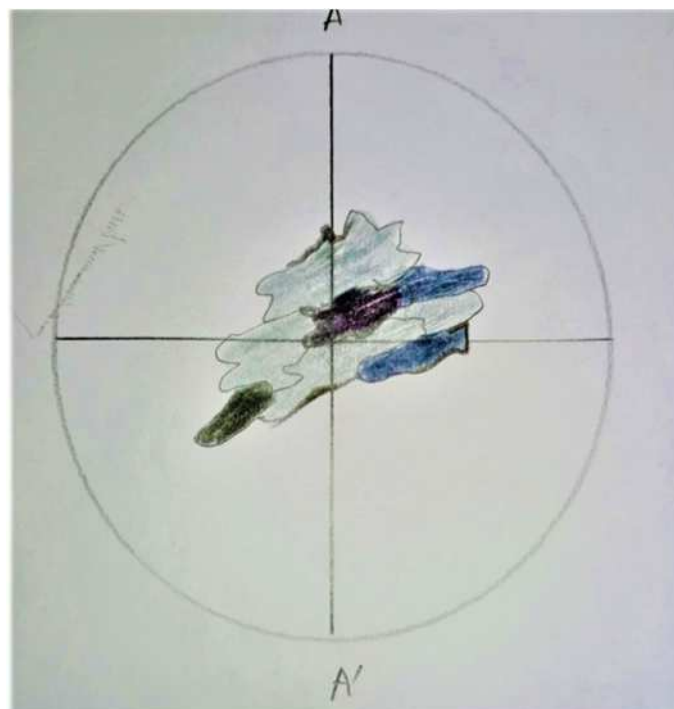


Figure 6: Polycrystalline quartz aggregate. The elongated grains are surrounded by other grains. It indicates the new grains (elongated grains) formed by SGR. The upper right grey grain is one old grain and the middle elongated grey grain is one new grain, (width of view 1.8 mm. CPL (after Passchier & Trouw 2005))

2.3 Grain boundary migration recrystallization (GBM)

This process, also known as high-temperature grain boundary migration recrystallization, takes place at higher temperature than SGR. The high temperature increases the mobility of the grain boundary to such an extent that it can move through the entire crystals to remove dislocations and subgrain boundaries, as shown in (Figure 7) (Passchier & Trouw 2005).

The new grains become larger than the older grains, and typically have interlobate or amoeboid boundaries (Figure 8).

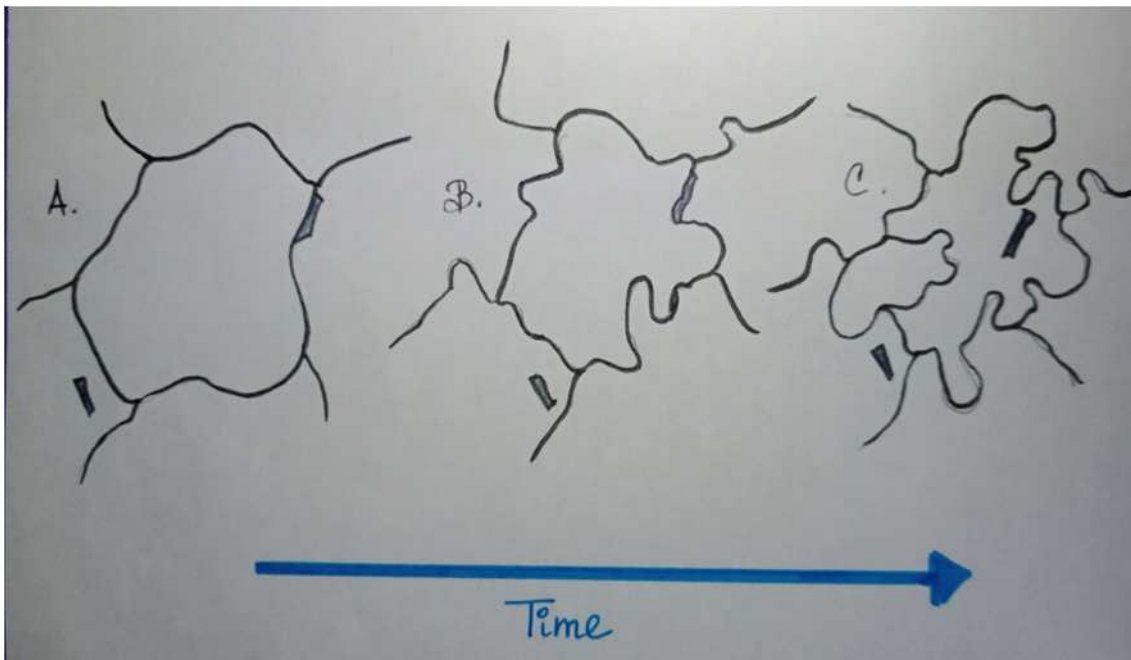


Figure 7: Grain boundary migration (GBM). It occurs at the highest temperature. At such higher temperature the mobility of the grain boundary increased so much that it moves freely (B.) all over the crystal lattice, sweeping away dislocations and sub-grain boundaries. Eventually forming new grain. It is evident that the new grains have ameboid grain boundaries. (C.). The old and new grains are difficult to differentiate. (Passchier & Trouw 2005)

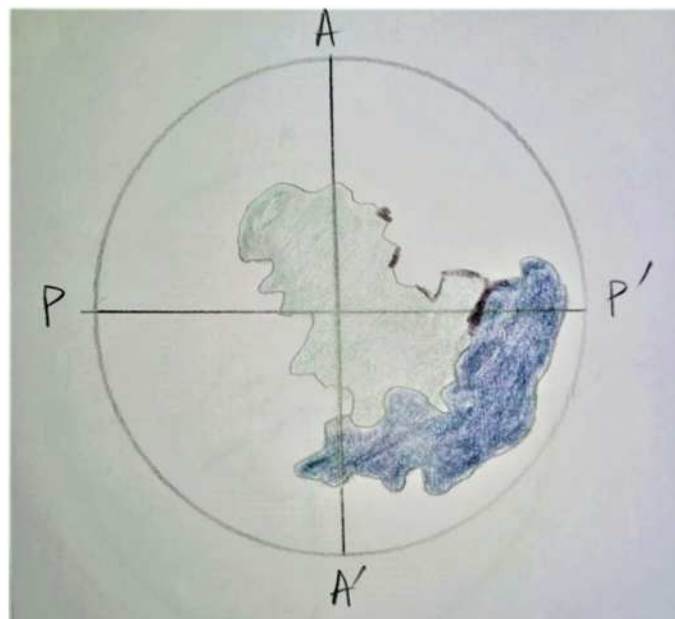


Figure 8: Polycrystalline quartz grains. Irregular grain boundary formed by grain boundary migration (GBM). The light grey grain moves towards the dark grey grain, finally a new grain will be formed. Quartzite, Yilgarn Craton, Australia. Width of view 1.8 mm. CPL (after Passchier & Trouw 2005)

In case of GBM, it is difficult to differentiate the new grains from the old ones. However, the secondary phases and impurities like the fluid and solid inclusions can produce some characteristic microstructures which may help to identify the grains formed by GBM recrystallization. Pinning, window and dragging microstructures, as described in Figure 9, are the examples of such microstructures.

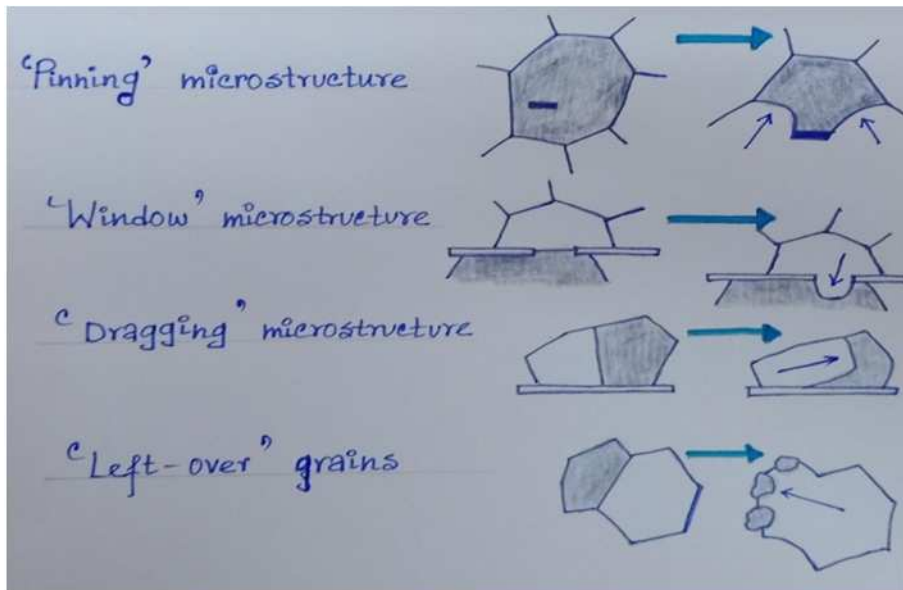


Figure 9: The new grains formed by GBM recrystallization cannot be differentiated easily. Some characteristic microstructures such as 'pinning', 'window', 'dragging', and 'left-over grains' are means to differentiate. These are formed by some fluid or solid inclusions present in the grains. The violet arrow indicates the direction of movement of the grain boundary occurred during GBM i.e. in the figure the grain boundaries move towards the grey part from the white part (after Passchier and Trouw 2005).

3. Temperature dependence of dynamic recrystallization mechanisms

During intracrystalline deformation the major recrystallization mechanisms i.e. BLG, SGR, GBM, start at different temperatures for different minerals (Figure 10).

BLG starts for quartz and calcite within 200°C to 300°C, whereas for feldspar it occurs at greater than 400° C. At these temperature ranges, the new grains are formed within the boundary of the old grain with higher dislocation density.

At intermediate temperature, dislocations are added to the grain boundary and climb accommodated dislocation creep initiates, which causes the sub-grain rotation forming new grains i.e. SGR recrystallization mechanism. For feldspar it occurs at ~600°C and for quartz ~400°C. The new grains are elongated in shape e. g. 'ribbon' feldspar.

At higher temperature(>800°C in feldspar and ~500°C in quartz) the mobility of the grain boundaries increases so much that they move freely all over the crystal lattice, to start GBM. It is therefore possible to determine the temperature range in which a mineral was deformed, if the mechanism of recrystallization operated on it can be identified from the microstructures (Passchier & Trouw 2005).

Increase in strain rate raises the temperature of transformation of one recrystallization mechanism to the other; i.e. when strain rate increases, BLG-SGR transformation and SGR-GBM transformation of a mineral take place at relatively higher temperature.

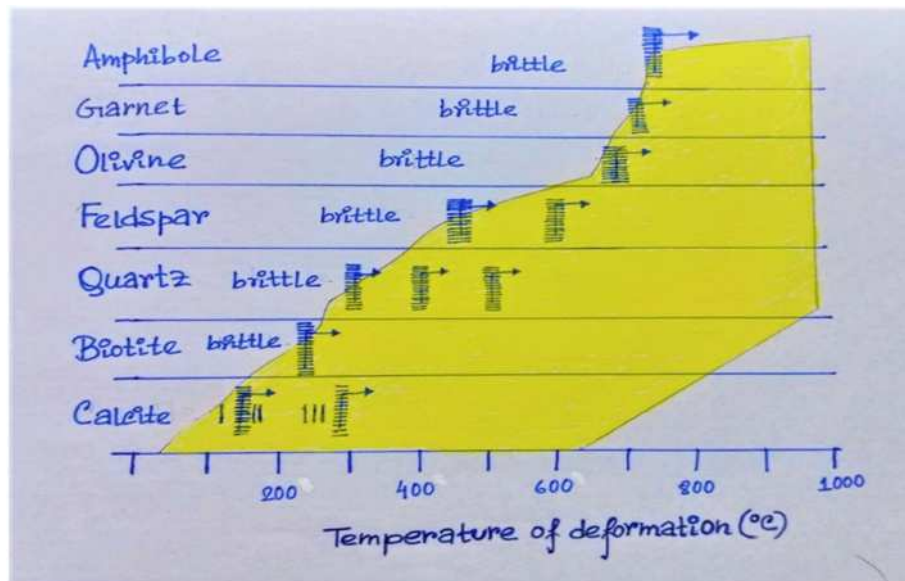


Figure 10: The three mechanisms of dynamic recrystallization, BLG, SGR, and GBM, occur successively with increasing temperature. The temperature ranges of these mechanisms are different for different minerals. This figure shows the temperature ranges of these three mechanisms for six common rock-forming minerals: amphibole, garnet, olivine, feldspar, quartz, and calcite. The arrow indicates the effect of strain rate – when strain rate increases, the temperature of transformation of one mechanism to another also increases. For example, in quartz, BLG – SGR transformation takes place at ~400°C. If strain rate increases, this transformation will take place at > 400°C. The yellow zone in the figure indicates crystalplastic field, (the zone of permanent deformation during intracrystalline deformation), in this field BLG, SGR, GBM occurs (After Passchier & Trouw 2005).

4. Conclusion

The microstructural features developed by dynamic recrystallization, if properly discerned, may provide valuable insights on the thermal and rheological conditions of deformation and metamorphism; and along with metamorphic mineral assemblages, can be applied successfully in paleobarometry and paleothermometry. Detailed qualitative and quantitative analyses of these microstructures are therefore essential in a comprehensive study of a deformed rock.

Acknowledgement

We would like to take the opportunity to thank our mentor Bhaskar Ghosh, department of Geology for guiding us through the process and helping us reach the completion of the task without any hindrance.

References:

- Passchier, C. W., Trouw, R. A. J., 2005. *Microtectonics*, 2nd Edition. Springer-Verlag Berlin Heidelberg.
- Vernon, R. H., 2004. *A Practical Guide to Rock Microstructure*. Department of Earth and Planetary Sciences, Macquarie University, Sydney Cambridge University Press

Fun Texture in Feldspar

Ankita Samaddar¹, Tanushri Bera², Debadrita Nag³ and Debarati Bhowmik⁴

Students of 2nd Semester Geology Honours Course

¹samaddarankita93@gmail.com, ²tanushribera13@gmail.com

³debadritanag@yahoo.co.in, ⁴bhowmicktuhina@gmail.com

1. Introduction

“Feldspar” is the name of a large group of rock-forming silicate minerals that make up over 50% of Earth’s crust. They are found in igneous, metamorphic and sedimentary rocks in all parts of the world. Feldspar minerals have very similar structures, chemical compositions, and physical properties. Common feldspars include orthoclase (KAlSi_3O_8), albite ($\text{NaAlSi}_3\text{O}_8$), and anorthite ($\text{CaAl}_2\text{Si}_2\text{O}_8$).

2. Structure of feldspar

Feldspars are tectosilicate. Any feldspar structure can be considered to have been derived from SiO_2 unit.

For example $\text{SiO}_2 \times 4 = 4\text{SiO}_2 = \text{Si}_4\text{O}_8$. Out of 4 Si of Si_4O_8 unit one may be replaced by Al. $\text{Si}_4\text{O}_8 - 1\text{Al} = \text{AlSi}_3\text{O}_8^-$

It will take up either Na or K to be electrically neutral. When Na is taken into structure, the resultant feldspar formed is $\text{NaAlSi}_3\text{O}_8$ (Albite). Similarly if K taken into structure, the resultant feldspar formed is KAlSi_3O_8 (orthoclase) (Figure 1).

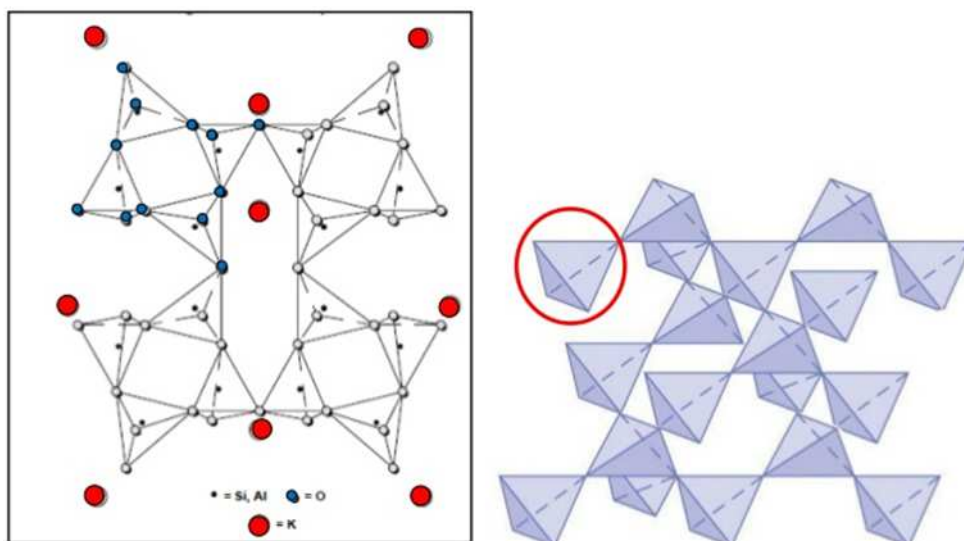
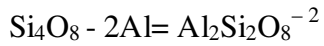


Figure 1: Structure of feldspar (Orthoclase).^[1]

Again replacing another Al we get-



It will take up Ca to be electrically neutral. When Ca is taken into structure, the resultant feldspar formed is $\text{CaAl}_2\text{Si}_2\text{O}_8$ (Anorthite).

3. Plagioclase feldspar

Type of Feldspar	End Members	Intermediate Members	Solid Solution Series
Plagioclase Feldspar – a group of feldspar minerals that essentially have the same formula but vary in their percentage of sodium and calcium.	Albite ($\text{NaAlSi}_3\text{O}_8$) Anorthite ($\text{CaAl}_2\text{Si}_2\text{O}_8$)	Oligoclase, Andesine, Labradorite, Bytownite	Form a solid solution series ranging from pure albite, $\text{NaAlSi}_3\text{O}_8$, to pure anorthite, $\text{CaAl}_2\text{Si}_2\text{O}_8$.

Table 1: Description of Plagioclase Feldspar

Discontinuities in this series are shown by the existence of peristerite and other intergrowth. It can be detected by electron optical and X-ray study.

Mineral	% Albite	% Anorthite
Albite	100-90% Ab	0-10% An
Oligoclase	90-70% Ab	10-30% An
Andesine	70-50% Ab	30-50% An
Labradorite	50-30% Ab	50-70% An
Bytownite	30-10% Ab	70-90% An
Anorthite	10-0% Ab	90-100% An

Table 2: Relative abundance of Albite (Ab) and Anorthite (An).



Figure 2: Hand specimen of plagioclase feldspar.^[2]

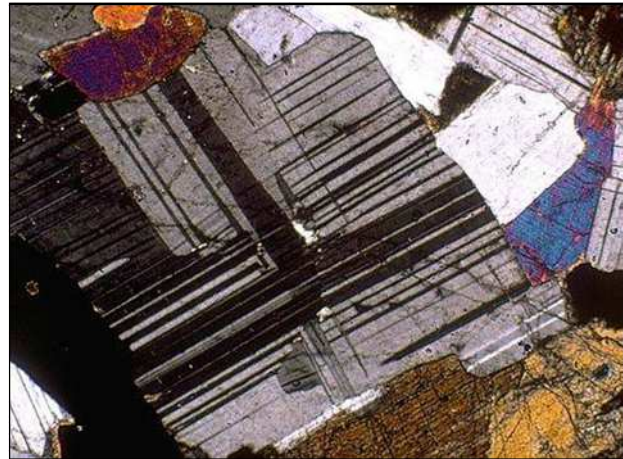


Figure 3: Plagioclase feldspar under microscope (under crossed polars).^[3]

4. Alkali feldspar

Types of Feldspar	End Members	Intermediate Members	Solid Solution Series
Alkali Feldspar minerals with compositions that range between $\text{NaAlSi}_3\text{O}_8$ and KAlSi_3O_8	Albite ($\text{NaAlSi}_3\text{O}_8$)	Anorthoclase ($(\text{Na,K})\text{AlSi}_3\text{O}_8$)	Albite and sanidine form a solid solution series between $\text{NaAlSi}_3\text{O}_8$ and KAlSi_3O_8 . Anorthoclase, with a composition of $(\text{Na,K})\text{AlSi}_3\text{O}_8$, occupies the intermediate position between them.
	Orthoclase (KAlSi_3O_8)	Sanidine ($(\text{K,Na})\text{AlSi}_3\text{O}_8$) (have a composition very close to KAlSi_3O_8) Microcline (KAlSi_3O_8) (usually have compositions that are very close to KAlSi_3O_8)	

Table 3: Description of Alkali Feldspar



Figure 4: Hand specimen of Alkali feldspar.^[4]

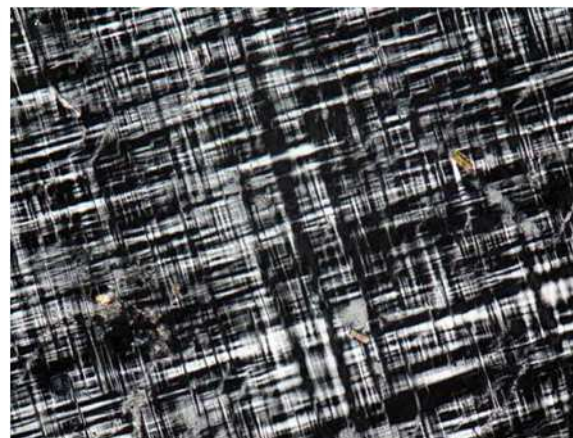


Figure 5: Alkali feldspar under light microscope.^[5]

5. Classification of feldspar

In the classification of igneous rocks of the International Union of Geological Sciences (IUGS), the feldspars are treated as two groups: the alkali feldspars and the plagioclase feldspar. This group consist of three end members namely orthoclase, albite and anorthite.

Albite and anorthite form a complete solid solution series. On the other hand orthoclase and albite form a solid solution series (Figure 6).

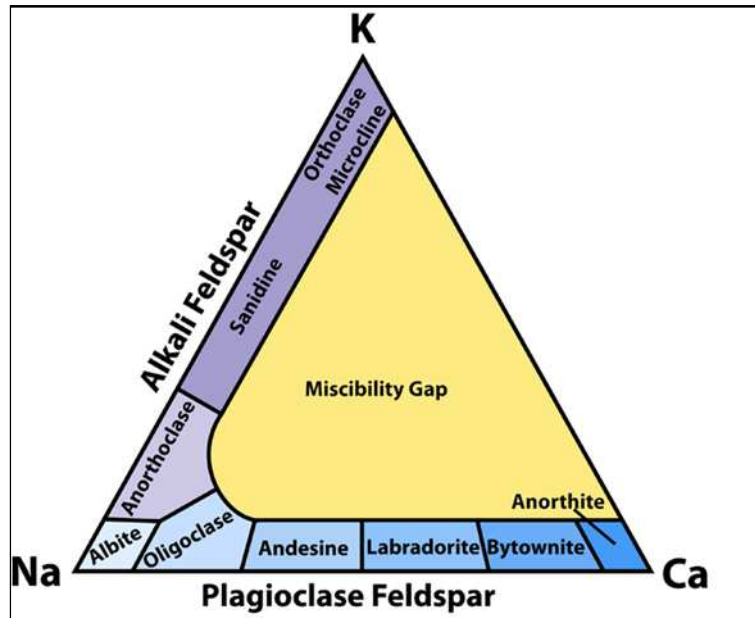


Figure 6 Triangular diagram showing classification of feldspar.^[6]

Alkali feldspar series		Plagioclase feldspar series	
1.	orthoclase (monoclinic) $KAlSi_3O_8$	1.	albite (0 to 10) $NaAlSi_3O_8$,
2.	sanidine (monoclinic) $(K,Na)AlSi_3O_8$,	2.	oligoclase (10 to 30) $(Na,Ca)(Al,Si)Al_2Si_2O_8$,
3.	microcline (triclinic) $KAlSi_3O_8$	3.	andesine (30 to 50) $NaAlSi_3O_8-CaAl_2Si_2O_8$,
4.	anorthoclase (triclinic) $(Na,K)AlSi_3O_8$	4.	labradorite (50 to 70) $(Ca,Na)Al(Al,Si)Si_2O_8$,
		5.	bytownite (70 to 90) $(NaSi,CaAl)AlSi_2O_8$,
			anorthite (90 to 100) $CaAl_2Si_2O_8$

Table 4: Classification of Feldspar

6. Order-disorder transformation and polymorphism in feldspar

The three alkali feldspar minerals $KAlSi_3O_8$ namely orthoclase, microcline and sanidine are polymorphs of each other. It means they have the same chemical compositions but different crystal structures at different temperature.

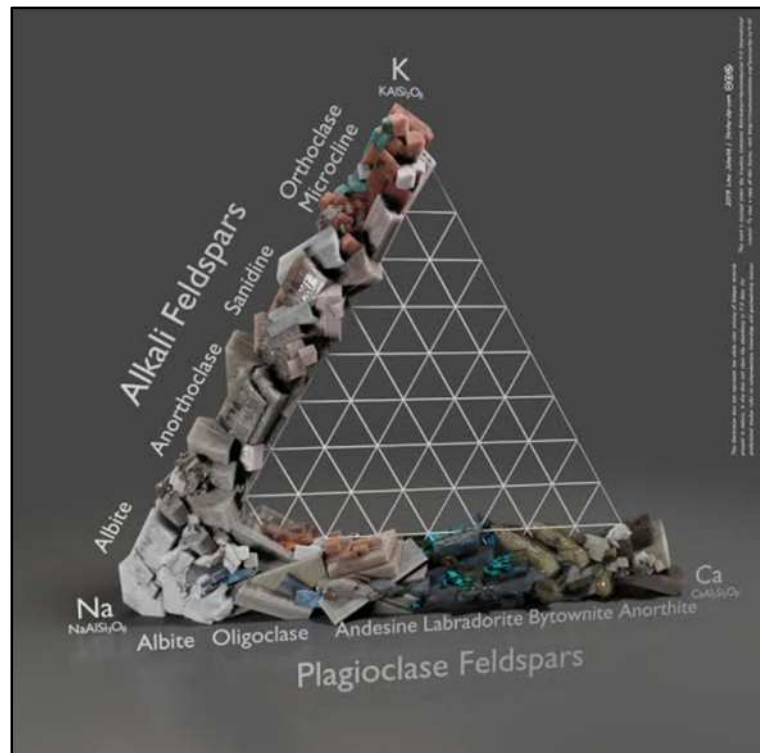


Figure 7- Classification of feldspar.^[7]

As the temperature of alkali feldspar ($KAlSi_3O_8$) decreases the crystal structure changes from that of sanidine (monoclinic) through orthoclase to microcline (triclinic). This is due to order-disorder transformations. Furthermore if the feldspar is allowed to cool very slowly then exsolution will occur. The solid solution will separate into a Na-rich phase and a K-rich phase. Thus one expects to find sanidine in rocks that were cooled very rapidly from high temperature i.e. volcanic rocks. Orthoclase and microcline will be found in plutonic igneous rocks as well as in metamorphic rock.

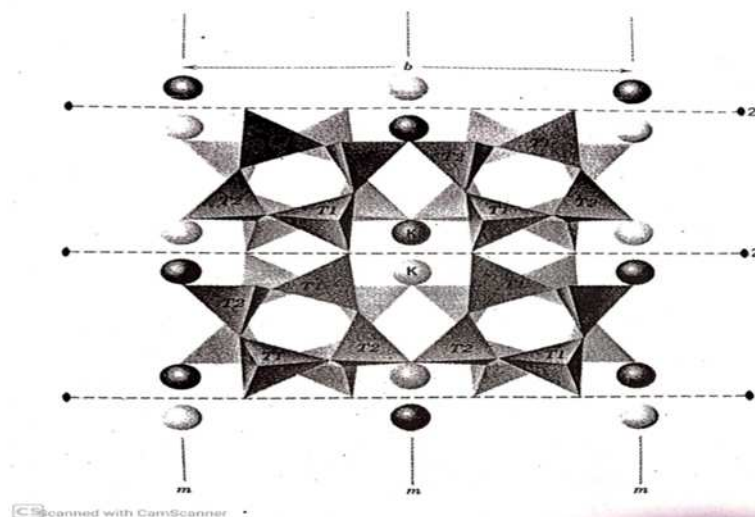


Figure 8 The general structure of feldspar (the high-temperature polymorph of $KAlSi_3O_8$ with space group $C2/m$) (Source- Mineral science (after Dana, J.D.) by Klein and Dutrow 23rd edition: p.472)

As the temperature of alkali feldspar ($KAlSi_3O_8$) decreases the crystal structure changes from that of sanidine (monoclinic) through orthoclase to microcline (triclinic). This is due to order-

disorder transformations. Furthermore if the feldspar is allowed to cool very slowly then exsolution will occur. The solid solution will separate into a Na-rich phase and a K-rich phase. Thus one expects to find sanidine in rocks that were cooled very rapidly from high temperature i.e. volcanic rocks. Orthoclase and microcline will be found in plutonic igneous rocks as well as in metamorphic rock.

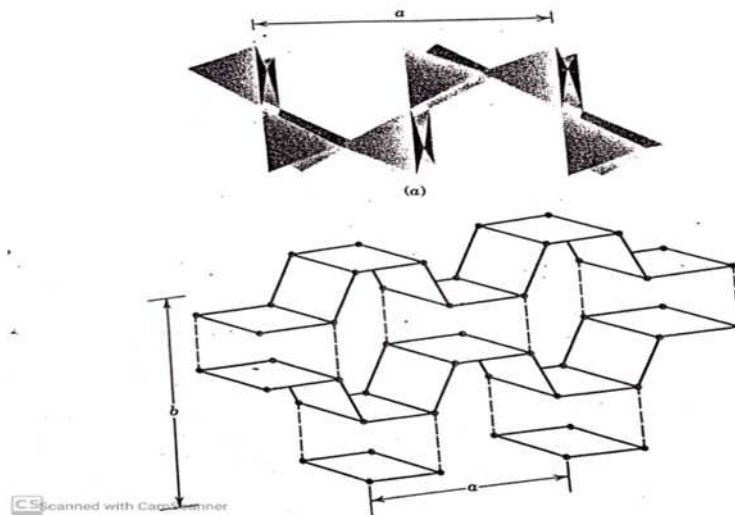


Figure 9 (a) The four membered rings in figure 8 are linked to form crankshaft-like chains that run parallel to the a axis. (After Papike, J.J. and M. Cameron. 1976)

(b) Schematic representation of the location and orientation of the four-member crankshaft like chains in the feldspar structure. Black dots are locations of Si. Dashed lines locate bonds between adjoining (Si,Al)₄ tetrahedral (Ribbe, 1987).

(Source- Mineral science (after Dana, J.D.) by Klein and Dutrow 23rd edition: p.473)

Name of Polymorph	Type of Al-Si distribution	Type of Polymorph of KAlSi ₃ O ₈	Symmetry
Microcline	Completely ordered what is known as low-temperature or maximum microcline (maximum refers to maximum triclinicity which results from the complete order). The tetrahedra that contain Al in this structure can be unambiguously located and the K ⁺ ions are no longer located in special positions.	a low temperature polymorph	Triclinic symmetry (space group C1) and lacks of mirror planes and rotation axes. Less symmetric
Orthoclase	Between the total order of microcline (Figure 10).	Intermediate polymorph	Monoclinic symmetry
Sanidine	Completely disordered, meaning that the Al and Si ions are randomly distributed among the two crystallographically distinct tetrahedral sites, T1 and T2. The K ⁺ ions, bounded to the nine nearest oxygens in large interstices occupy special positions on mirror planes perpendicular to b axis. The Si-Al tetrahedral framework consists of four-membered rings of tetrahedra that are linked into chains (of a crankshaft type) parallel to the a axis (Figures 8 and 9).	High Temperature polymorph	Monoclinic symmetry has mirror planes and rotation axes. More symmetric.

Table 5: Types of Polymorphism

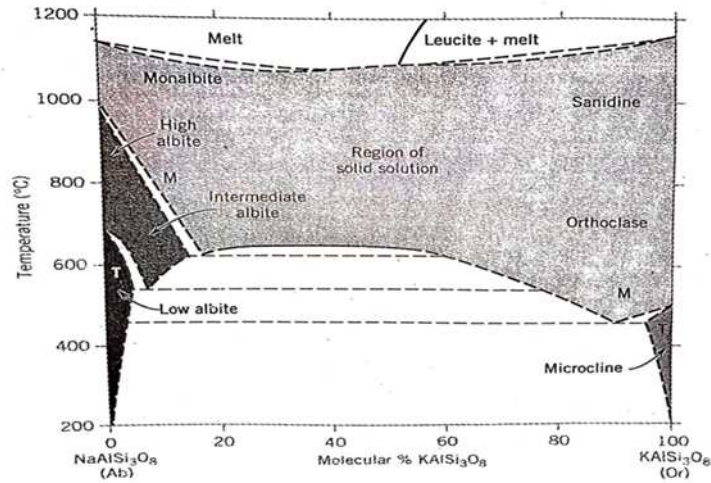


Figure 10: Schematic phase diagram for the system $\text{NaAlSi}_3\text{O}_8$ (Ab) - KAlSi_3O_8 (Kspar) showing a large miscibility gap at temperatures below approximately 650°C.

Here M and T mean monoclinic and triclinic respectively. Orthoclase, with space group $C2/m$, crystallizes at intermediate temperature (Smith, J.V. and W.L. Brown, 1988 (Source- Mineral science (after James.D.Dana) by Klein and Dutrow 23rd edition- Pg-473)

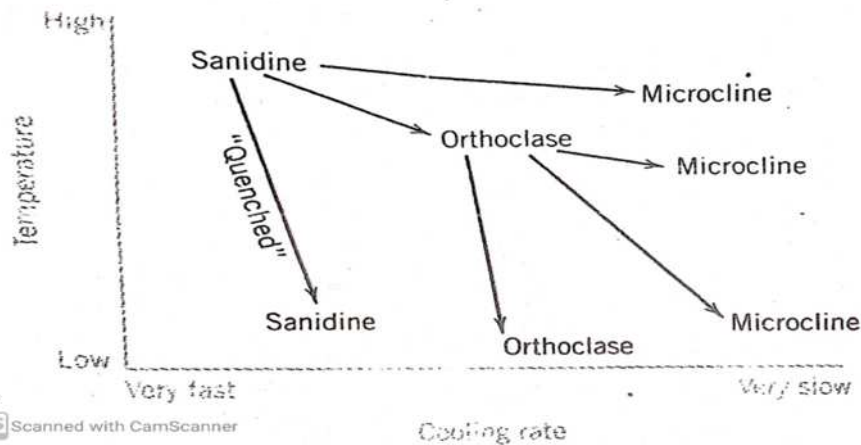


Figure 11- The various possible temperature-cooling rate paths that an originally high-temperature K-feldspar (sanidine) can follow. The path marked quenched depicts path in which the original high-temperature sanidine is cooled so rapidly that all characteristics of the high temperature state are preserved in the final product. (Putnis, A and J.D.C. McConnell, 1980).

(Source- Mineral science (after James.D.Dana) by Klein and Dutrow 23rd edition pg 474)

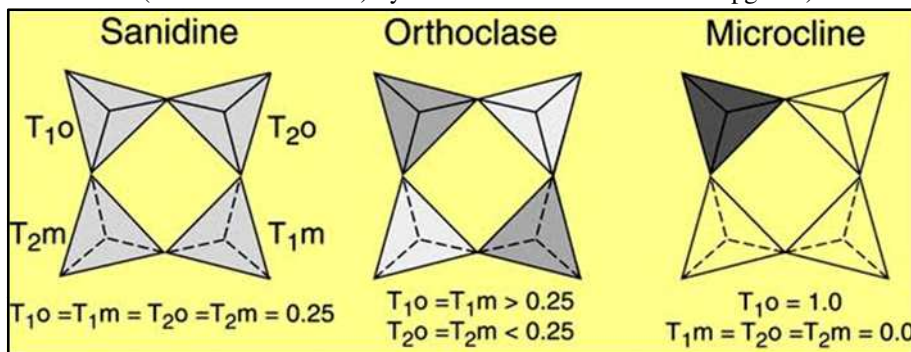
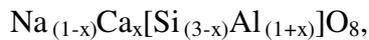


Figure 12: Structure of Sanidine, Orthoclase and Microcline.^[8]

7. The Albite-Anorthite series

The general structure of the members of the Albite-Anorthite series is very similar to that of microcline. The general formula of a feldspar in this series may be written as:



where x ranges from 0 to 1. The structural interpretation of the region of essentially complete solid solution is complicated because of the varying ratio of Al/Si from albite, $\text{NaAlSi}_3\text{O}_8$, to anorthite, $\text{CaAl}_2\text{Si}_2\text{O}_8$

Type of Feldspar	Al-Si Distribution	Symmetry
Low Albite	a highly ordered	generally triclinic
High albite or Monoalbite (occurs at very high temperature)	a highly disordered	generally monoclinic
Anorthite	perfectly ordered	Triclinic with space group $P1\bar{1}2$ at room temperature. At elevated temperatures body-centred with space group $I1\bar{1}2$

Table 6: Classification of Albite-Anorthite Series



Figure 13: Hand specimen of Albite.^[9]



Figure 14: Hand specimen of Anorthite.^[10]

8. Solid- Solution System

Pure albite crystallizes at 1118°C and pure anorthite melts at 1500°C . Thus from the Figure 15 it can be concluded that a solid solution containing 50% albite and 50% anorthite ($\text{Ab}_{50}\text{An}_{50}$) begins to melt at 1220°C point F, and the melting is complete at 1410°C , point A. Crystals that are in equilibrium with liquid will always be enriched in anorthite component relative to the liquid. As crystallization continues with lowering of temperature the composition of the plagioclase will change along the solidus, continually reacting with the liquid to produce crystals more enriched in the Ab component. Meanwhile, the composition of the liquid will change along the liquidus, thus also becoming more enriched in the Ab component. During crystallization the proportion of the solid continually increases while that of the liquid continually decreases. Thus as the composition of the liquid becomes more

sodic, approaching E, its volume steadily decreases. Thus it can be seen that the amount of liquid in equilibrium with the solid of composition F will be extremely small.

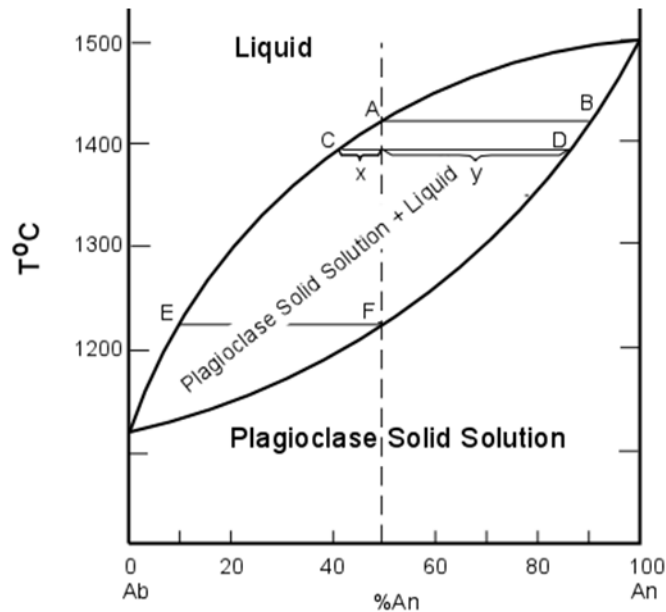


Figure 15: Phase diagram of albite anorthite system at constant pressure equal to that of atmosphere (atmospheric pressure =1 bar). Here the upper curve is called the liquidus and the lower curve is called the solidus. At temperatures above the liquidus everything is liquid, below the solidus everything is solid (crystals of plagioclase solid solution). At temperatures between the solidus and liquidus crystals of plagioclase solid solution coexist in equilibrium with liquid. Composition X is completely liquid above the liquidus (above 1410°C). The composition of this plagioclase can be found by drawing an isotherm in figure (line of constant temperature, a horizontal line in this diagram) through the temperature 1410°C. Where this isotherm intersects the solidus (at point B), the composition of the solid can be found by drawing a vertical line to the base of the diagram. Cooling to the liquidus at point A results in the crystallization of a small amount of plagioclase solid solution. Thus it is seen that the first crystals precipitated from composition X will have the composition $Ab_{10}An_{90}$.^[11]

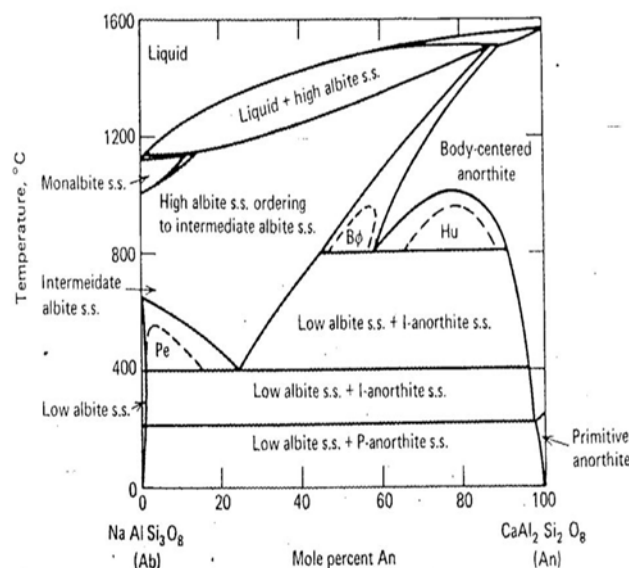


Figure 16: Schematic phase diagram for Albite Anorthite series showing a range of almost complete solid solution at high temperatures and broad miscibility regions at lower temperature.

(Source: Mason and Moors 1982: p. 101)

9. Texture

Texture is an important criterion for the naming a rocks. Three types of exsolution textures found in this series are not visible to the naked eyes but may be detected because of iridescence. These discontinuities in the solid solution series between albite and anorthite are on a fine scale, however, most properties, such as specific gravity or refractive index, show a generally linear change with chemical composition.

Types of exsolution textures	Compositional Range of occurrence
Peristerite_ intergrowths	An ₂ to An ₁₅
Bøggild intergrowths (their presence is indicated by the play of colours in labradorite)	in some plagioclase with composition between An ₄₇ and An ₅₈
Huttenlocher intergrowths	An ₆₀ to An ₈₅ region

Table 7: Exsolution Texture

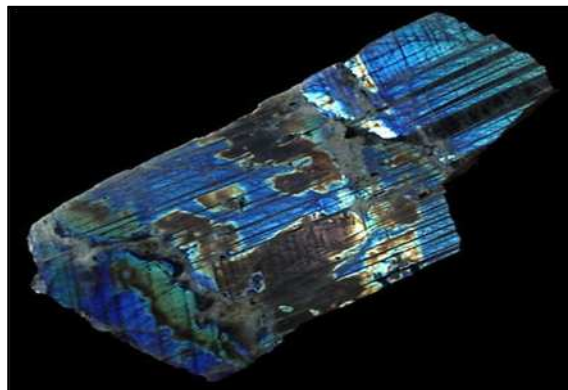


Figure 17: Play of colour in Labradorite.^[12]

10. The Albite-Orthoclase series

The albite-orthoclase series shows a complete solid solution only at high temperatures. For example, members of the sanidine high albite series are stable at elevated temperatures but at lowest temperature, two separate phases, low albite and microcline becomes stable. As can be seen from Figure 10, the compositional ranges of low albite and microcline are very small. When a homogeneous feldspar of composition Or₅₀Ab₅₀, in which the Na⁺ and K⁺ ions are randomly distributed is allowed to cool slowly, then segregation of Na⁺ and K⁺ ions will result because the size requirements of the surrounding structure become more stringent. The Na⁺ will diffuse to form Na-rich regions in the structure, causing the originally homogeneous feldspar to become heterogeneous intergrowth.

11. Exsolution System

Many minerals that show complete solid solution at higher temperatures do not show such solid solution at lower temperatures. When this is the case, the phenomenon of exsolution

occurs. Exsolution implies that one or the other of the mineral phases in the solution must “exsolve” or come out of solution with the other mineral phase.

At temperatures just below the solidus, alkali feldspar solid solutions are stable. At lower temperatures, along the curve labelled “solvus” the solid solution is no longer stable. In this case the exsolution phenomena occurs below the solidus and so is a “sub-solidus” reaction.

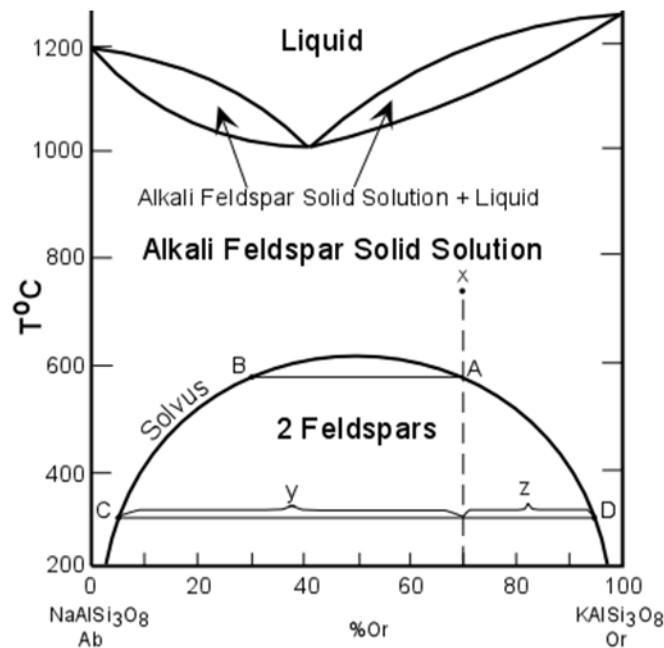


Figure 18: Phase diagram of the Albite-Orthoclase system which exhibits such exsolution behaviour at low temperatures. At high temperatures the diagram shows that albite (Ab) or NaAlSi₃O₈ and orthoclase (Or) or KAlSi₃O₈ form a complete solid solution series.^[13]

Temperature	Stability	Composition (The composition of coexisting exsolved phases can be found by drawing an isotherm until it intersects the solvus)
750°	Stable	Composition of the alkali feldspar solid solution is 70% orthoclase and 30% albite (Or ₇₀ Ab ₃₀).
About 590° (obtained at point A of Figure 18)	Solid solution is no longer stable and begins to exsolve	Solid solution having the composition of (point B from Figure 18) Or ₃₂ Ab ₆₈ coexists with an alkali feldspar solid solution with the composition of (point A from Figure 18) Or ₇₀ Ab ₃₀ .
300°	Exsolution occurs	Original composition X (from Figure 18) has exsolved into two alkali feldspar solid solutions, one with the composition of point C (from Figure 18) and one with a composition of point D (from Figure 18).

Table 8: Exsolution phenomenon at different temperatures

Complete exsolution is only common in metamorphic rocks. More often, especially in granitic rocks, the two exsolved phases do not separate as individual crystals, but occur as intergrown crystals with exsolution lamellae of one crystal occurring within the other crystal.

In the alkali feldspars (KAlSi_3O_8) containing such exsolution lamellae the result is to produce a texture called perthitic texture.

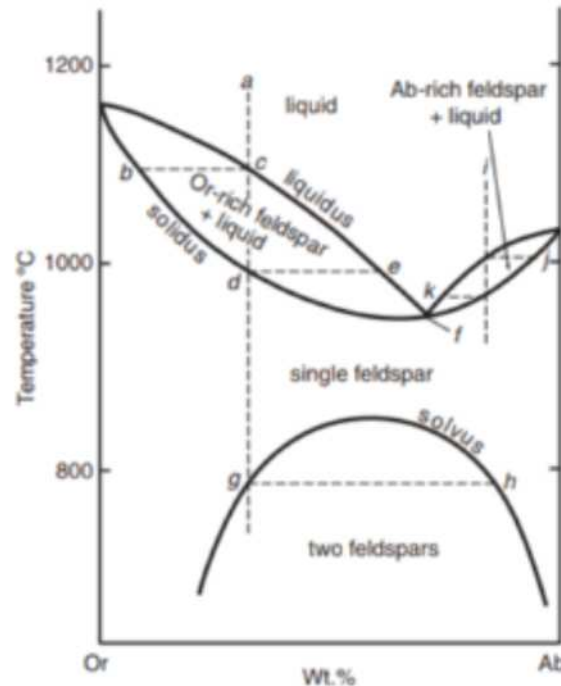


Figure 19: T-X phase diagram of albite-orthoclase system at 0.2 GPa H_2O pressure
(Source: Winter 2009: p. 116)

12. Texture

When a high temperature feldspar cools, albite separates and appears as small grains, blebs or streaks within it. The resulting mixtures are termed perthites. Perthitic texture may be coarse and easily visible as slight variation in colour in the crystal, or it may be microscopic and practically invisible. The coarseness of the texture depends mostly on the rate at which the feldspar was cooled. The slower the cooling, the coarser the texture. The separation most commonly results in thin layers of albite in a host crystal of K-feldspar (KAlSi_3O_8). Such intergrowths are known as perthites and are the result of exsolution. In the albite-orthoclase series the exsolution lamellae are roughly parallel to $\{100\}$ (Klein 2002).

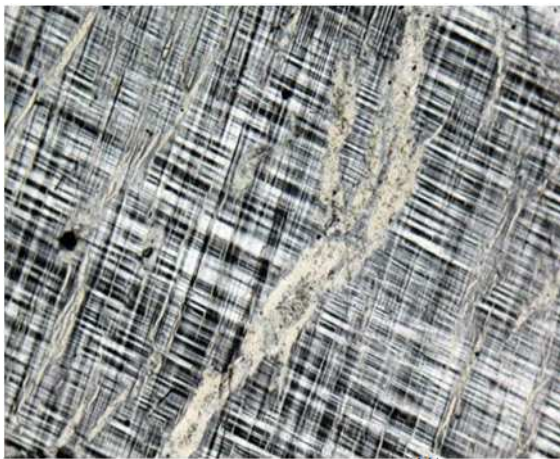


Figure 20: Perthite under microscope.^[14]

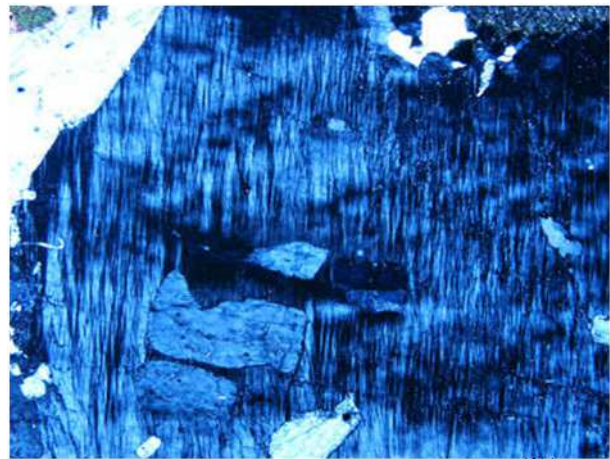
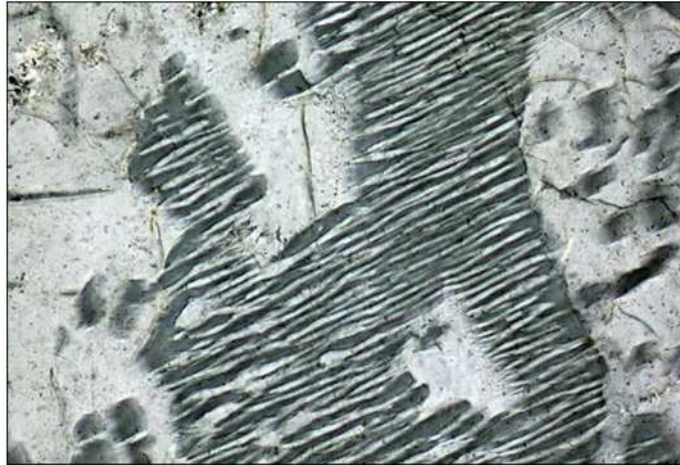


Figure 21: Microperthite under microscope.^[15]

Intergrowth	Visibility
Macropertthite	visible to naked eyes,
Microperthite	visible only by optical microscope
Cryptoperthite.,	detectable only by X-ray or electron microscope techniques,

Table 9. Types of intergrowths

Figure 22: Antiperthite under microscope.^[16]

More rarely, the host mineral is a plagioclase feldspar and the lamellae are of alkali-feldspar (KAlSi_3O_8) composition; this is called antiperthite.

13. Conclusion

From the above discussion it can be concluded that ‘Feldspar’, a large group of rock forming silicate minerals in the Earth's crust, form different textures in their structures resulting in varying colours with change of temperature sometimes. They are of two types—alkali feldspar and plagioclase feldspar. They show polysynthetic twinning textures that can give important information about their genesis.

Acknowledgement

We would like to express our sincere gratitude to our mentor Chandrabali Mukhopadhyay, Department of Geology, Jogamaya Devi College for her valuable suggestions.

References

- Klein C., 2002, The Manual of The Mineral Science, 23rd edition, John Wiley & Sons (after James. D. Dana)
- Mason, B & Moore,. B, 1982, Principles of Geochemistry, 4th edition, John Wiley & Sons, New York.
- Papike, J. J., Cameron, M., 1976. Crystal chemistry of silicate minerals of geophysical

interest. Reviews of Geophysics and Space Physics 14:67.

Putnis, A., McConnell, J. D. C., 1980. Principles of mineral behaviour. Oxford, England, Figure 7.8, reprinted with permission)

Ribbe, P. 1987. Feldspar. McGraw-Hill Encyclopedia of science and Technology, 6th ed., v.7, 38-47, New York, McGraw-Hill Book Co., copyright 1987. Reproduced with permission of The McGraw-Hill Companion.

Smith, J. V., W. L. Brown. 1988. Feldspar minerals 1. Spring Verlag, New York. (Fig 1.2)

Winter, J. D, 2009, Principles of Igneous and Metamorphic Petrology, 2nd edition, Prentice Hall

Weblinks

- [1] <https://image.slidesharecdn.com/lecture3-feldspar-130407160732-phpapp02/95/lecture-3-feldspar-group-and-its-application-5-638.jpg?cb=1515417190>
- [2] http://www.pitt.edu/~cejones/GeoImages/1Minerals/1IgneousMineralz/Feldspars/KSpar_IrregFract.jpg
- [3] <https://plagioclasefeldspar.weebly.com/uploads/4/3/2/7/43273749/864011344.jpg>
- [4] <https://image.shutterstock.com/image-photo/natural-specimen-microcline-feldspar-split-260nw-774382924.jpg>
- [5] [https://www.alexstrekeisen.it/immagini/pluto/microclino2013\(2\).jpg](https://www.alexstrekeisen.it/immagini/pluto/microclino2013(2).jpg)
- [6] <https://geology.com/minerals/photos/feldspar-classification.gif>
- [7] <https://cdnb.artstation.com/p/assets/images/images/018/669/617/large/lina-jakaite-feldspars-1920x1920-cc-by-nc-lina-jakaite-strike-dip-com.jpg?1560265278>
- [8] <https://www.cefns.nau.edu/geology/naml/Meteorite/Images/FeldsparOrdering.png>
- [9] https://upload.wikimedia.org/wikipedia/commons/f/f6/Albite_-_Crete_%28Kriti%29_Island%2C_Greece.jpg
- [10] <https://en.wikipedia.org/wiki/File:Anorthite-221029.jpg>
- [11] <https://www.tulane.edu/~sanelson/images/phdfig3.gif>
- [12] <https://www.tulane.edu/~sanelson/images/phdfig4.gif>
- [13] [https://www.alexstrekeisen.it/immagini/pluto/pertitimicroclino0025\(8\).jpg](https://www.alexstrekeisen.it/immagini/pluto/pertitimicroclino0025(8).jpg)
- [14] <https://people.carleton.edu/~bhaileab/Petrology/Thinsections/images/biaxial%20minerals/feldspars/BH250-13%20microperthitex.jpg>
- [15] [https://www.alexstrekeisen.it/immagini/pluto/antipertite\(51\).jpg](https://www.alexstrekeisen.it/immagini/pluto/antipertite(51).jpg)
- [16] <https://www.astronomynotes.com/solarsys/carbon-thermostat.png>

Plate Tectonics and Carbon Dioxide Balance in Atmosphere

Nabanita Barik¹, Nrittwika Barui² and Dakshi Sarkar³

Students of 4th Semester Geology Honours Course

¹www.nabanitabarik16@gmail.com, ²nrittwika@gmail.com, ³dakshisarkar98@rediffmail.com

1. Introduction

Plate tectonic processes influence all the major factors that are currently thought to determine the earth's long-term changes in climate (Figure 1). The concentration of CO₂ in the atmosphere, at any particular point in time, is thought to be determined largely by the amount of volcanism at that time (Condie 1997).

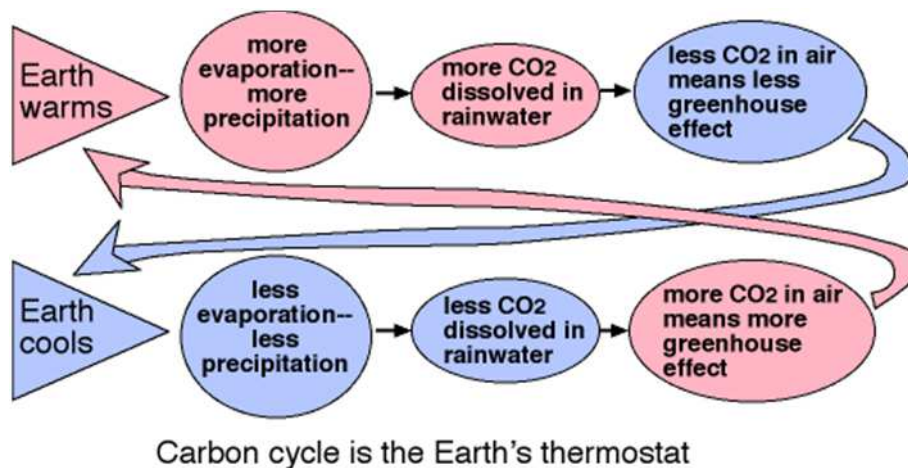


Figure 1: Carbon dioxide effect on Earth Climate^[1].

Thus, the exceptionally high level of CO₂ associated with “Greenhouse Earth” of the Cretaceous period (Figure 2) are related to super plume activity and high rates of sea floor spreading and subduction, all three giving rises to enhanced volcanic activity. Conversely, systematic decreases in plume activity, and plate accretion and destruction, would cause global cooling (Figure 3).

2. Plate Tectonics

Tectonic plates are pieces of the rocky outer layer of the Earth known as the crust.^[2] There are a number of different types of plate boundary.

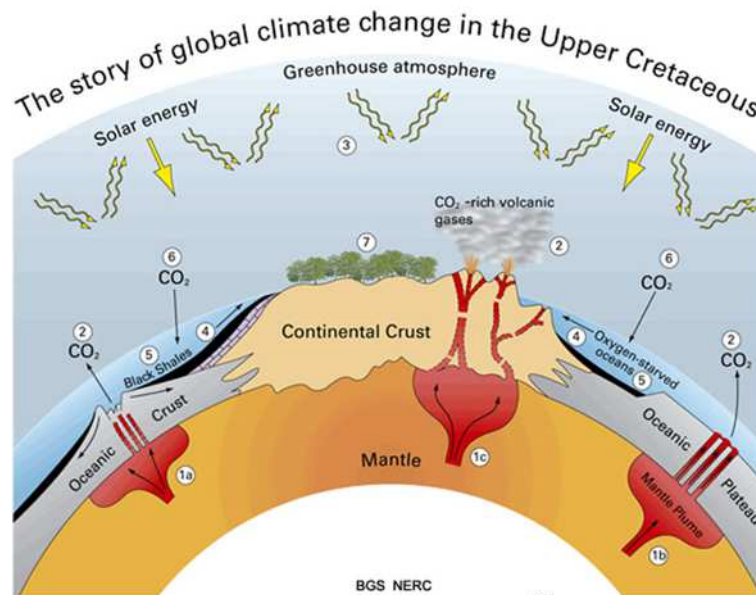


Figure 2: Greenhouse Earth.^[3]

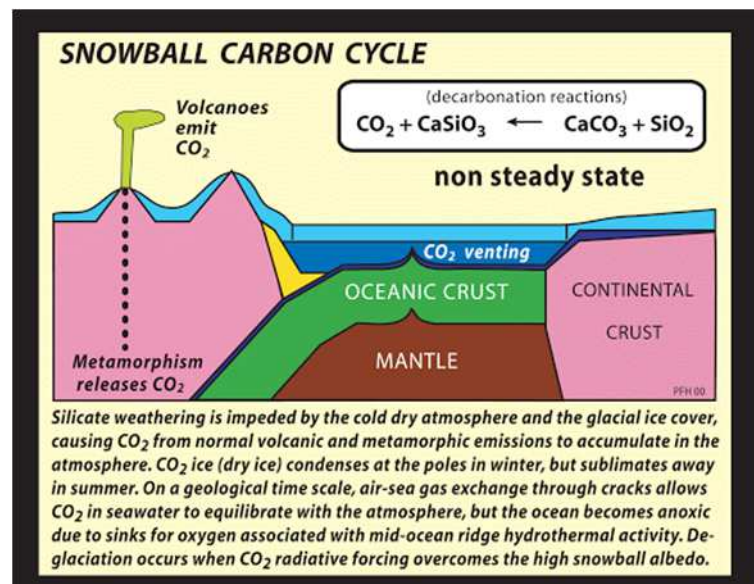


Figure 3: Snowball Earth.^[4]

2.1 Destructive plate boundary

Destructive plate boundary is sometimes called a convergent or tensional plate margin (Figure 4A). This occurs when oceanic and continental plates move together. The oceanic plate is forced under the lighter continental plate.

An example of a destructive plate boundary is where the Nazca plate is forced under the South American Plate.

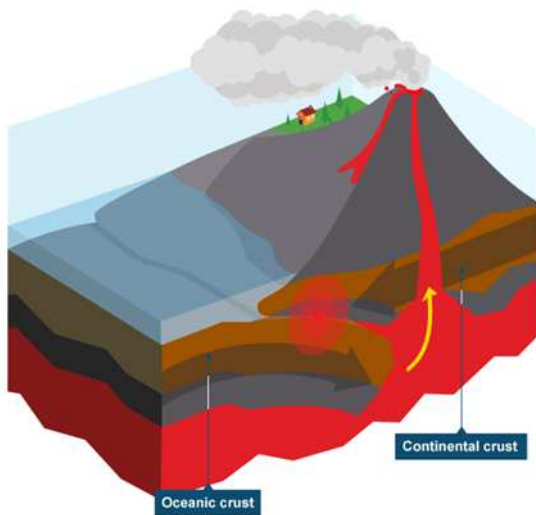


Figure 4A: Convergent plate boundary.^[5]

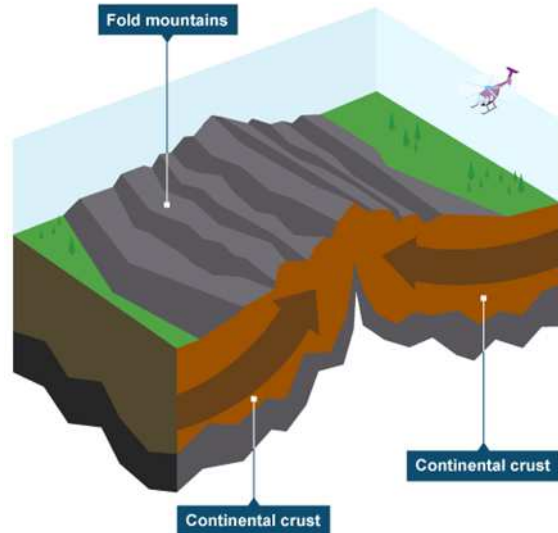


Figure 4B: Collision zones.^[6]

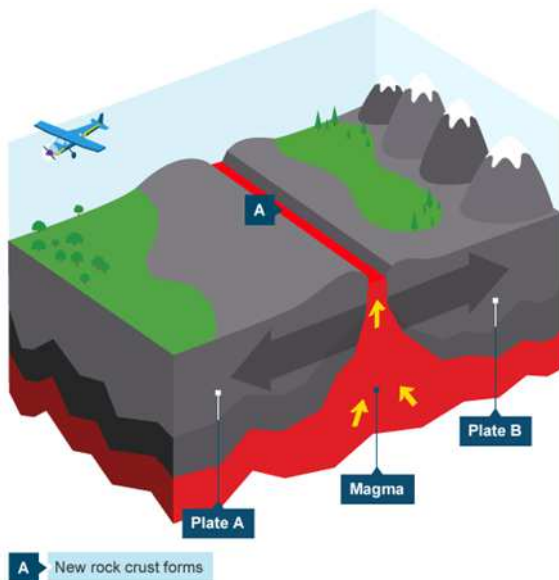


Figure 4C: Divergent plate margin.^[7]

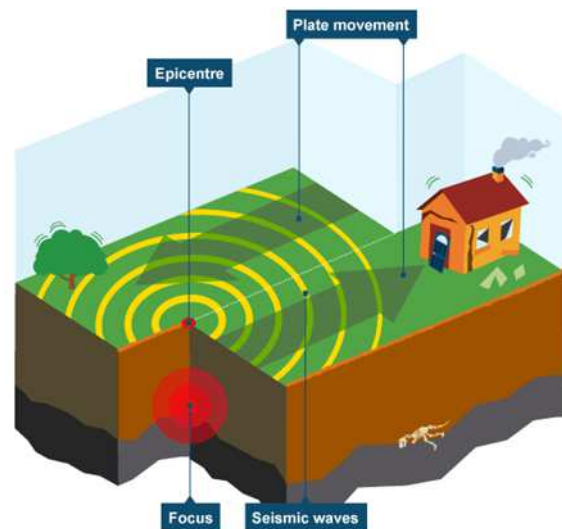


Figure 4D: Transform plate margin.^[8]

2.2 Collision zones

Collision zones form when two continental plates collide (Figure 4B). Neither plate is forced under the other, and so both are forced up and form fold mountains.

2.3 Constructive plate boundary

A constructive plate boundary, sometimes called a divergent plate margin (Figure 4C), occurs when plates move apart. Volcanoes are formed as magma wells up to fill the gap and eventually new crust is formed.

An example of a constructive plate boundary is the Mid-Atlantic Ridge.

2.4 Conservative plate boundary

A conservative plate boundary, sometimes called a transform plate margin (Figure 4D), occurs where plates slide past each other in opposite directions, or in the same direction but at different speeds. This occurs at the San Andreas Fault in California.

3. Significance of carbon dioxide in Mid-Oceanic Ridge

The sea floor spreading theory is one hypothesis introduced to suggest a mechanism of controlled CO₂ levels in the atmosphere, causing the observed variations between warm CO₂ rich greenhouse intervals and CO₂-depleted global cooling intervals.^[9]

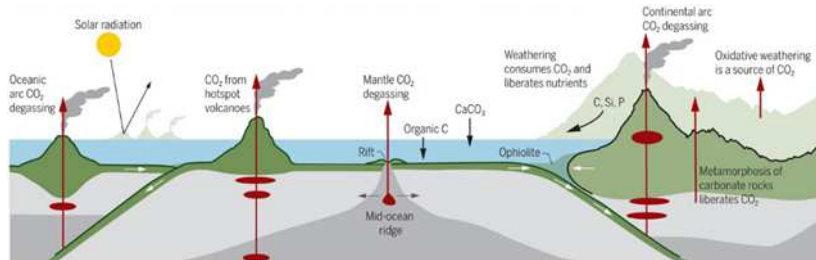


Figure 5: Carbon dioxide degassing at mid oceanic ridge.^[10]

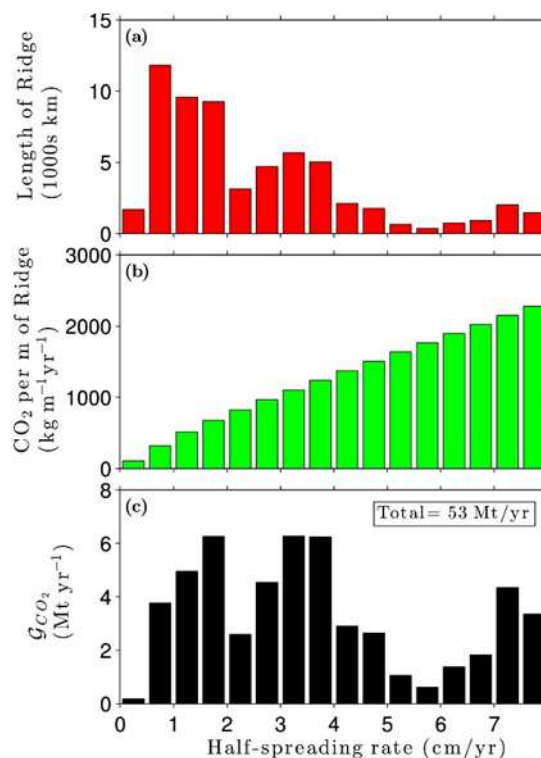


Figure 6: Variation in mid oceanic ridge CO₂ emissions.^[11]

This theory focuses the control of CO₂ levels on plate tectonics processes. During plate tectonics, carbon is cycled endlessly between the Earth’s interior and its surface. It is this cycling of carbon in different stages that defines whether global warming or global cooling intervals predominate.

Rock deep within the Earth exists as magma, which contains a rich supply of gases. As the magma rises to the surface during volcanic activity, CO₂ escapes at the plate margins—such as at oceanic ridges where volcanoes are commonly found. Most CO₂ enters the atmosphere at the margins of divergent plates where the hot magma carrying CO₂ erupts right into the ocean water. These areas are the oceanic ridges. One of the best known is the Mid-Atlantic Ridge (Figures 5 & 6).

Carbon dioxide is a relatively inert and abundant magmatic gas (Gerlach & Graeber 1985) that is relatively insoluble in melt and therefore exsolves at depth (Pan et al. 1991, Papale et al. 2006). CO₂ is emitted both actively through channelizing conduits (Aiuppa et al. 2014, de Moor et al. 2016b) and diffusely through the porous volcanic edifice (Allard et al. 1991, Chiodini et al. 1996, 1998, 2001, Hernández et al. 1998, 2001, Hernández Perez et al., 2003). As a fluid, its transportation occurs in two different ways: (1) Diffusion according to the Maxwell–Stefan diffusion model which is used instead of Fick's law for multicomponent systems (Maxwell 1965, Bird et al. 2001), and (2) viscous flow which is described by Darcy's law in a porous media (Bird et al. 2001). Gas transport is thus assumed to be the result of both diffusion and viscous flow contributions (Chiodini et al. 1998, Carapezza & Granieri 2004).

4. Significance of Carbon-dioxide in island arc

Convergent boundaries are places where two plates are moving towards each other or colliding. Most plate convergence happens where an oceanic plate is pushed or subducted beneath another plate, either oceanic or continental, forming a line of volcanoes on the overriding plate. This line of volcanoes is known as a magmatic arc and specifically as an island-arc if built on oceanic crust or an Andean arc if built on continental crust. When continents on this plate collide, the rocks that were deposited along their margins, typically under water, are uplifted in the collision zone and exposed to weathering processes^[12]. The weathering of this rock, particularly the limestone and carbonate rocks, causes chemical reactions where the CO₂ in the atmosphere reacts with the product of weathering and forms new carbonate (CaCO₃) that gets deposited in the oceans^[13] (Figure 7).



Figure 7: From Sea Floor to Terrestrial Weathering.^[14]

Continental collisions are thus associated with the overall removal of CO₂ from the atmosphere and help promote global cooling (Figure 8).

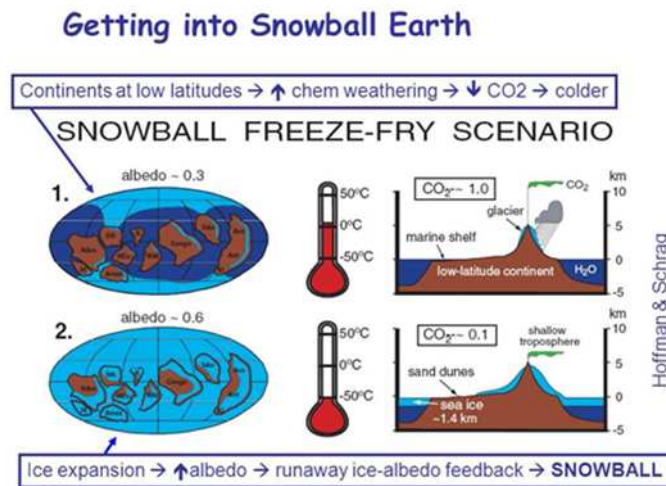


Figure 8: Snowball Earth Timeline^[15].

5. Plate tectonic control on atmospheric CO₂ level

A mechanism capable of regulating the strength of the atmospheric greenhouse effect, and thus counteracting the spatial and temporal variations in solar luminosity, exists via the long-term carbon cycle (Figure 9), which controls atmospheric CO₂ concentrations (Berner 2004).

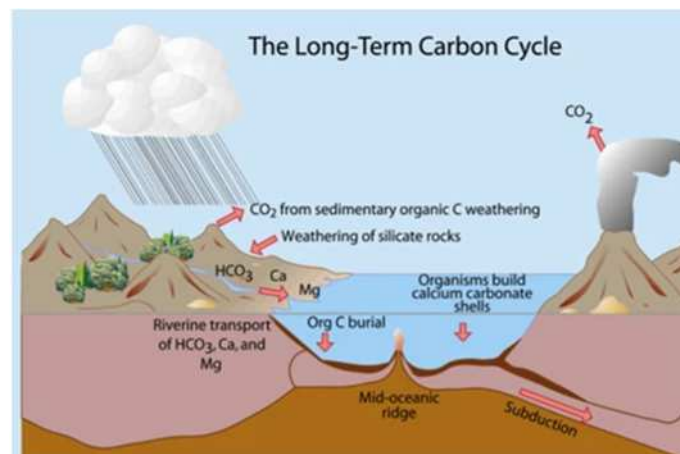


Figure 9: Long-term carbon cycle.^[16]

The long-term carbon cycle refers to the cycling of CO₂ between the atmosphere and ocean, carbonate rocks on the seafloor, and the mantle. Weathering of silicate minerals on continents and in the oceanic crust draws CO₂ out of the atmosphere and ocean, depositing it on ocean plates in the form of carbonate rocks. CO₂ resides on the seafloor until it is subducted, where some portion of the carbon reaches the deep mantle, and the rest is returned to the atmosphere through metamorphic degassing and arc volcanism. The carbon in the mantle eventually degasses back to the atmosphere and ocean at mid-ocean ridges, completing the cycle.

Plate tectonics plays a vital role in the operation of the long-term carbon cycle (Figure 10). Plate tectonics drives volcanism at ridges and arcs, the major sources of atmospheric CO₂, and facilitates silicate weathering, the primary sink of atmospheric CO₂, by providing a continuous supply of fresh, weatherable rock through orogeny and volcanic resurfacing.

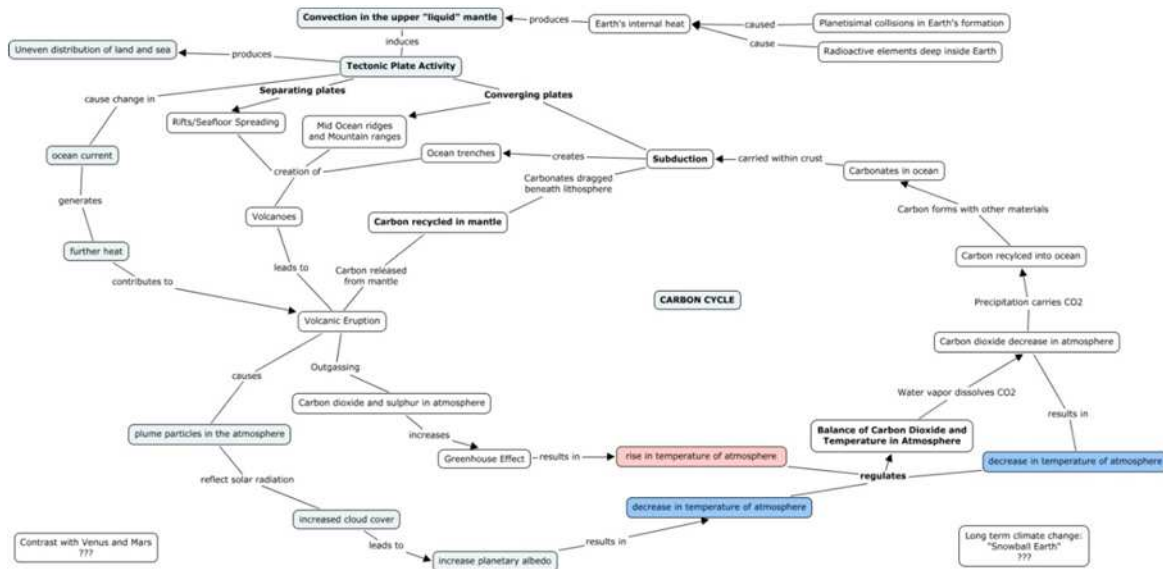


Figure 10: Plate Tectonic Activity and Carbon Cycle.^[17]

6. Conclusion

Plate tectonics is a scientific theory describing the large-scale motion of seven large plates and the movements of a larger number of smaller plates of the Earth's lithosphere. Plates interact at three types of plate boundaries: divergent, convergent and transform. Most of the Earth's geologic activity takes place at plate boundaries. Climate trends controlled by changes in solar luminosity, continent distribution and atmosphere composition. Plate tectonics affect not only in geography but also atmosphere composition through volcanic degassing of CO₂ at subduction zones and Mid-Ocean Ridges.

Acknowledgement

We hereby express our sincere gratitude to our mentor Chandrabali Mukhopadhyay, Department of Geology, Jogamaya Devi College, who helped in several ways while preparing this project.

References

- Berner, R. 2004. The Phanerozoic Carbon Cycle. Oxford Univ. Press.
- Condie, K. C., 1997. Plate tectonics and crustal evolution, 4th Ed., Butterworth-Heinemann, Oxford, 249p.

Weblinks

- [1] <https://www.astronomynotes.com/solarsys/carbon-thermostat.png>
- [2] <https://www.bbc.co.uk/bitesize/guides/zyhv4wx/revision/2>
- [3] <https://www.bgs.ac.uk/discoveringGeology/climateChange/greenHouseEarth.html>
- [4] <http://www.snowballearth.org/slides/Ch8-7.gif>
- [5] <https://bam.files.bbc.co.uk/bam/live/content/zkfk2hv/large>
- [6] <https://bam.files.bbc.co.uk/bam/live/content/z8y8mp3/large>
- [7] <https://bam.files.bbc.co.uk/bam/live/content/zdvdxnb/large>
- [8] <https://bam.files.bbc.co.uk/bam/live/content/zw3w6sg/large>
- [9] www.climate-policy-watcher.org/earth-surface-2/control-of-co2-by-seafloor-spreading.html
- [10] <https://science.sciencemag.org/content/sci/364/6436/126/F1.large.jpg>
- [11] https://ars.els-cdn.com/content/image/1-s2.0-S0012821X15003945-gr009_lrg.jpg
- [12] www.astrobio.net/biosphere/earths-breathable-atmosphere-tied-plate-tectonics/
- [13] www.climate-policy-watcher.org/plate-tectonics-and-climate.html
- [14] https://earthobservatory.nasa.gov/ContentFeature/CarbonCycle/images/san_gabriel_river.jpg
- [15] <https://i.pinimg.com/originals/7f/c4/5d/7fc45dcd18866ffb1511cdc9012066bf.jpg>
- [16] https://d32ogoqmya1dw8.cloudfront.net/images/eslabs/carbon/long_term_geological_carbon.jpg
- [17] <https://cmapspublic3.ihmc.us/rid=1KXSZGGHT-B4WJ9L-1XLY/Tectonic%20Plate%20Activity2.cmap>

Dendrochronology and Relative Age Dating

Aettree Karmokar¹, Bipasa Roy² and Susmita Mandal³

Students of 3rd Year Geology Honours Course

¹aettreekarmokar99@gmail.com, ²roy9bipasa31@gmail.com, ³mandalsusmita575@gmail.com

1. Introduction

Dendrochronology provides some of nature's most accurate evidences of the past. The rings in the cross-section of the tree trunk may hold evidences of drought and climatic changes, insect attacks, lightning strikes and even earthquake, forest fire and volcanic eruptions.

A tree ring consists of two different layers:

(A) A light-coloured layer (Figure 1) formed during the time of spring

(B) A dark coloured layer (Figure 1) during the dry late autumn

Scientists rely on data that are collected from tree rings to find out the extent, speed and effects of local or worldwide changes in the past.

Dendrochronology is a dating technique that utilises the common growth signal in trees of the same species growing in the same area under similar ecological conditions (Schweingruber 1996, Cleaveland and Stahle 2004).

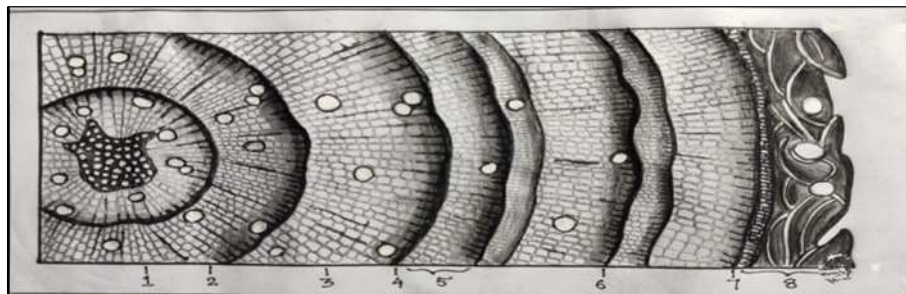


Figure1: Cross section of a typical conifer stem showing: (1) pith, (2) resin ducts, (3) earlywood cells, (4) latewood cells (dark), (5) annual rings (6) false intra annular rings, (7) cambium and (8) bark (Representative figure after Ferguson 1970, p.188)

2. Historical Background

In the early 15th century Leonardo da Vinci recognized a relationship between tree ring widths and precipitation. By the mid-19th century, the ecological foundation of dendrochronology was established based on Theodore Harting's study of wood structures and annual tree ring development. Later, by the early 20th century dendrochronology and tree ring studies developed into a science largely through the works of American astronomer Andrew Ellicott Douglass (Figure 2) (in Smithand Lewis 2007).

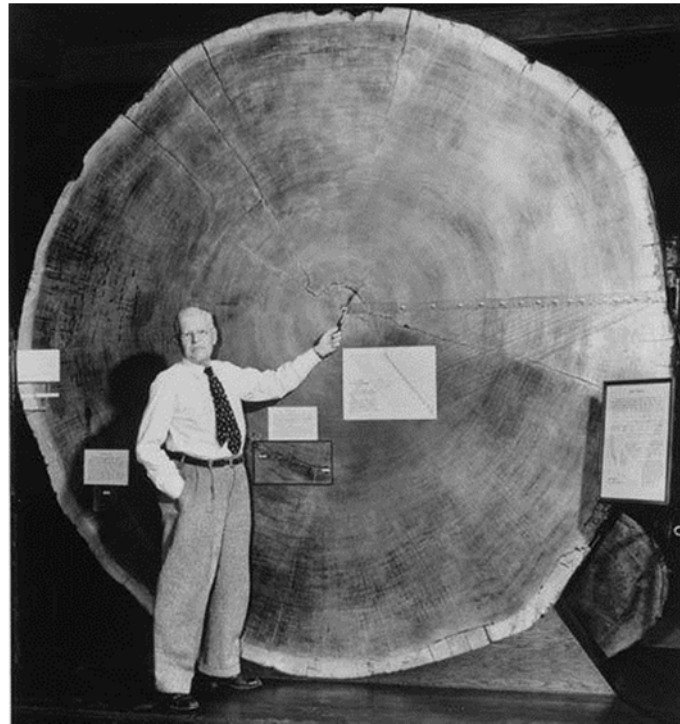


Figure 2: A.E. Douglass^[1].

3. Process of Dendrochronology

Figure 3 shows the sequential steps of dendrochronology.

Figure 4 represents the measurement of tree ring followed by development of entire tree ring chronology.

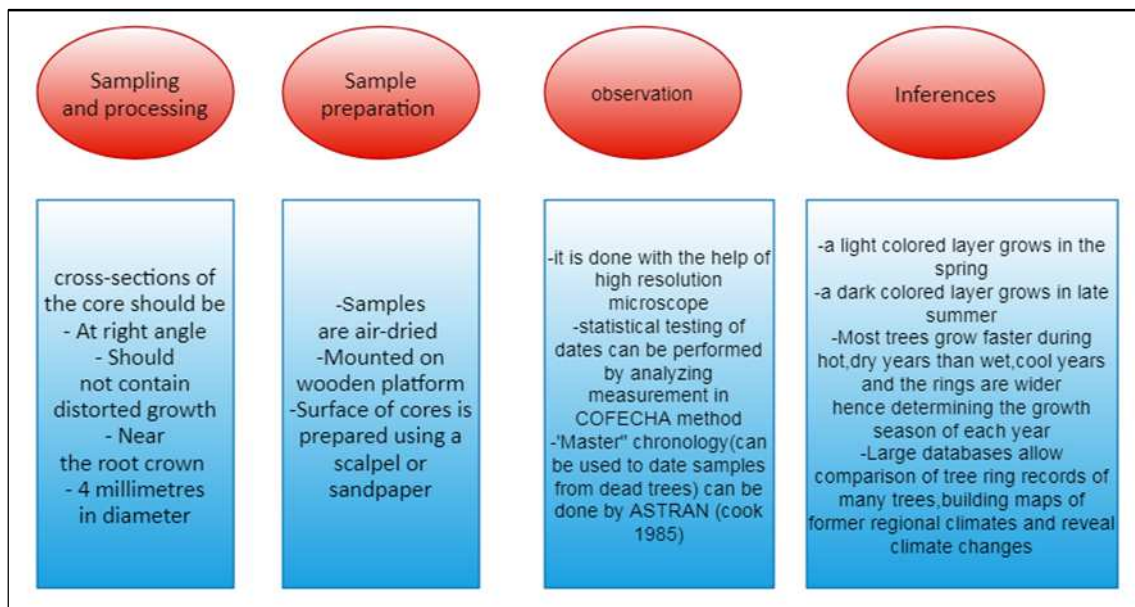


Figure 3: Process of Dendrochronology (see Torbenson 2015)

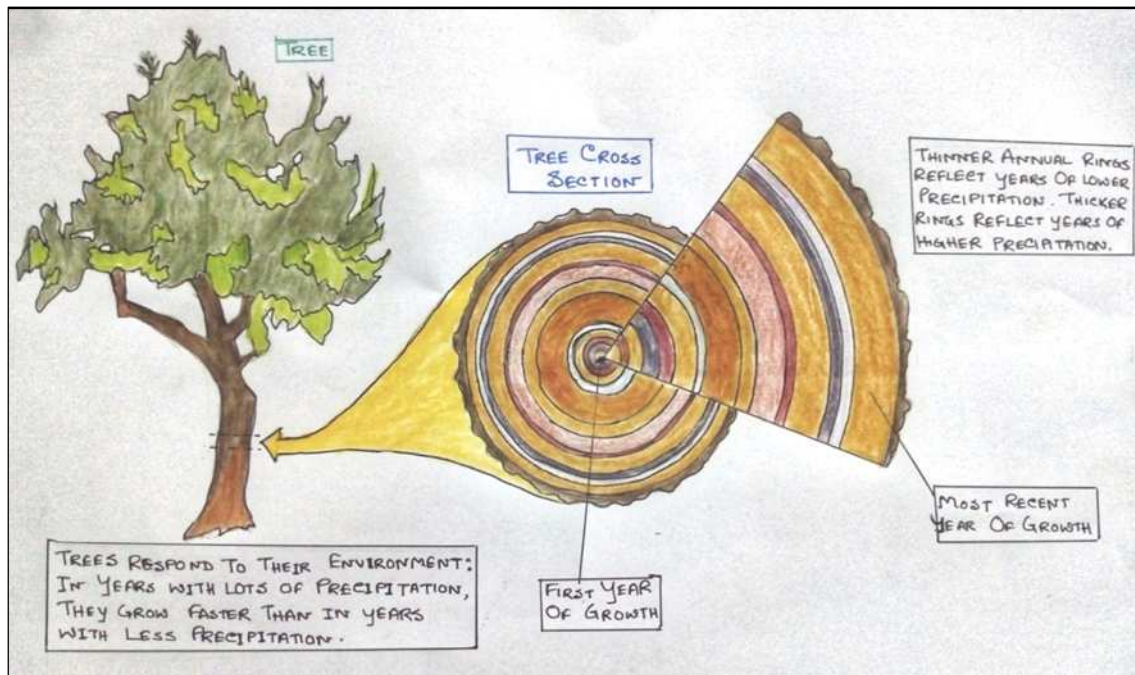


Figure 4: Inferences from dendrochronological study^[2].

4. Factors Influencing the Development and Formation of Tree Rings Having Same Cross-section

Abiotic Factors

Temperature: An increase in temperature forms denser tree rings due to increased productivity (Grace 1988), while fall in the temperature, snowfall, fire, or storm will make the tree rings wider.

Precipitation: Changes in the intensity of precipitation will induce formation of the tree rings of variable thicknesses due to their differences in growth pattern under different conditions (Figure 5).

Wind: A unidirectional wind results in the deformation of the tree-crown and it forms an eccentric stem cross-section (Figure 6).

Light: A tree growing beneath a dense canopy receives only poor illumination, resulting in a drastic reduction in ring width than a large tree receiving direct sunlight which forms wider rings (Figure 7) (Schweingruber 1993).

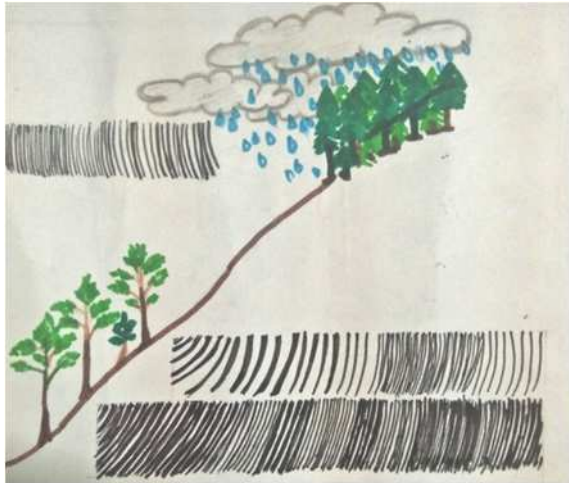


Figure 5: variation of tree rings due to change in precipitation (Schweingruber 1993).

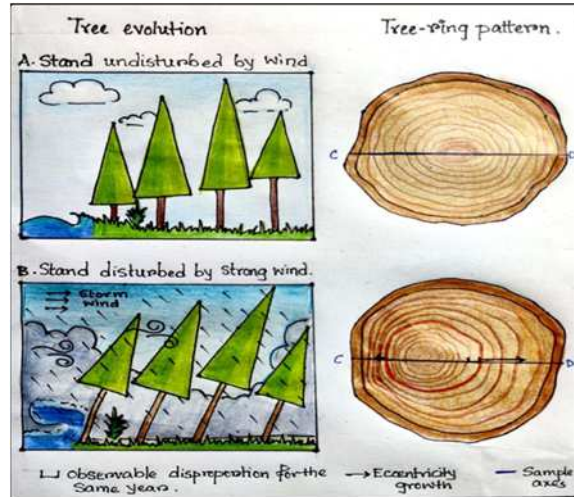


Figure 6: Growth rings in areas of heavy wind (after Pouzet et al. 2018).

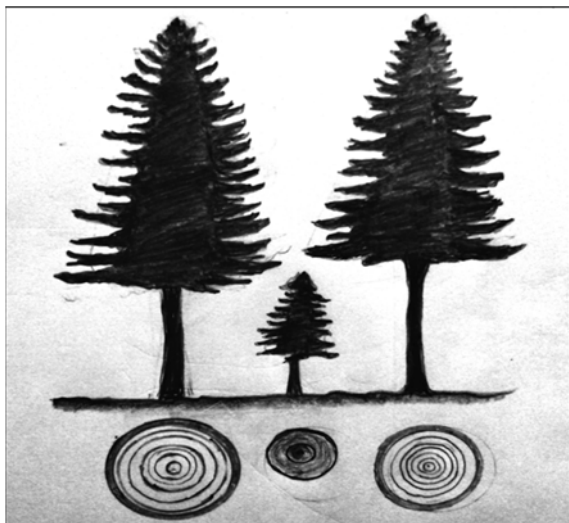


Figure 7: Tree rings variation due to sunlight (Schweingruber 1993.)

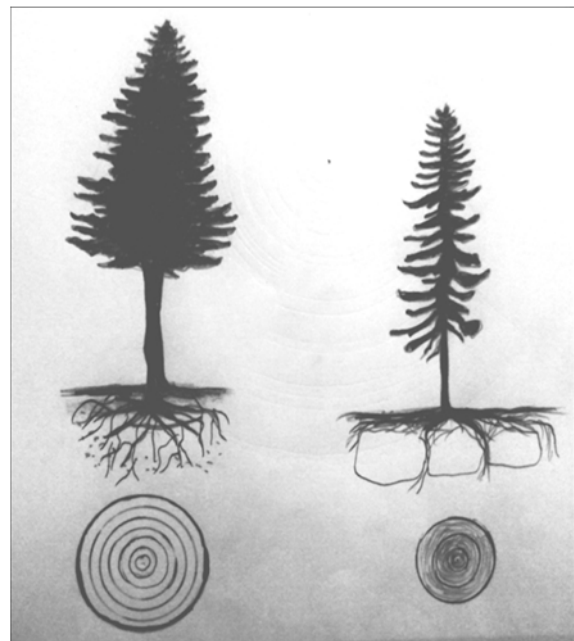


Figure 8: Different root systems in variable soil type showing differing tree rings (Schweingruber 1993.)

Biotic Factors:

Biotic factors include soil, tree age, genetic differences, human disturbances, herbivore impact, pest outbreaks, diseases and CO₂ concentration.

Large trees which are deep-rooted within fine, moist subsoil with a compact crown show wide tree rings than shallow-rooted trees growing in rocky, dry subsoil with loose crowns^[3] (Figure 8).

5. Applications of Dendrochronology

In Geological Past

Glaciology: Establishment of the number of rings in trees may be used to date glacial deposits and moraines (Luckman 1988)

As surface becomes devoid of ice, germinating trees from nearby areas may colonize the place. Hence the minimum age of glacial retreat in an area can be determined from the pith of the oldest tree in that landform (Lauren 1950) (Figure 9). Furthermore, the rates of ice front recession over time can be determined through multiple sampling.

Dating glacial retreats through dendrochronology is often accompanied by lichenometry to minimize uncertainty (Torbenson 2015.)

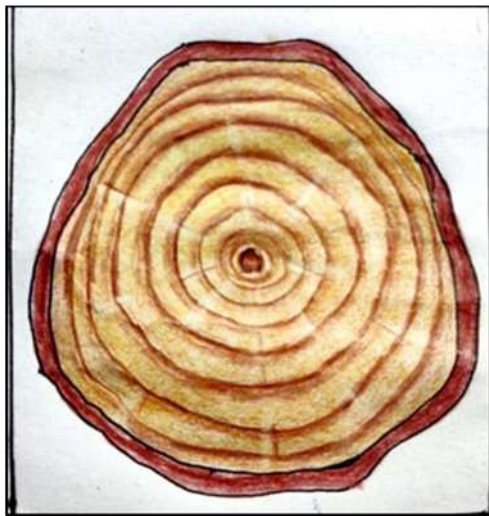


Figure 9: A cross-section from a young sub-Alpine fir (*Abies lasiocarpa*) illustrating the annual concentric ring (after Lewis 2006).

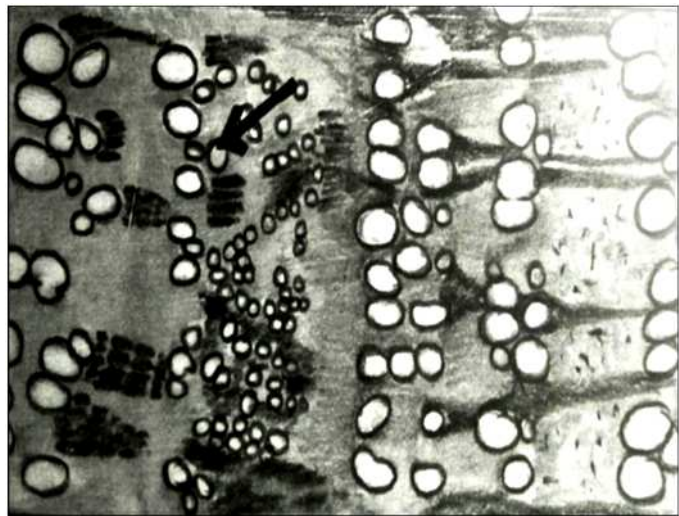


Figure 10: Shrunken and extending vessels growth left-to-right due to flooding (Torbenson 2015).

Volcanic events: Briffa et al. 1988, using tree ring density chronologies established the impact of major volcanic events in the Northern Hemisphere since the 15th century.

In 1756-58, sub-fossil material from Kamchatka, Russia was used to date an eruption of Shiveluch volcano.

An anomalous series of narrow rings in the nearby region of Mount St. Helens may be explained by pyroclastic surges caused by the 1842-43 eruption of the mountain.

Cinder cone eruption results in increase in levels of Na, S and P in the ring (Torbenson 2015).

In Recent Times (Holocene)

Seismology: Trees may fall over and/or be buried by rapid debris flow or landslides activated by the earthquakes (Jacoby 1997). The study of the cross section along the West Coast of the

United States has helped to link it to a large Cascadia earthquake in 1700 A. D. showing high synchronization in tree ring pattern of the event (Atwater and Yamaguchi 1991).

Flooding: Yanosky (1983) studied the considerably larger cells (Figure 10) in the latewood of 1972 than in any other year around the Potmac River, Washington D. C. This anomalous growth of tree cells in the cross section was linked with the flood in that year (Torbenson 2015).

6. Comparative Study with Other Methods

Correlation is a basic statistical tool in dendrochronology, which is widely used to identify the monthly or seasonal climate variation related to ring width pattern (Fritts 1973). Dendrochronology or tree-ring dating provides absolute dates in two different ways, i.e. directly or by calibrating radiocarbon methods.

Relative age dating is a scientific technique of determining the relative order of past events, without necessarily finding their absolute age. Cross-dating of ring width patterns in living trees allows for the identification of comparable patterns in undated wood samples; thereby providing a way to develop tree ring chronologies that extend back in time beyond the age of living trees or to date an event.

As the wood can be dated directly and by radiocarbon, scientists use bristlecone pines to calculate a calibration curve and convert radiocarbon results into accurate calendar dates. With the help of dendrochronology combined with the technique of absolute age dating, the accuracy of sample dating is more dependable (Cleaveland & Stahle 2004, Smith & Lewis 2007)

7. Advantages and Disadvantages of Dendrochronology

Advantages

Tree rings provide valuable chronological information when there are no absolute dates. It can also facilitate the reliability of radiometric dating method.

In places where sub-fossils or archaeological material do not exist, the germination date of the oldest living tree becomes the ultimate limit of dating of the samples.

Disadvantages

Not all trees show coherent inter-annual growth variability over space making it difficult for cross dating.

The temporal range to which trees can be dated may differ depending on species and region. Some samples may not show the presence of all the rings from pith to bark due to low preservation rate or sampling difficulties.

Despite this disadvantages, by combining dendrochronology with other methods like absolute age dating, lichenometry etc. (geomorphic method of geochronologic dating which uses lichen growth to determine the age of exposed rock), it not only acts as a dependable informer about a tree's history but also that of the ecosystem in which it lives (Torbenson 2015).

8. Conclusion

Dendrochronology has proved to be an invaluable tool for dating events. Dendrochronology not only offers the potential of unequalled dating exactness but it can also help the researchers to know about the spatial extent of past landscape change. The on-going development of long tree-ring chronologies offers opportunities to develop paleoenvironmental reconstructions at local to hemispheric scales. Since evidence of geomorphic processes recorded in trees can be caused by different factors, it is suggested to use multiple lines of evidence, like death and establishment, sudden changes in growth rate, structural features and in some cases chemical composition (Torbenson 2015).

Acknowledgement

We would like to express our gratitude to our mentor Keya Bandyopadhyay for her sincere guidance and valuable suggestions.

References

- Cleaveland, M.K., Stahle D. W. 2004. Introduction to Dendrochronology. Lab exercise #4: Tree-ring Reconstruction of Precipitation, 1-14 (Study material of SUNY College of Environmental Science and Forestry: Source: www.esf.edu/for/bevilacqua/for496/Lab04_treering_reconstruction_of_ppte.pdf)
- Ferguson, C. W., 1970. Concepts and techniques of dendrochronology, University of California Press Berkeley, Los Angeles, London.
- Pouzet, P. et al., 2018. Sedimentological and dendrochronological indicators of coastal storm risk in western France. *Ecological Indicators*, 90, pp.:401-415.
- Schweingruber, F. H., 1993. Trees and wood in dendrochronology: morphological, anatomical, and tree-ring analytical characteristics of trees frequently used in dendrochronology, Berlin: Springer Science & Business Media. 1-419.
- Smith, D., Lewis, D., 2007. Dendrochronology. University of Victoria, Victoria. Amsterdam: Elsevier. 1-7

Torbenson, M. C. A. 2015. 4.2.8. Dendrochronology. University of Arkansas. British Society of Geomorphology. ISSN 2047-0371.1-1

Weblinks

- [1] <https://alchetron.com/cdn/a-e-douglass-fe759e78-7172-4673-8cde-c41ae55dbf6-resize-750.jpeg>
- [2] <https://www.crowcanyon.org/index.php/dendrochronology>
- [3] <https://en.wikipedia.org/wiki/Dendrochronology>

Mohr Circle: Its Applications in the Representation and Measurement of Stress

Anwesa Sen¹ and Debapriyaa Chakraborty²

Students of 3rd Year Geology Honours Course

¹senanwesa29@gmail.com, ²jhimli.chakraborti@gmail.com

1. Introduction

This article deals that representation and measurement of stress can be a matter of no stress at all. An easy and convenient method for this, the Mohr diagram, was introduced in the nineteenth century by the German engineer Otto Mohr (Fossen 2016). It expresses the relationship between the orientation of a plane and the values of normal and shear stress components acting on it in an “XY-type” plot where the horizontal and vertical axes represent σ_n (normal stress) and σ_s (shear stress) respectively.

2. How to measure stress by Mohr Circle

The principal stresses are plotted on the σ_n axis (abscissa) – the tensile and the compressional stresses are plotted on the negative and the positive sides of this axis respectively.

The Mohr Circle is the circle constructed in this coordinate system, with its centre on the abscissa, and its diameter representing the differential stress, i.e. the difference between σ_1 and σ_3 .

If θ is the angle between normal to the plane and σ_1 , then angle between radius to the point on the circle and horizontal axis is 2θ .

Both the positive and negative values of the normal and the shear stresses can be represented in this diagram.

3. Normal and shear stresses on a plane in a homogeneous stress field as a function of the principal stresses

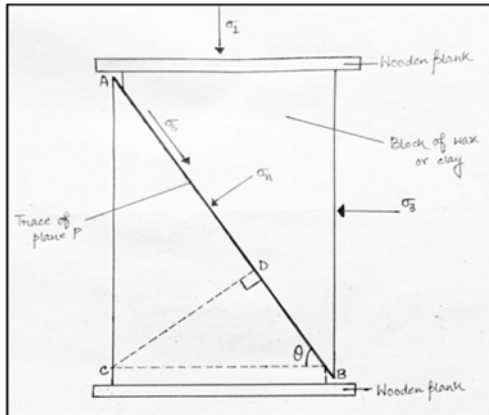


Figure 1: Determination of the normal and shear stresses on a plane whose normal makes an angle θ with σ_1 . (After Van der Pluijm & Marshak 2004)

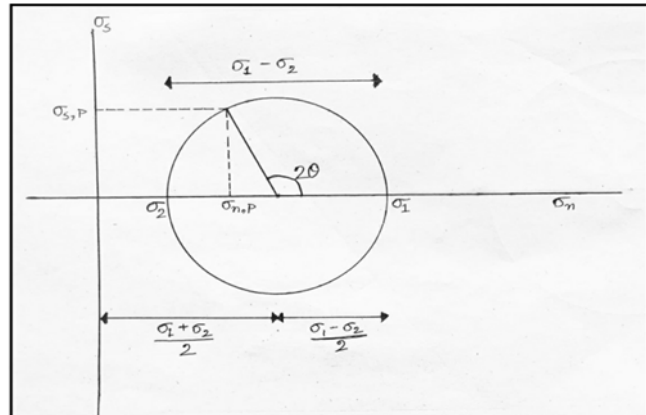


Figure 2: Mohr circle representing two-dimensional stress. (see Van der Pluijm & Marshak 2004).

Let the length of the given plane be l , breadth b and thickness t .

Total force in the vertical direction: $F_1 = \sigma_1 bt$

Total force in the horizontal direction: $F_3 = \sigma_3 bt$

Area of the given plane is $bt \sec \theta = lt / \sin \theta$

Normal force acting on given plane due to $F_1 = F_1 \cos \theta = \sigma_1 bt \cos \theta$

Normal stress on given plane due to $F_1 = \sigma_1 bt \cos \theta / bt \sec \theta = \sigma_1 \cos^2 \theta$

Normal force acting on given plane due to $F_3 = F_3 \sin \theta = \sigma_3 lt \sin \theta$

Normal stress on given plane due to $F_3 = \sigma_3 lt \sin \theta / lt / \sin \theta = \sigma_3 \sin^2 \theta$

Total normal stress acting on the given plane $\sigma_n = F_1 + F_3$

$$= \sigma_1 \cos^2 \theta + \sigma_3 \sin^2 \theta$$

$$= \sigma_1 \cos^2 \theta + \sigma_3 (1 - \cos^2 \theta)$$

$$= \sigma_1 \cos^2 \theta + \sigma_3 - \sigma_3 \cos^2 \theta$$

$$= (\sigma_1 - \sigma_3) \cos^2 \theta + \sigma_3$$

$$= (\sigma_1 - \sigma_3) \frac{1}{2} (2 \cos^2 \theta) + \sigma_3$$

$$= \frac{1}{2} (\sigma_1 - \sigma_3) (1 + \cos 2\theta) + \sigma_3$$

$$= \frac{1}{2} \{ \sigma_1 - \sigma_3 + \sigma_1 \cos^2 \theta - \sigma_3 \cos 2\theta \} + \sigma_3$$

$$= \frac{1}{2} (\sigma_1 - \sigma_3) + \sigma_3 + \frac{1}{2} (\sigma_1 - \sigma_3) \cos 2\theta$$

$$\sigma_n = \frac{1}{2} (\sigma_1 + \sigma_3) + \frac{1}{2} (\sigma_1 - \sigma_3) \cos 2\theta \quad \text{Eq. (i)}$$

Total shear stress acting on the given plane $\sigma_s = F_1 - F_3$

$$\begin{aligned}
 &= \sigma_1 \cos^2 \theta - \sigma_3 \sin^2 \theta \\
 &= \sigma_1 \cos \theta \sin \theta - \sigma_3 \cos \theta \sin \theta \\
 &= (\sigma_1 - \sigma_3) \cos \theta \sin \theta \\
 &= \frac{1}{2}(\sigma_1 - \sigma_3) 2 \cos \theta \sin \theta \\
 \sigma_s &= \frac{1}{2}(\sigma_1 - \sigma_3) \sin 2\theta. \qquad \text{Eq. (ii)}
 \end{aligned}$$

4. Construction of the Mohr circle for stress

In a Mohr diagram for two-dimensional stress we draw two mutually perpendicular axes, representing σ_n along the X-axis and σ_s along the Y-axis (Pluijm & Marshak 2004). In Figure 1, the maximum principal stress (σ_1) and the minimum principal stress (σ_2) act on a plane P that makes an angle θ with the σ_1 direction; we then plot σ_1 and σ_2 on the X-axis (Figure 2). Then construct a circle through points σ_1 and σ_2 , with O, the midpoint at $(\sigma_1 + \sigma_2)/2$ as centre (A), and a radius (B) of $(\sigma_1 - \sigma_2)/2$. To obtain the equation of Mohr circle the equations mentioned above (i & ii) are rearranged and squares are taken on both sides of equation and we get the equation $(\sigma_n - A)^2 + \sigma_s^2 = B^2$ from which the centre and radius can be obtained also. Then draw a line OP that makes an angle of 2θ with σ_1 . Thus, the construction of Mohr diagram is complete and we can read off the value of σ_n, P along the σ_n -axis, and the value of σ_s, P along the σ_s -axis for plane P, as shown in Figure 2.

The angle between plane normal and σ_n are doubled in the Mohr space, two points representing perpendicular planes are separated by 180° in the Mohr diagram. This is why the two principal stresses both plot on the horizontal axis.

The Mohr diagram used in geologic applications is generally constructed so that compression is positive and tension is negative.

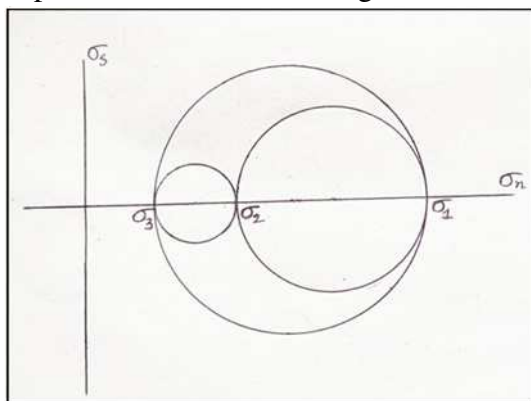


Figure 3: Mohr circle representing three-dimensional stress (see Van der Pluijm & Marshak 2004)

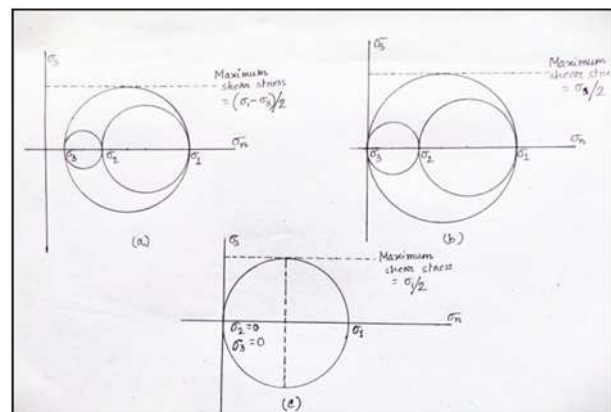


Figure 4: Mohr circle representing three-dimensional stress. (Source: Van der Pluijm.& Marshak. 2004)

For three-dimensional stress, all the three principal stresses are plotted along the horizontal axis, and three Mohr circles are constructed in a single Mohr diagram (Figure 3). Three-

dimensional Mohr constructions combine three Mohr circles of two-dimension: $(\sigma_1 - \sigma_2)$, $(\sigma_1 - \sigma_3)$, and $(\sigma_2 - \sigma_3)$.

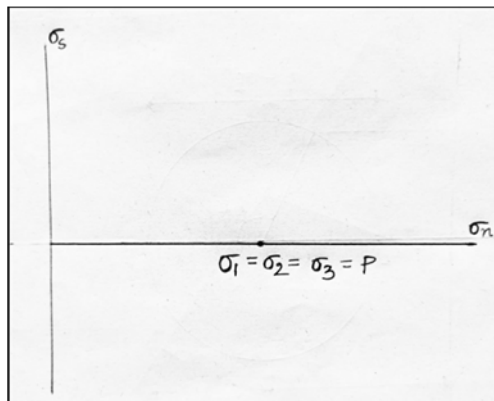


Figure 5: Hydrostatic stress.
(Source: Van der Pluijm & Marshak 2004)

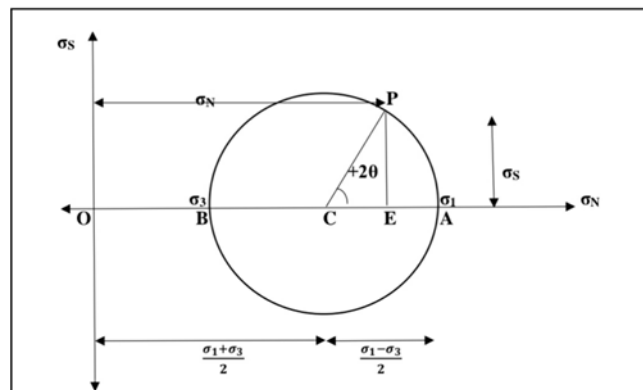


Figure 6: Measurement of stress using Mohr circle.
(after Van der Pluijm & Marshak 2004)

Representation of different states of stress using Mohr circle

Figure 4a shows the case for general triaxial stress, in which all three Principal stresses have nonzero values ($\sigma_1 > \sigma_2 > \sigma_3 \neq 0$).

Biaxial (plane) stress, in which one of the principal stress is zero (e.g., $\sigma_3 = 0$) is shown in Figure 4.b.

Uniaxial compression ($\sigma_2 = \sigma_3 = 0$; $\sigma_1 > 0$) is shown in Figure 4(c), and similarly uniaxial tension can be represented as ($\sigma_1 = \sigma_2 = 0$; $\sigma_3 < 0$).

Isotropic stress, often called hydrostatic pressure, is represented in Figure 5 by a single point on the σ_n -axis of the Mohr diagram (positive for compression, negative for tension), because all three principal stresses are equal in magnitude ($\sigma_1 = \sigma_2 = \sigma_3$) (Pluijm & Marshak 2004).

5. The procedure for measurement of stress using Mohr circle

In a coordinate system with σ_n - axis as abscissa; σ_s - axis as ordinate and origin at O.

The principal stresses σ_1 and σ_3 are given. On a certain scale, the stresses are plot on the σ_n -axis as OA and OB.

By convention, compressive stress is plotted on the positive direction, tensile stress is plotted on the negative direction of σ_n - axis.

Mohr's circle is drawn with AB as diameter and C as centre. Then segment $OC = \frac{1}{2}(\sigma_1 + \sigma_3)$; the radius, $AC = \frac{1}{2}(\sigma_1 - \sigma_3)$

Plot the plane making an angle 2θ at C from the σ_n -axis. Taking anticlockwise as $+2\theta$, clockwise as -2θ .

Let, P be a point on the circle, it signifies as a plane, where $\angle ACP = 2\theta$.

Let, EP be a perpendicular on σ_n - axis.

Normal stress on plane P is;

$$OE=OC+CE;$$

In $\triangle CEP$, $CE= CP \cos 2\theta$; CP is the radius of the Mohr's Circle.

$$CP=1/2(\sigma_1 - \sigma_3);$$

$$OE=1/2(\sigma_1 + \sigma_3) + 1/2(\sigma_1 - \sigma_3) \cos 2\theta$$

Shear stress on plane P is;

$$EP= CP \sin 2\theta; [\text{From } \triangle CEP]$$

$$EP= 1/2(\sigma_1 - \sigma_3) \sin 2\theta$$

(Ghosh 1993)

6. Conclusion

Under this topic we have described the concept and applications of Mohr Diagrams, and how to measure the normal and shear stresses acting on planes of all possible orientations through a point in a stress field (Fossen 2016). To represent a state of stress in stress ellipsoid, all the normal stress components must have the same sign i.e., either all of them must be compressive or all of them must be tensile. In Mohr Circle, however, both compressive and tensile stresses can be represented together, unlike that of the stress ellipsoid. It is therefore a more convenient way than stress ellipse/ellipsoid for representation of stress in two or three dimensions.

Acknowledgement

We thank our mentor Bhaskar Ghosh, Department of Geology, Jogamaya Devi College, Kolkata for the constant inspiration and guidance we received from him. We also thank Adrija Chakraborty, Final Year M. Sc. Tech, student, Department of Applied Geology, Indian Institute of Technology (Indian School of Mines), Dhanbad for guiding us in certain parts of our present work.

References

- Fossen, H. 2016. Structural Geology, 2nd Edition. Cambridge University Press
- Ghosh, S. K., 1993. Structural Geology Fundamentals and Modern Developments, 1st Edition. Pergamon Press
- Van der Pluijm, B. A. and Marshak. S. 2004. Earth Science: An Introduction to Structural Geology and Tectonics, 2nd Edition., W. W. Norton & Co. New York.

Mohr Circle: Its Applications in the Representation and Measurement of Strain

Debasrita Bhattacharjee¹, Shrestha Pal² and Sumana Roy³

Students of 3rd Year Geology Honours Course

¹debasrita9.db@gmail.com, ²shresthapal98@gmail.com, ³sumanaroy1999@gmail.com

1. Introduction

The Mohr diagram is a well-known method for graphical representation of two-dimensional and three-dimensional stresses, from which the normal stress and shear stress acting on a plane of given orientation can be measured conveniently. This article describes the application of Mohr circle in the representation of infinitesimal strain and finite strain, and its application in the measurement of longitudinal and angular strain.

Usually quadratic elongation and shear strain are used in construction of Mohr circle for strain in which the incremental strain axes are parallel to the finite strain axes (i.e. for coaxial strain). The construction for non-coaxial strain adds a component of rotation to the deformation. In Mohr space, this rotational component moves the centre of the Mohr circle off the reciprocal longitudinal strain axis (Van der Pluijm & Marshak 2004).

2. Representation of longitudinal strain and shear strain as a function of the principal strains

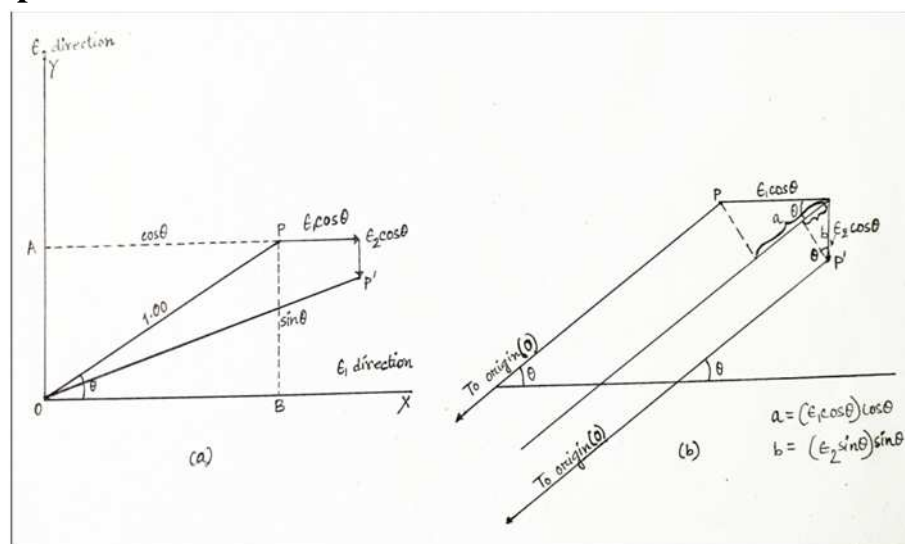


Figure 1: Diagrams for derivation of normal strain.

*NOTE: In Figure1, the $(\epsilon_2 \cos\theta)$ should be $(\epsilon_2 \sin\theta)$ for both (a) and (b).
(Source: Means 1976).

The line OP of unit length is inclined at θ° to the ϵ_1 direction. Point P lies at distances of $\sin\theta$ and $\cos\theta$ from x and y axes respectively. This is the situation before strain occurs.

Let us consider an infinitesimal strain occurs such that O remains at the origin but P is displaced a small distance to P'. The displacement of P to P' has a component $\epsilon_1 \cos\theta$ parallel to the x axis. That is, any line parallel to the x axis will be stretched by an amount $\Delta l = \epsilon_1$ times of its original length.

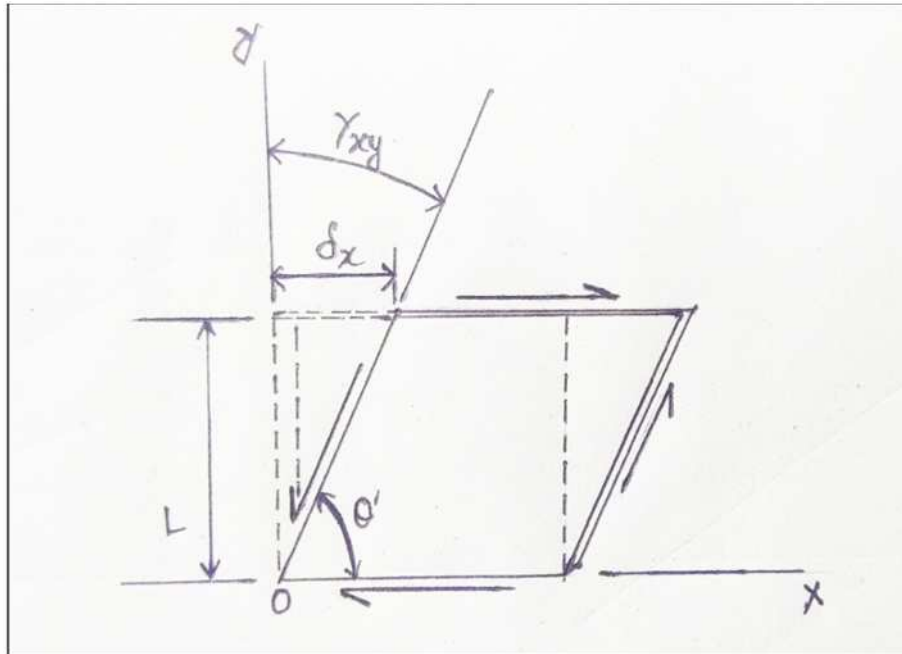


Figure 2:Diagrams for derivation of shear strain^[1] ('L' indicates the original length; γ_{xy} = shear strain; Original angle = θ ; Changed angle after shearing= θ' ; δx = change in length).

And for line AP in particular, this is, $\Delta l = \epsilon_1 (AP) = \epsilon_1 \cos\theta$.

Likewise, any line parallel to the y axis will be shortened a small amount and for BP this is $\epsilon_2 \sin\theta$.

It is assumed that $\epsilon_1 \cos\theta$ and $\epsilon_1 \sin\theta$ are infinitesimally small compared to the distance OP, so that the lines OP and OP' are drawn parallel to each other. x displacement of $\epsilon_1 \cos\theta$ will lengthen the original distance OP by an amount 'a' equal to $\epsilon_1 \cos^2\theta$. At the same time, the y displacement of $\epsilon_2 \sin\theta$ will shorten OP by an amount of $\epsilon_2 \sin^2\theta$ (indicated by 'b'). Thus, the normal strain of a line at θ° to the ϵ_1 direction is

$$\epsilon = \epsilon_1 \cos^2\theta + \epsilon_2 \sin^2\theta.$$

From the above equation it is obtained that,

$$\epsilon = \epsilon_1/2 + \epsilon_1 \cos^2\theta/2 + \epsilon_2/2 - \epsilon_2 \cos^2\theta/2$$

$$\text{Or, } \epsilon = (\epsilon_1 + \epsilon_2)/2 + \{(\epsilon_1 - \epsilon_2) \cos^2\theta\}/2$$

This equation gives the normal strain or elongation of any line in a principal plane, where ϵ_1 and ϵ_2 are the two principal strains and θ is the angle between the line and the ϵ_1 direction (Means 1976).

x displacement of $\epsilon_1 \cos\theta$ will rotate the original line OP by an amount equal to $\epsilon_1 \cos\theta \sin\theta$. At the same time 'y' displacement of $\epsilon_2 \sin\theta$ will rotate OP by an amount of $\epsilon_2 \cos\theta \sin\theta$. Thus, shear strain of a line at θ° to the ϵ_1 direction is

$$\gamma/2 = \epsilon_1 \cos\theta \sin\theta - \epsilon_2 \cos\theta \sin\theta$$

$$\gamma/2 = (\epsilon_1 - \epsilon_2) \cos\theta \sin\theta$$

$$\gamma = (\epsilon_1 - \epsilon_2) 2 \cos\theta \sin\theta$$

$$\gamma = (\epsilon_1 - \epsilon_2) \sin 2\theta$$

3. Representation of infinitesimal strain using Mohr circle

Infinitesimal strain refers to a very small amount of strain, assumed to be indefinitely close to zero. For such a small magnitude of strain, the numerical values for the angular shear Ψ (in radians) and the shear strain γ can be considered equal.

The equation for elongation of any line in a principal plane is represented as

$$\epsilon = (\epsilon_1 + \epsilon_2)/2 + \{(\epsilon_1 - \epsilon_2) \cos 2\theta\}/2$$

Where ϵ_1 and ϵ_2 are principal strains and θ is the angle between the line and the ϵ_1 direction.

The above equation is comparable to the equation for normal stress given as

$$\sigma_n = (\sigma_1 + \sigma_2)/2 + \{(\sigma_1 - \sigma_2) \cos 2\theta\}/2$$

The equation for shear strain of a line at θ degrees to ϵ_1 is:

$$\gamma = (\epsilon_1 - \epsilon_2) \sin 2\theta$$

This equation has similarity with the corresponding equation for shear stress:

$$\sigma_s = \{(\sigma_1 - \sigma_2) \sin 2\theta\}/2.$$

Comparing the above four equations we draw the following inferences.

The infinitesimal strain can also be represented by a Mohr circle.

In the Mohr circle for strain, the quantity plotted on the abscissa is the longitudinal strain.

In the Mohr circle for strain, the quantity plotted on the ordinate is the one-half of the shear strain.

Three important properties of infinitesimal strain emerge once it is accepted that a Mohr circle accurately represents the state of strain:

There are two lines upon which the shear strain is maximum. These lie at 45 degrees to the ϵ_1 direction.

The magnitude of the maximum shear strain is equal to the difference between the principal strains. It may be positive or negative.

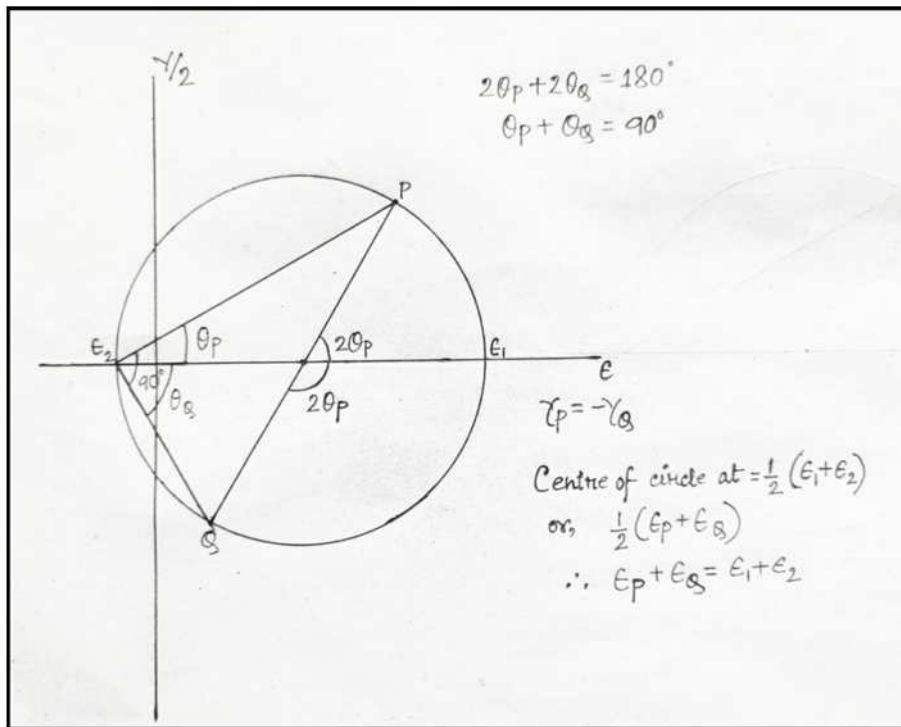


Figure 3: Mohr circle for infinitesimal strain showing how the sum of the normal strains of any two perpendicular lines is a constant equal to $\epsilon_1 + \epsilon_2$ (Means 1976: p.156)

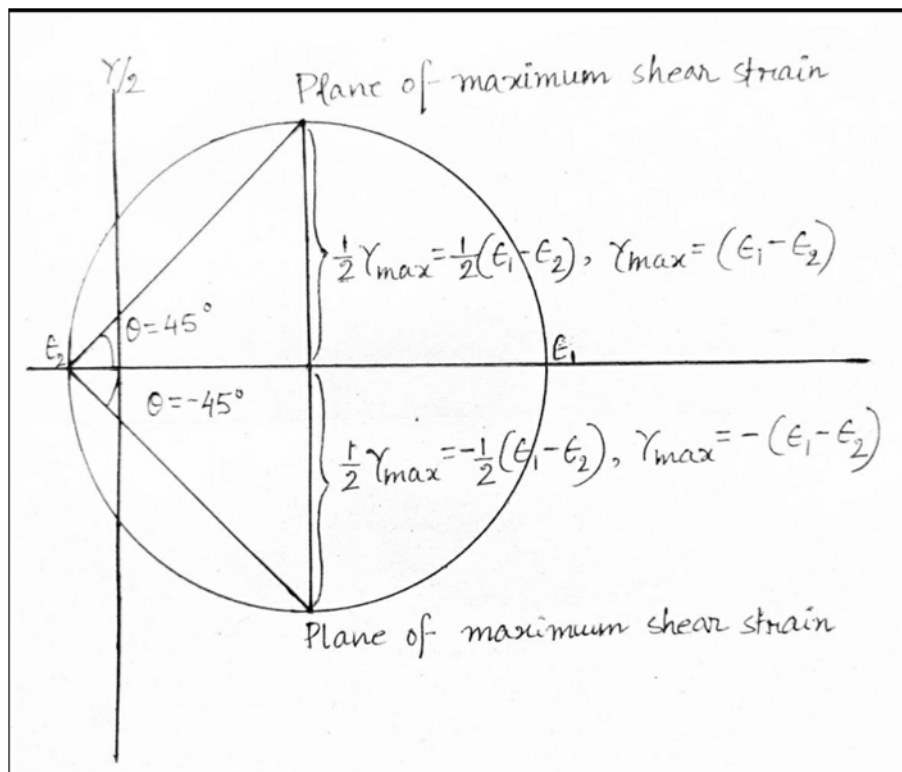


Figure 4: Mohr circle for infinitesimal strain showing how maximum shear strain occurs on two lines at 45 degrees to the ϵ_1 direction. (Means 1976: p.156)

Any two lines P and Q at right angles to each other are represented by points at the opposite ends of a diameter on the Mohr circle.

Therefore, on any pair of perpendicular lines the shear strains are equal in magnitude but opposite in sign. The sum of normal strains on those planes equals the sum of the principal strains.

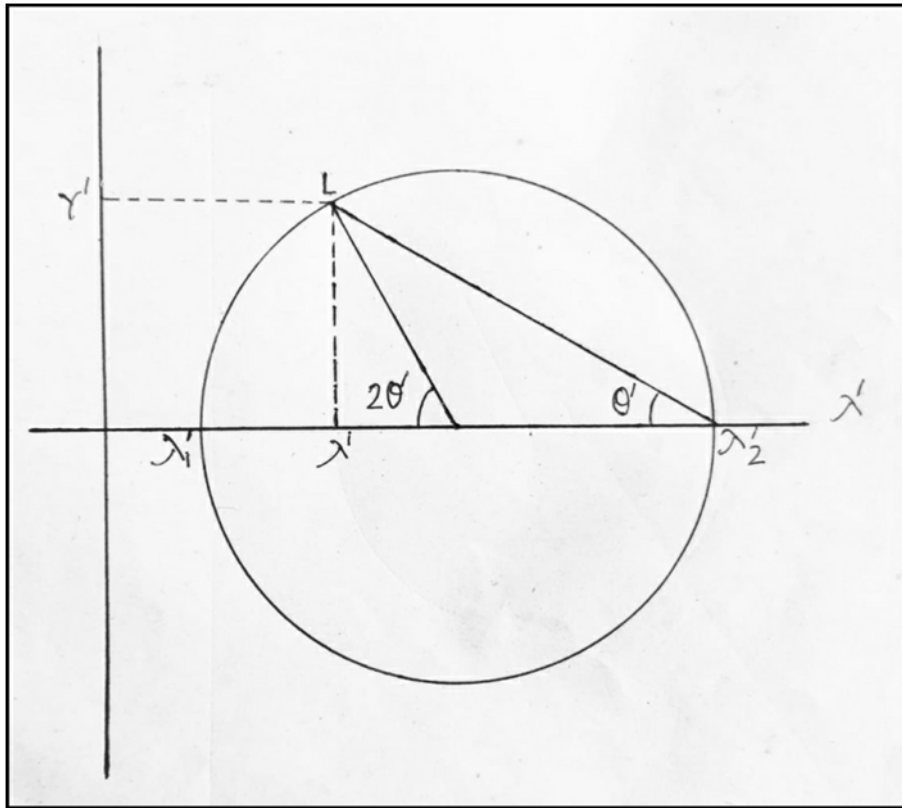


Figure 5: Mohr circle for a state of two-dimensional finite strain. The coordinates of any point L on the circle are the quantities λ' and γ' , described in the text, for a line inclined at Θ' degrees to the λ' direction on the deformed object (Means, 1976).

4. Representation of finite strain using Mohr circle

The measure of strain that compares the initial and final strain configurations is called finite strain (or total strain).

Equations of the Mohr circle for finite strain are as follows:

$$\lambda_n' = (\lambda_1' + \lambda_2')/2 + \{(\lambda_1' - \lambda_2') \cos 2\theta'\}/2 \text{ [Eq. (4.1)] and}$$

$$\gamma_s' = \{(\lambda_2' - \lambda_1') \sin 2\theta'\}/2 \text{ [Eq. (4.2)]}$$

The quantities will plot on a circle with λ_1' and λ_2' at the opposite ends of its diameter on the abscissa.

λ' is $1/\lambda$ where λ is the quadratic elongation of a line at θ' degrees to the λ_1 direction.

γ' is γ/λ where γ is the shear strain of a line at θ' degrees to the λ_1 direction and λ is the quadratic elongation of the same line.

λ_1' is $1/\lambda_1$ where λ_1 is the greater principal strain and λ_2' is $1/\lambda_2$ where λ_2 is the lesser principal strain both expressed as a quadratic elongation.

θ' is the angle measured in the deformed state from the λ_1 direction to the line. Anticlockwise values of θ' measured on the deformed object are reckoned positive.

Conclusion

In homogeneous or inhomogeneous field of deformation, strain at a point is represented by strain ellipsoids. But in this method, if we draw a strain ellipsoid where the principal strains are very low, it would look like the original undistorted sphere. That is why it is not very useful for representation of very small magnitude of strain. But the Mohr diagram can be applied for the representation of both infinitesimal and finite strain. The Mohr diagram also measures the longitudinal and shear strain easily and more conveniently than any other method. Wider use of Mohr diagram can therefore be recommended in the analysis of strain.

Acknowledgement

We would like to acknowledge and thank our mentor Bhaskar Ghosh, Department of Geology, Jogamaya Devi College for his relentless help and supervision during the preparation of this essay. We would also like to thank Monomita Chattopadhyay, M. Sc. 2nd year, Department of Geology and Geophysics, IIT Kharagpur for helping us by giving her thoughtful comments.

References

- Means, W. D., 1976. Stress and Strain Basic Concepts of Continuum Mechanics for Geologists, Springer-Verlag, 1st Edition.
- Van der Pluijm B. A. & Marshak. S., 2004, Earth Science: An Introduction to Structural Geology and Tectonics, W. W. Norton & Co. New York, 2nd Edition.

Weblink

- [1] <https://www.youtube.com/watch?v=Gj653EeL5Bg> (1:48min)

Development of the Extension Fractures and the Shear Fractures in Nature

Ankita Mukherjee¹, Upasna Karmakar² and Tiyasa Ghosh³

Students of 3rd Year Geology Honours Course

¹heythsanki@gmail.com, ²upasnakarmakar@gmail.com, ³tiyasaghosh100899@gmail.com

1. Introduction

It wasn't anyone's "fault" but there's a "fracture"!

Fractures are surfaces along which rocks or minerals are broken or have lost cohesion. They are classified as follows, based on the relative motion that has occurred across fracture surface during formation (Van der Pluijm & Marshak 2004).

Extension fracture: Relative motion is perpendicular to and away from the fracture surface (Figure 1).

Shear Fracture: Relative displacement is parallel to the fracture surface. There are two types.

- (a) Mode II Fracture (Sliding Fracture): Relative motion is perpendicular to fracture edge or fracture front (Figure 2).
- (b) Mode III Fracture (Tearing Fracture): Relative motion is parallel to fracture edge or fracture front (Figure 3).

Mixed Mode Fracture: Relative displacement is oblique to the fracture surface (Figure 4).

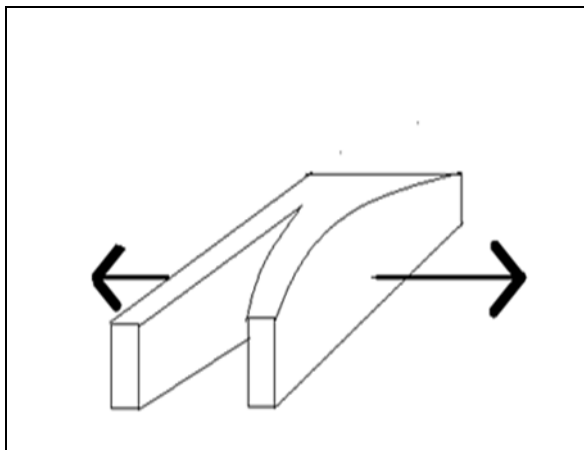


Figure 1: Extension Fracture/Mode I fracture/Tensile fracture, Relative displacement is parallel to the fracture (sketch by the authors, after Twiss & Moores 2007).

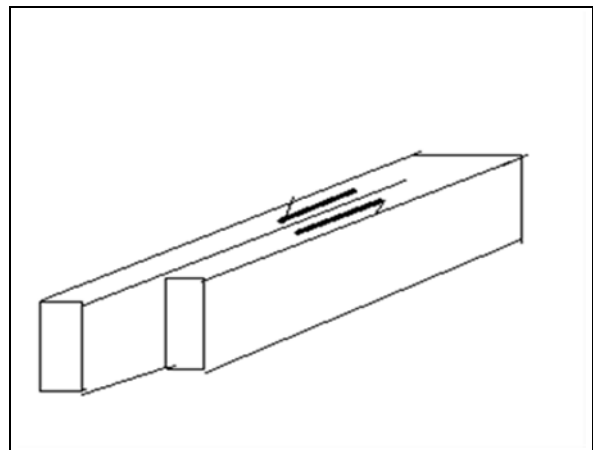


Figure 2: Shear fractures mode II fracture/Sliding fracture/In plane fracture Relative displacement is a sliding parallel to the fracture and perpendicular to the edge of fracture (sketch by the authors, after Twiss & Moores 2007).

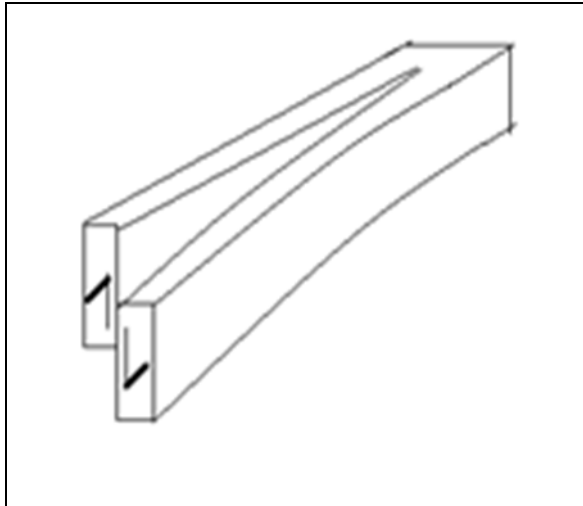


Figure 3: Shear fractures mode III/Tearing fracture/Out of plane fracture- Relative displacement is a sliding parallel to the fracture and to edge of the fracture. (Sketch by the authors, after Twiss & Moores 2007)

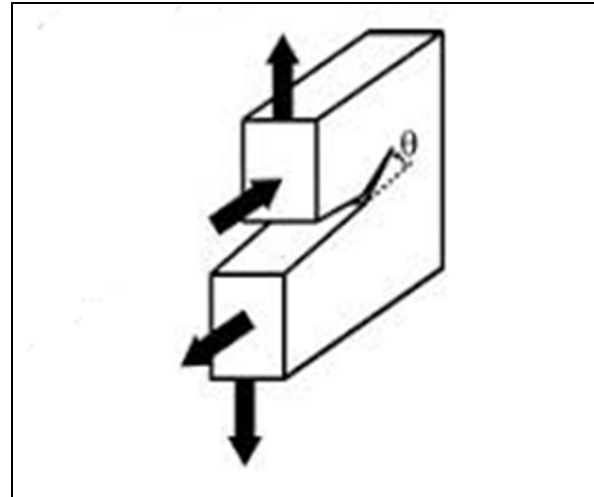


Figure 4: Mixed Mode Fracture^[1].

2. Mechanism of formation of the extension fractures

Criterion for extension fractures

Tensile fractures are those extension fractures which are formed in response to a minimum principal stress that is tensile, i.e. the principal stresses are negative. (Fossen 2016)

Tensile strength^[1] (say T_0) of a material can be defined as the maximum stress that the material can withstand before breaking.

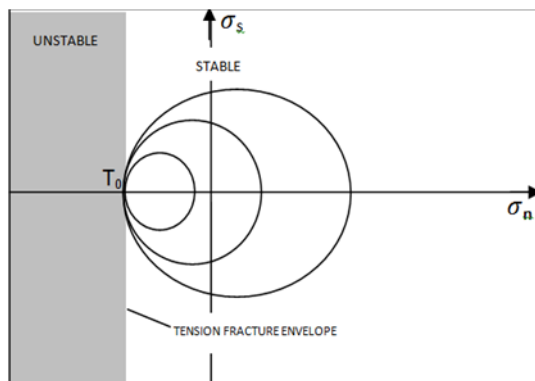


Figure 5: Fracture criterion for tensile fractures. The tension fracture envelope divides the Mohr diagram into areas of unstable stress (shaded) and stable stress (unshaded); this is for a critical state of stress (sketch by the authors, after Twiss. & Moores 2007).

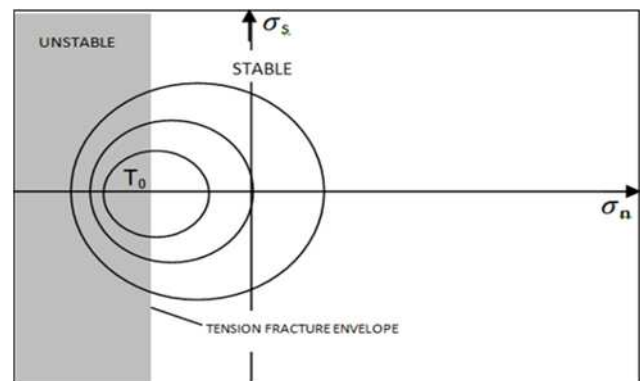


Figure 6: Fracture criterion for tensile fractures. The tension fracture envelope divides the Mohr diagram into areas of unstable stress (shaded) and stable stress (unshaded); this figure is for unstable state of stress (sketch by the authors, after Twiss. & Moores 2007).

A rock remains stable when subjected to tensile stresses $< T_0$. When tensile stress = T_0 , the rock fractures (Figure 5) and when it exceeds T_0 , the rock is in unstable condition (Figure 6). The following equation provides a fracture criterion.

$$\sigma_n^* = T_0$$

σ_n^* = critical normal stress required to fracture, T_0 = tensile strength of the rock

As observed in experiments, extension fractures develop perpendicular to the minimum principal stress direction (σ_3). Therefore, the stress on the fracture plane plots at $2\theta_f = 180^\circ$ from σ_1 (Figure 8). The normal and shear stress acting on the fracture plane is thus seen to plot exactly at the point of tangency between the critical Mohr's circle and the tension fracture envelope.

Thus it can be inferred that a tension fracture is such a plane where normal stress reaches critical value T_0 and is perpendicular to the tensile stress σ_3 .

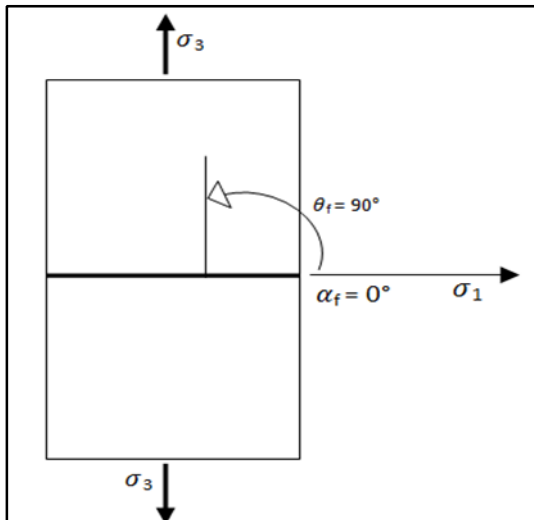


Figure 7: Diagram in physical space. (Sketch by the authors, after Twiss & Moores 2007)

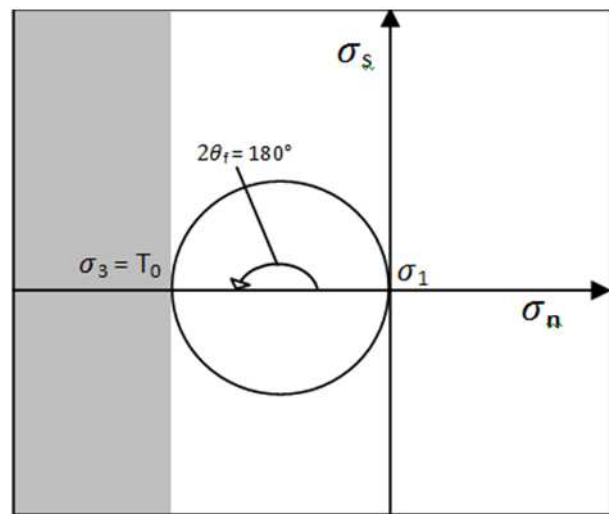


Figure 8: critical Mohr diagram for tension fracture under uniaxial tensile stress (sketch by the authors, after Twiss & Moores 2007)

3. Mechanism of formation of the shear fractures

A macroscopic fracture that grows with a component of shear parallel to the fracture and hence relative movement parallel to the fracture surface is shear fracture.

Shear fractures show fracture parallel slip. Experiments conducted under confined compression which shows shear fractures commonly develop in conjugate pairs and initiated in laboratory rock cylinders at typical angle of 30° to σ_1 . These develop under temperature and confining pressures corresponding to the upper part of the crust and also near brittle plastic transition zone where they tend to grow into wider bands and zones of cataclastic flow.

The normal stress acting on the fracture in addition to shear stress, friction resists sliding on the fracture during its formation (Figure 9).

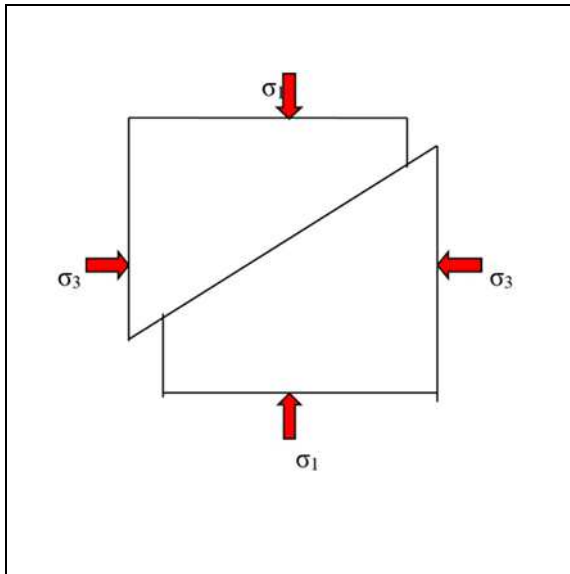


Figure 9: Experimental deformational structure that develops under contraction (sketch by the authors after Van der Pluijm & Marshak 2004).

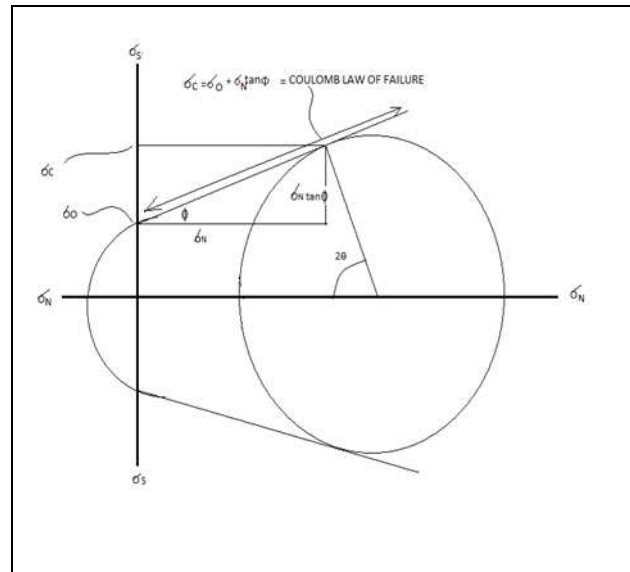


Figure 10: Critical state of stress and Coulomb fracture criterion. This figure shows the envelope of failure for a rock. The point of failure shown on the Coulomb envelope has x,y coordinates that reveal the magnitudes of normal stress and shear stress on the fracture at time of failure. (sketch by the authors after Davis & Reynolds 1996)

4. The Coulomb fracture criterion

Coulomb's law of failure is based on dynamic models developed by Coulomb (1773) and Mohr (1900), the strength of a rock to resist shear fracturing is derived from two sources.

1) Natural cohesive strength of the rock (σ_0)

2) The internal frictional resistance (σ_f) to shearing. The stress required to fracture rock must be large enough to overcome these two. Coulomb proposed a criterion of failure which states that a shear fracture can develop when the shear stress acting on a plane is large enough to overcome the cohesive strength as well as the frictional resistance to movement along the fracture plane.

$$\sigma_c = \sigma_0 + \sigma_f$$

where, σ_c = the critical shear stress required for faulting, σ_0 = the cohesive shear strength, and σ_f = the frictional resistance.

Any Mohr circle tangent to the lines represents a critical state of stress that causes shear fracturing. Straight line approximation to the shear fracture envelope is known as the Coulomb fracture criterion.

In this criterion the shear stress value is the critical shear stress (σ_c) which is necessary for fracturing. Part of its magnitude is cohesive strength (σ_0). It can be read directly from the Mohr diagram. Rest of the σ_c is stress required to overcome internal frictional resistance to

triggering movement on the fracture The frictional resisting force is proportional to the normal force and independent of the area of the surface of contact.

$$\sigma_f \propto \sigma_n$$

$$\sigma_f = \mu \cdot \sigma_n$$

where, σ_n = the applied normal force and μ = the coefficient of internal friction (Coulomb coefficient), when the angle of internal friction is ϕ , the coefficient of friction $\mu = \tan \phi$. So, $\sigma_c = \sigma_0 + \mu (\sigma_n)$. The stress level at which shear fractures will form in compression is strongly influenced by ϕ , the angle of internal friction. Based on the geometry of Mohr diagram, we have

$$\phi = 90^\circ - 2\theta$$

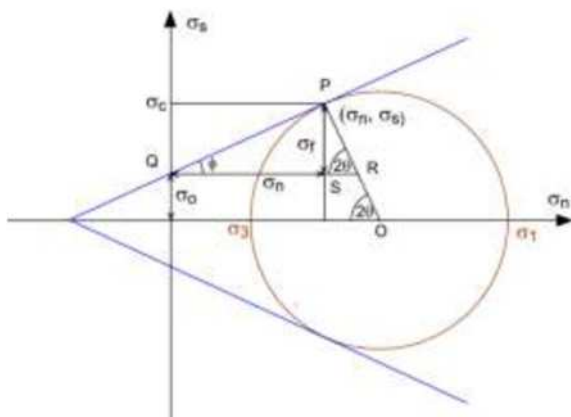


Figure 11: Relationship of frictional resisting force (σ_f), cohesive shear strength (σ_0) and critical shear stress (σ_c) for shear failure (figure provided by :Adrija Chakraborty, Final Year M.Sc.Tech, Department of Applied Geology, Indian Institute of Technology (Indian School of Mines), Dhanbad)

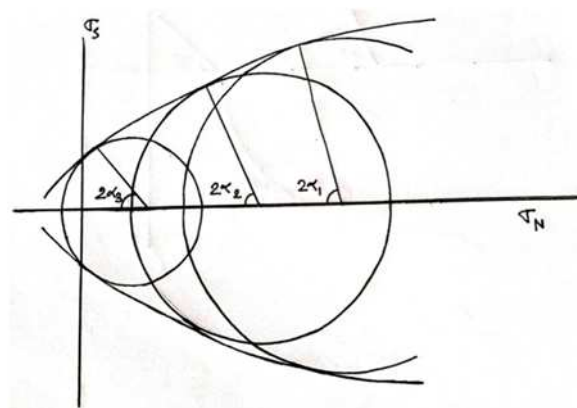


Figure 12: Mohr failure envelope. The slope of the envelope steepens towards the σ_s axis (sketch by the authors after Van der Pluijm & Marshak 2004)

On satisfying this criterion, a shear fracture can develop.

For any critical stress state the criterion is satisfied at the two points where the Mohr circle is tangent to the two lines given by the equation. These two differently oriented planes called conjugate shear planes (Twiss & Moores 2007, Davis & Reynolds 1996).

5. The Mohr failure envelope

Mohr conducted studies showing that straight line relationship only works for a limited range of confining pressures. At lower confining pressure the line representing the stress state at failure curved with a steeper slope and at higher confining pressure the line curved with shallower slope.

Change in slope of the failure envelope indicates that angle between shear fracture plane and σ_1 depends on the stress state. At lower confining pressures, angle is smaller, and at high confining pressures, angle is steeper.

Mohr-Coloumb Criterion (both for positive and negative values of σ_s) defines a failure envelope on Mohr diagram. Failure envelope separates the field of stable and unstable stresses.

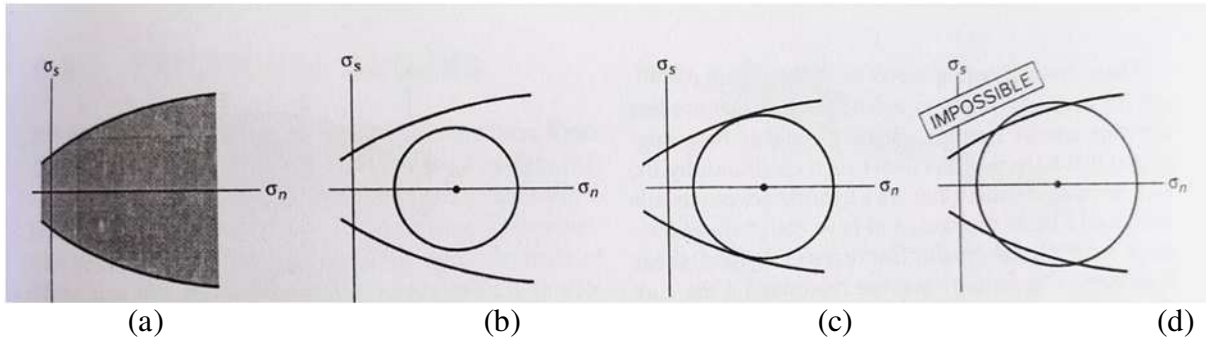


Figure 13: A brittle failure envelop as depicted on a Mohr diagram. Within the envelope (shaded area) stress state are stable but outside the envelope stress state are unstable.

- (a) A stress state that is stable because the most circle which passes through values for σ_1 and σ_3 and defines the stress state falls entirely inside the envelope.
- (b) A stress state that instant of failure. The circle touches the envelope
- (c) A stress state that is impossible

(sketch by the authors after Van der Pluijm & Marshak 2004)

6. The Von Mises Criterion

At high confining pressures, samples may begin to deform plastically. Under such conditions, concept of failure envelope no longer applies. Critical shear stress (the yield stress) leads to creep. Thus, the failure envelops runs parallel to the normal stress axis (constant shear stress). This yield criterion, known as von Mises Criterion, indicates that plastic yielding is effectively independent of the differential stress once the yield stress has been achieved.

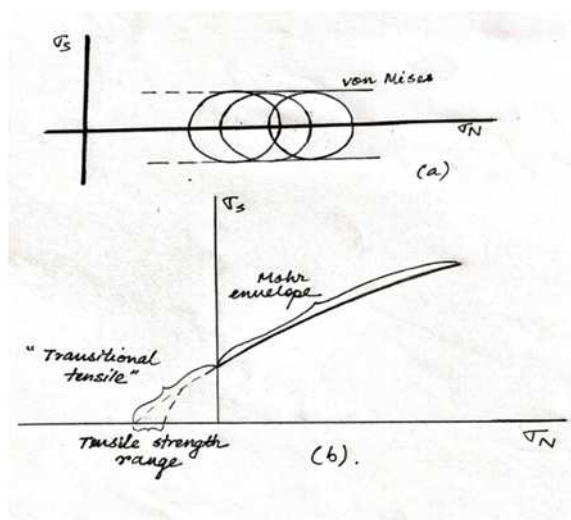


Figure 14: (a) Mohr diagram illustrating the Von Mises yield criterion. The criterion is represented by lines parallel to the σ_n axis (b) The extrapolation of a Mohr envelope to its intercept with the σ_n axis illustrating the transitional tensile regime and the tensile strength. (sketch by the authors after Van der Pluijm & Marshak 2004)

7. Conclusion

The topics discussed in the above section focuses mainly on the types of fractures and their development. They are formed by brittle deformation and are developed in a rock body when they reach a critical state of stress. Some fracture criteria such as those of Coulomb and Mohr have been discussed here, which define the stresses and the orientations of the fracture surfaces at various states of stress.

Acknowledgement

This article would not be possible without the constant guidance from our mentor Bhaskar Ghosh, Department of Geology, Jogamaya Devi College. We would also like to thank our senior Miss Adrija Chakraborty, Final Year M. Sc. Tech, Department of Applied Geology, Indian Institute of Technology (Indian School of Mines), Dhanbad, for sharing her valuable suggestions on the article.

References

- Davis, G. H., Reynolds, S. J., 1996. Structural geology of rocks and regions, 2nd edition John Wiley & Sons Inc.,
- Fossen, H., 2016. Structural Geology, 2nd Edition. Cambridge University Press.
- Twiss. R. J., Moores, E. M., 2007, Structural Geology, 2nd Edition. W. H. Freeman, New York, 2nd edition.
- Van der Pluijm B. A., Marshak., S., 2004, 2nd Edition. Earth Science: An Introduction to Structural Geology and Tectonics, W. W. Norton & Co. New York.

Weblink

- [1] ALT: <https://ars.els-cdn.com/content/image/1-s2.0-S0142961209006218-gr1.sml>

Appendix

[1] (Section 2, tensile strength): Often the terms ‘tensile strength’ and ‘yield strength’ are confused with each other. Tensile strength is the maximum strength a material can withstand, before it breaks or fails. However, when a material is stressed by an amount that is less than its yield stress, it will only undergo elastic (reversible) strain, and no permanent deformation of the material will occur. The level of stress that corresponds to the yield point is referred to as the yield strength of the material.



आत्मदीपो भव

JDC GEOBYTES 2020

**Department of Geology
Jogamaya Devi College**